ELECTRON MEDIATION THROUGH CHALCOGENOCYANATES : SYNTHESIS, CHARACTERIZATION AND ELECTRON TRANSFER PROPERTIES OF THIOCYANATO AND SELENOCYANATO BRIDGED BINUCLEAR MIXED - VALENCE COMPLEXES

A Thesis Submitted
In Partial Fulfilment of the Requirements
for the Degree of

DOCTOR OF PHILOSOPHY

by

VAITHIANATHAN PALANIAPPAN

to the

DEPARTMENT OF CHEMISTRY

INDIAN INSTITUTE OF TECHNOLOGY, KANPUR

DECEMBER, 1987

TO MY PARENTS & TEACHERS

CHM-1987-D-PAL-E

STATEMENT

I hereby declare that the matter embodied in this thesis is the result of investigations carried out by me in the Department of Chemistry, Indian Institute of Technology, Kanpur, India, under the supervision of Professor U.C. Agarwala.

In keeping with the general practice of reporting scientific observations, due acknowledgement has been made wherever the work described is based on the findings of other investigators.

V. PALANIAPPAN

Kanpur

December 24, 1987.

DEPARTMENT OF CHEMISTRY
INDIAN INSTITUTE OF TECHNOLOGY KANPUR, INDIA
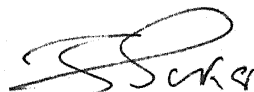
CERTIFICATE OF COURSE WORK

This is to certify that Mr. V. Palaniappan has satisfactorily completed all the courses required for the Ph.D. programme. These courses include,

Chm 505	Introductory Organic Chemistry
Chm 521	Chemical Binding
Chm 524	Modern Physical Methods in Chemistry
Chm 525	Introductory Physical Chemistry
Chm 542	Advanced Inroganic Chemistry II
Chm 545	Introductory Inorganic Chemistry
Chm 800	General Seminar
Chm 801	Graduate Seminar
Chm 900	Post-Graduate Research

Mr. V. Palaniappan was admitted to the candidacy of the Ph.D. programme in July 1983 after he successfully completed the written and oral qualifying examinations.

(P.S. Goel)
Professor and Head,
Department of Chemistry,

(S. Sarkar)
Convener
Departmental Post-Graduate
Commmittee, Department of
Chemistry, IIT, Kanpur-16

CERTIFICATE

Certified that the work contained in this thesis, entitled: "ELECTRON MIGRATION THROUGH CHALCOGENOCYANATES; SYNTHESIS, CHARACTERIZATION AND ELECTRON TRANSFER PROPERTIES OF THIOCYANATO- AND SELENOCYANATO-BRIDGED BINUCLEAR MIXED-VALENCE COMPLEXES" has been carried out by Mr. V. Palaniappan under my supervision and the same has not been submitted elsewhere for a degree.

(U. C. Agarwala)
Thesis Supervisor

Kanpur

December 24 , 1988.

ACKNOWLEDGEMENTS

Chidambaram and other friends for making Core Labs a habitable place.

- Dr. M.I. Khan, Mohan Rao, Minu Gupta, D.S. Pandey, Anjali Mishra and Rajendra Prasad for bearing my presence in the lab.

- Mrs. J. Chandrasekaran, Mrs. and Dr. K. Raghavan and Dr. V. Mohan for their encouragement.

- Messrs Clement Ravichandar, and K. Srinivasan and Murali for their help.

- Mr. K. Rajagopalan, Mr. Jain and Mr. Nayab Ahmed, for their technical assistance.

- Office staff of the Chemistry Department for their assistance in many ways.

- Ms. Jyoti Seth, Mr. G. Kumaravel, Mrs. ¯and Dr. V. Muruganandam, for my association with them has helped me to get over many difficulties.

- My parents for their faith in me which keeps me going.

- CSIR, New Delhi for a fellowship and the authorities of IIT, Kanpur for facilities.

<div align="right">V. PALANIAPPAN</div>

LIST OF ABBREVIATIONS AND NOTATIONS

M-NCX   :   N-Isomer of chalcogenocyanate complex

M-XCN   :   X-Isomer of chalcogenocyanate complex
(X = S or Se)

M-CNX   :   Both the isomers or the nature of bonding is not
                     specifieid

ET   :   Electron transfer

C-T ion   :   Creutz-Taube ion

(22),   (23):   Three different stages of oxidation states for
and (33)   the dimeric compounds

Pyz   :   Pyrazine

bpy   :   2,2'-Bipyridine

IL   :   Intraligand

LF   :   Ligand field

LMCT   :   Ligand to metal charge transfer

MLCT   :   Metal to ligand charge transfer

MMCT   :   Metal to metal charge transfer

HOMO   :   Highest occupied molecular orbital

LUMO   :   Lowest unoccupied molecular orbital

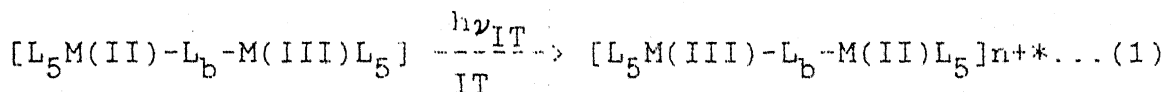RR   :   Resonance Raman

NIR   :   Near infrared

PREFACE

Thiocyanate ion and the chalcogenocyanates (NCO^-, NCS^-, $NCSe^-$ and $NCTe^-$ ions) in general are versatile ambidentate ligands. Their ambidenticity is manifested by a large number of linkage isomers synthesized till date. They have played a crusading role in solving many of the mechanistic problems of inorganic coordination chemistry. Furthermore, these ions exhibit bridging properties resulting in the synthesis of a large number of oligomeric and polymeric chalcogenocyanato bridged metal complexes, where they have been recognized to be a good mediator for electron transfer. Thiocyanate ion takes part in electron transfer reactions by both inner sphere and outer sphere mechanisms. Following the continued interest on the chemistry of the chalcogenocyanates and their capabilities as bridging ligands in di-, tri- and polynuclear complexes, an effort to quantify the electron mediation properties of the thiocyanate bridge was needed. To accomplish this, the synthesis and a detailed study of the thiocyanato and selenocyanato bridged complexes of the 8th group metals, viz., Fe, Ru and Os were planned.

As a first step, the synthesis and a detailed study of the mononuclear thiocyanato and selenocyanato complexes were undertaken. The linkage isomers such as, $[(NH_3)_5RuNCS]^{2+}$ and $[(NH_3)_5RuSCN]^{2+}$, $[(NH_3)_5RuNCSe]^{2+}$ and $[(NH_3)_5RuSeCN]^{2+}$, $[(CN)_5FeNCS]^{3-}$, $[Cl(bpy)_2RuNCS]$ and $[Cl(bpy)_2RuSCN]$ and $[Cl(bpy)_2RuNCSe]$ and $[Cl(bpy)_2RuSeCN]$ were identified and characterized using vibrational spectroscopy and other

physicochemical methods. These complexes were later reacted with appropriate mononuclear units ($[ML_5X]^{n-/n+}$ where X is a labile ligand) to generate the discrete binuclear complexes. Different building blocks such as $[(NH_3)_5Ru]^{n+}$, $[(CN)_5Fe]^{n-}$ and $[(bpy)_2Ru]^{n+}$ were used in the process.

The binuclear complexes were characterized by various physicochemical techniques such as, microanalytical methods, vibrational (IR, Raman and resonance Raman), electronic (absorption and emission), n.m.r. (^1H and ^{13}C) and Mossbauer spectroscopy and electrochemical methods (cyclic voltammetry). All the thiocyanato- and selenocyanato bridged binuclear mixed valence compounds exhibited fairly intense intervalence transfer (IT) bands (Eqn. 1):

$$[L_5M(II)-L_b-M(III)L_5] \xrightarrow[IT]{h\nu_{IT}} [L_5M(III)-L_b-M(II)L_5]n+* \ldots (1)$$

in the near infrared region of their electronic spectra. This in combination with the conceptual model proposed by Hush was used in evaluating the electron mediation properties of the bridge.

A few of the several important results, those emerged from this study, are:

(i) In the case of $[(NH_3)_5MCNX]^{2+}$, where M = Ru and Os and X = S and Se and the coligands are mainly σ-donors the X-bonded (S or Se) isomers are favored over the N-bonded isomers. If the coligands are substituted by π-acceptors, as in the cases of $[(CN)_5FeCNX]^{3-}$ and $[Cl(bpy)_2RuCNX]$, the N-bonded isomer is

favored over the X-(S or Se) bonded isomers. These results are in concordance with the earlier studies.

(ii) In the binuclear complexes, the interaction between the metal centers via the chalcogenocyanate bridge is suggested to occur through a π-overlap, viz., $d\pi(M)-3\pi*(NCX^-)-d\pi(M)$.

(iii) The electron mediation properties of the chalcogenocyanate bridges in the mixed-valence compounds, as obtained from the delocalization factor, α^2, are interesting. For example,

Complex	α^2 (X $\equiv$ S)	α^2 (X $\equiv$ Se)
$[(NH_3)_5RuNCXRu(NH_3)_5]^{4+}$	Delocalized	-
$[(CN)_5FeNCXFe(CN)_5]^{6-}$	5.3×10^{-3}	5.0×10^{-3}
$[Cl(bpy)_2RuNCXRu(bpy)_2Cl]^{2+}$	1.9×10^{-3}	1.9×10^{-3}

The inference is that the change in the "spectator ligands" (from σ-donor to π-acceptor) affects the delocalization of the optical electron as one would expect. A further point is that the interaction between the metal centers could be "tuned" as to our requirements by deliberately changing the nature of the coligands. This will have large impact on biological electron transfer processes, where the driving force (a function of redox asymmetry) plays an important role.

(iv) The asymmetry of the chalcogenocyanate bridge is not as manifested as it might look from a purely chemical point of view.

The reason for this could be the pseudosymmetric π-overlap (vide infra). The pair of LUMO π^*-acceptor orbitals on the chalcogenocyanate ions ($3\pi^*$-orbitals) are localized mostly ($>92\%$) on the central carbon atom and the contributions from the end atoms, viz., N and S or Se, are meager. Thus, the π-overlap could even, be thought of as occurring on [M-C-M] unit rather than [M-NCX-M] unit. The bridge is more a symmetric one rather than asymmetric.

(v) The anionic nature of the bridge, NCX^- (X = S or Se) seems to increase the stability of the mixed-valence species (cf. Table) by a favorably higher contribution from the electrostatic factors to the total free energy change of the comproportionation reaction, ΔG_{tot}°. $\Delta G_{tot}^{\circ} = \Delta G_{es}^{\circ} + \Delta G_{del}^{\circ} + \Delta G_{struct}^{\circ} + \Delta G_{mag}^{\circ} + \Delta G_{induct}^{\circ}$.

(vi) The difference between thiocyanate and selenocyanate ions, as for the π-acceptor properties are concerned is very small. However, the available evidences suggest that the selenocyanate ion has a favorable edge over the thiocyanate ion.

(vii) The electrochemical studies of the binuclear complexes show that the successive two one-electron redox processes occur within a short range of potential. This may be a desirable property, as, now one could imagine the thiocyanato bridged polymeric coordination compounds to exhibit a multielectron redox process within a short range of potential and this is a primary requirement for any compound to act as an electrocatalyst for multielectron redox processes such as

photodissociation of water, etc. As the thiocyanate ion acts as the bridging species in one-, two- and three dimensional networks of coordination complexes, the synthesis of the appropriate polymeric compounds could be planned in future.

Details of these experiments and results are presented in the thesis, the plan of which is as following:

Section I gives a brief overview of the status (both theory and experiment) of the mixed-valence compounds. with a stress on the Hush model.

Section II deals with experimental procedures used to synthesize these complexes along with the description of the various instrumental methods involved in the characterization of these complexes.

Section III describes the characterization of the linkage isomers synthesized in our study.

Section IV describes the characterization part of the synthesized complexes using various physicochemical techniques. The observed IT absorption data for the mixed-valence compounds are treated in terms of the Hush model, to arrive at the numerical values of the different parameters, e.g., interaction parameter H_{AB}, delocalization factor, α^2 and etc.

Section V gives a brief summary and a few recommendations for the further research.

CONTENTS

SECTION I. GENERAL INTRODUCTION

1.1 Introduction - Electron Transfer

Electron transfer (ET) reactions are ubiquitous and are main focus of the mechanistic inorganic chemistry.[1] The interest in ET reactions stems partly due to the versatile variable valency exhibited by transition metals, which plays a key role in the catalysis of redox processes in biological and chemical systems and partly from our needs to understand the **vectorial** charge transport, unique of several metalloproteins[2] and the photosynthetic unit.[3] The wide range of oxidation states available over a comparatively narrow range of energy in transition metals, often makes electron transfer reactions facile, both thermodynamically and kinetically. The large number of investigations carried out till date, do not seem to provide a clear picture of the several aspects of ET reactions. Several questions, such as, 'what is/are the distance dependence on the rate of the ET reaction?' 'what are the reasons for the considerably large rates of ET across the so-called insulators, σ-bond framework?'[4] and 'what is the mechanism by which electron transport in metalloproteins occurs over a large distance, viz., 25 Å?' etc., are yet to be answered. Nevertheless the situation is not so hopeless.

The outcome of these investigations has put us in a comfortable position in the solutions of a number of problems. Thus, the chemical approach to the artificial cells for the storage of energy demonstrated recently,[5] is an evidence for this. Further, a large number of investigations have been devoted to excited state electron transfer taking advantage of the modified redox behaviour of the reagents in their excited states.[6] The one/many electron couple of certain complexes has been efficiently coupled to generate O_2[7], H_2O[6] and Cl_2[8], respectively from H_2O, OH^- and Cl^- and with several organic substrates.[9] The catalytic effectiveness of the transition metal 2,2'-bipyridine complexes; in the "water-oxidation" reaction with large turnover numbers is a well recognized fact now.

1.2 Introduction - Chalcogenocyanates

The chalcogenocyanate ions (NCO^-, NCS^-, $NCSe^-$ and $NCTe^-$ ions) in general, and thiocyanate ion in particular are the most favorite ligands of inorganic chemists since Werner's time. Large amount of investigations, though, have been devoted to these classical ligands, they still pose some of the unsolved problems of inorganic chemistry. The results of the studies on the chalcogenocyanates until 1980 have been compiled in the form of two comprehensive reviews by Norbury[10] and Jackson and coworkers.[11] A few of the important, recently recognized

characteristics of the thiocyanate and in general chalcogenocyanate chemistry, which have given impetus for further research, are the following:

(i) The versatile linkage isomerism[10-22] exhibited by thiocyanate and selenocyanate ions with transition metals has been recognized beyond doubts. For instance, the **simultaneous formation** of both the linkage isomers (N- and S-bonded and N- and Se-bonded in thiocyanate and selenocyanate ions, respectively) in a reaction between a metal ion and the thiocyanate/selenocyanate ion has been proved independently by Agarwala and coworkers[14,15] and Jackson and coworkers.[13] However, in these reactions the thermodynamically stable isomer is favored over the unstable one. This is not in agreement with some of the earlier studies,[16-18] which suggested the formation of **only one** thermodynamically stable isomer. The formation of the thermodynamically unstable isomer suggests that the formation of the linkage isomers are controlled by kinetic reasons. Under conditions of kinetic control, it is observed, by Haim and coworkers[19] and Espenson and coworkers,[20] that the thermodynamically unstable isomers are formed initially and then they undergo spontaneous isomerization to the corresponding stable isomer. The unstable isomers are observed as transient intermediates with lifetimes ranging from seconds and minutes (respectively for $[(CN)_5CoONO]^{3-}$ and $[(H_2O)_5CrNC]^{2+}$ ions) to hours (for $[H_2O)_5CrSCN]^{2+}$ ion).[19]

(ii) A series of thiocyanate bridged oligomeric ruthenium ammine complexes has been reported by Agarwala and coworkers.[21] Though, at first the thiocyanate bridge in these ruthenium complexes was thought to be weak, it was later realized that it was not so. However, a quantification of these results as to the nature of the thiocyanate bridge is necessary to understand further, the nature of the bridge.

(iii) Thiocyanate ion has been recognized to be a good mediator in electron transfer reactions.[22] In fact, thiocyanate ion is one of the two ligands (azide and N- and S-bonded thiocyanates) which are favorites of the chemists for the study of the ligand effects on electron transfer reactions. Several important mechanistic features were first elucidated using these ligands.[19] Interestingly, thiocyanate ion participates in electron transfer reactions by both inner sphere and outer sphere mechanisms. Further, the electron transfer properties of the bridge in a inner sphere mechanism, in general, is directly related to its stability.

(iv) In the light of (ii) and (iii) it is envisaged that the thiocyanate bridged oligomeric and polymeric compounds might have certain parallel implications to Meyer's oxo-[7-9] and pyrazine[23] bridged oligomeric ruthenium-2,2'-bipyridine complexes, which are used as catalysts in multielectron transfer reactions such as "water-oxidation". In this context, synthesis

and characterization of heretofore unknown compounds could be important in their own right.

(v) Another important observation is the very little difference in the π-acidities of the N- and S- end coordination of the NCS$^-$ ion to transition metals.[24] Keeping in view the intrinsic chemical asymmetry of the thiocynate ion, this behaviour is surprising. However, the solution for this question becomes apparent if one takes into account the HOMO and LUMO[25,26] of the NCS$^-$ group for the ligand $\rightarrow$ M π-bonding and M $\rightarrow$ ligand π-backbonding in the [M-NCS] unit. The HOMO and LUMO orbitals of thiocyanate have been computed by several workers using semiempirical methods. Rabalais and coworkers[25] suggest that the LUMO ($3\pi *$) of NCS$^-$ ion has maximum contribution from the 2p orbitals of the central carbon atom ($>$ 92%) and the contributions from the orbitals of the end atoms are practically zero, i.e., the LUMO is effectively localized on the central carbon atom. However, the completely filled HOMO (2π) of the NCS$^-$ ion has totally opposite shape.[26] Here, the contributions from the end atoms are the maximum, while that of the carbon is practically nil. However, the participation of HOMO in the π-bonding (L $\rightarrow$ M) is considerably less effective compared to the participation of LUMO in the π-backbonding (M $\rightarrow$ L). Hence, the coordination of NCS$^-$ ion to metal centers should effectively disturb the π-electron density around carbon atom of the thiocyanate group which has been proved by ESCA measurements on a

series of tetra- and hexathiocyanato complexes of transition metals.[27]

It is, therefore, expected that the participation of LUMO of the NCS^- ion in the π-backbonding of a thiocyanate bridged dinuclear complex should lead to a near-symmetric situation rather than an asymmetric one. This, in turn, is important in the context of electron transfer properties of a bridge, as the redox asymmetry of $[M-L_b-M]$ unit is directly related to the rate of electron transfer across the bridge.[2d] Thus, a study of the thiocyanate bridged oligonuclear complexes in terms of electron transfer properties of the bridging ligand should be able to resolve the extent of participation of the HOMO and LUMO of the bridging ligand in the bridging properties. This, in turn, would enrich our knowledge about the mechanism of electron transfer, i.e., through space,[28,29] through bond[4,29] and/or "superexchange" pathway,[28,29] apart from giving a quantitative picture of the bridging properties of the chalcogenocyanates.

It was, thus, felt that in continuation to our earlier efforts, a study of the bridging properties of thiocyanate and selenocyanate ions between two metal centers may be worthwhile. The results of such a study form the basis for this thesis.

1.3 Electron Transfer in Complex vis-a-vis Simple Moieties

Over the last two decades, the guiding principle to work on electron transfer reactions has been the classical theory

developed by Marcus,[30] Hush[31] and others.[32] However, last decade saw a rapid growth of the non-classical aspects, i.e., electron and nuclear tunneling reactions.[33] These quantum mechanical phenomena are critical for understanding many details of the inorganic electron transfer and mainly the bio-inorganic electron transfer reactions.

Two approaches have generally been followed by investigators to unravel the mysteries of the ET reactions.[1a] The first approach involves the study of the electron transfer reactions in structurally complex metalloproteins and enzymes[2,3] with slight modifications and in their model compounds.[5] Considerably interesting results have been obtained by the study of the donor spacer-acceptor systems,[4] especially porphyrin-linker-quinone (PLQ) and carotenoid-porphyrin-quinone (CPQ) systems[34] which seem to mimic the photodriven vectorial charge transfer in photosynthetic pigments. Studies on the Ru-modified metalloproteins such as blue copper proteins[35] and cytochrome-c[2d] suggest unbelievably large rates for ET over surprisingly large distances, viz., 10-25 Å. The structural and **conformational** aspects of the polypeptide chains in metalloproteins and their role in electron mediation is one of the major questions being probed now.[36]

Though the results obtained using this approach is enormously important, the second approach has solved some of the fundamental questions about ET reactions. This approach[28,33a]

involves the design and synthesis of discrete donor-.acceptor complexes, especially oligomeric metal complexes with or without bridging units and studying ET in these complexes. The different possibilities these systems offer, are important. For example, one can vary the driving force for the ET reaction by varying the redox asymmetry of the metal centers,[37] or one can vary the distance between the donor and acceptor (both are metal centers in the case of the oligomeric transition metal complexes) to study the distance[2a] dependence on the rate of the electron transfer and etc.

An overview of the results of the electron transfer reactions, which has emerged by the second approach is given below. Needless to mention, the terms and symbols which are used throughout the thesis are also introduced.

1.4 Mixed Valency

Though mixed-valence complexes, e.g., prussian blue, have been recognized for the past two centuries[38] much importance has not been attached to it until late sixties. However, a reawakening of interest in this area occured during 1967, after the two important papers by Robin and Day[39] and Hush[40] appeared, followed by the deliberate synthesis of the prototype of the robust mixed-valence complexes, Creutz-Taube complex, $[(NH_3)_5Ru-Pyz-Ru(NH_3)_5]^{5+}$ ion (C-T ion).[4] It was then followed by the synthesis of a large number of discrete oligonuclear ligand

bridged mixed-valence compounds with a variety of bridging ligands.[28,37,38] The ET properties of these compounds were studied using the intervalence transfer absorption (IT), a photoinduced metal to metal charge transfer (MMCT).

1.5 Hush Model and Robin and Day Classification Scheme

In his brilliant paper[40a] Hush offered a theoretical bridge between the physical properties of mixed-valence complexes and the electron transfer chemistry in solution. The theory developed is as following. A binuclear molecular AB is considered in which Ap and Bq represent two metal centers in different oxidation states, p and q. For simplicity, it is assumed that p-q = 1. Then, a ground state wave function, ψ_a, can be written as (1)

$$\psi_a = \psi(Ap)\,\psi(Bq) \qquad \qquad .. (1)$$

One electron transfer from A to B produces an excited state, which can be written as (2)

$$\psi_b = \psi(Aq)\,\psi(Bp) \qquad \qquad .. (2)$$

If these functions have the same symmetry, they can be mixed by an off-diagonal matrix element $\langle \psi_a | H_{AB} | \psi_b \rangle$, say H_{AB}. The mixing of some excited state into the ground state to generate a

new ground state whose wave function could be written as (3)

$$\Psi_g = C_a\Psi_a + C_b\Psi_b \qquad \qquad .. (3)$$

In terms of MO-theory, when the overlap between Ψ_a and Ψ_b is negligible, i.e, $\langle \Psi_a | \Psi_b \rangle = 0$, the energy of the ground state with respect to the energy of the unmixed function Ψ_a becomes (4)

$$E_g = 0.5 [E_{ab} - (E_{ab}^2 + 4 H_{AB}^2)^{1/2}] \qquad \qquad .. (4)$$

The quantity, E_{ab} is the energy difference betwen the energies of unmixed functions Ψ_a and Ψ_b.

Zero overlap between Ψ_a and Ψ_b has been assumed for the sake of simplicity. However, in reality, if any interaction occurs between Ψ_a and Ψ_b, there must be non-zero overlap. Thus, this theory is adequate to deal with compounds having a small degree of interaction. When the mixing is large, appropriate values for overlap integral should be considered.

The coefficients in (3) are given by

$$C_b/C_a = E_g/H_{AB} = 0.5 [R-(R^2 + 4)^{1/2}] \qquad \qquad .. (5)$$

where $C_a^2 + C_b^2 = 1$ and $R = E_{ab}/H_{AB}$. In the case of zero-

interaction the ratio C_b^2/C_a^2 becomes zero and the oxidation states of metals are completely localized and in other cases the ratio is non-zero. Thus, the value of H_{AB} determines the degree of mixing between ψ_a and ψ_b. However, if $E_{ab} = 0$, then from (4)

$$E_g = -H_{AB}; \quad R = 0 \text{ and } C_a/C_b = 1 \qquad \ldots (6)$$

Under these conditions the ground state is a 50:50 mixture of ψ_a and ψ_b. Completely delocalized limit of oxidation states of the metal centers represented by $(p + q)/2$ is the result of this.

The energy of the excited state, relative to the unmixed ground state and the coefficients in (7) are given in (8)

$$\psi_e = C_a \psi_a + C_b \psi_b \qquad \ldots (7)$$

$$E_e = 0.5 \, [E_{ab} + (E_{ab}^2 + 4 \, H_{AB}^2)^{1/2}] \text{ and}$$

$$C_b/C_a = E_e/H_{AB} = 0.5 \, [R + (R^2 + 4)^{1/2}] \qquad \ldots (8)$$

The electronic transition between these two mixed states is termed as "intervalence transition" (IT) and represents a Franck-Condon hopping of an electron between the two metal centers. The energy of this IT transition (9) is given as E_{IT} (or E_{op}) = $E_e - E_g$;

$$[p,q] \rightleftharpoons [q,p]^* \qquad \ldots (9)$$

it may occur anywhere from very low energy in the near infrared to high energy in the ultraviolet region.

In a symmetric mixed-valence compound the IT transition occurs as shown in (10)

$$[X_5M^{II}-L_b-M^{III}X_5]^{n+} \dashrightarrow [X_5M^{III}-L_b-M^{II}X_5]^{n+}{}^* \qquad ..(10)$$
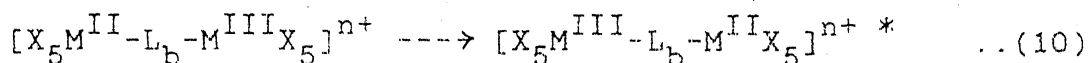
The situation is depicted in Fig. 1(a) in terms of the potential energy surfaces of the reactant and product. The free energy for net electron transfer is zero as the reactant and product are the same. As M-X distance and the solvation spheres around the two ions will be different, after the Franck-Condon transition, the M^{II} ion enjoys the M^{III} environment and the M^{III} ion enjoys the M^{II} environment (hence high energy state). There is, thus, activation energy for the optical electron transfer from the inner-sphere reorganization (E_{in}) and outer-sphere reorganization (solvent; E_{out}). E_{IT}, thus, is non-zero.

Robin and Day[39] proposed a classification scheme which presents a useful framework for handling these compounds. The α^2, which is termed as mixing coefficient or the delocalization factor and represented by (5) and (6) forms the basis for the classification. Totally localized systems were called class I, (α approaches zero). Totally delocalized systems were called class III ($\alpha = 0.5$) while intermediate systems ($\alpha < 0.25$;
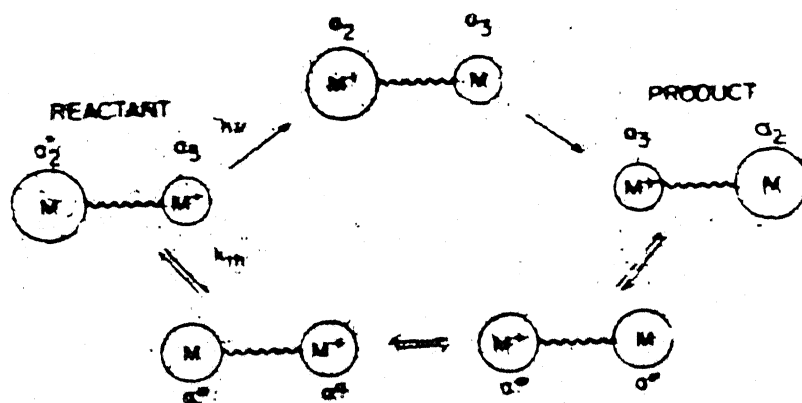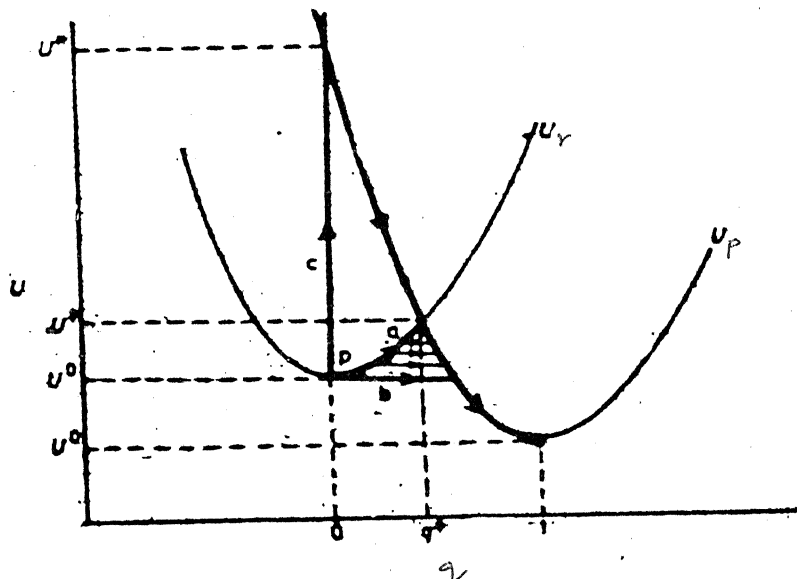
Fig.1 (a) Electron transfer reaction, $r \rightarrow p$ in terms of potential energy curves (a) thermal mechanism; (b) tunneling mechanism (c) vertical transition.

(b) Thermal and optical ET in a symmetrical binuclear mixed- valence compound.

localized with slight delocalization) were called class II. A sub-classification of class III called discrete compounds as class III-a, while infinitely delocalized solids were called as class III-b.

A number of useful relationships relating the IT transition with the fundamental properties of the systems are given below.[37] More detailed discussions on these relationships can be obtained from the original papers. As mentioned earlier, these relationships are applicable only to systems with a small mixing (α^2 is small), i.e., Robin and Day class II systems. To begin with, the Franck-Condon maximum of optical transition is related to the activation energy of the thermal transfer (Fig. 1(b).

$$E_{IT} = 4 \Delta G_{th}^{*} \qquad ..(11)$$

Further, for a symmetrical one electron transfer, i.e., as in equation (10), the absorption maximum and the FWHM, $\Delta \bar{\nu}_{1/2}$ of the IT band are interrelated. At the high temperature limit (300 K)

$$\Delta \bar{\nu}_{1/2} = [16 \, kT \, \ln \, (2) \, \bar{\nu}_{IT}]^{1/2} \qquad ..(12)$$

$$= [2310 . \bar{\nu}_{IT}]^{1/2} \qquad ..(13)$$

It is useful to compare the observed and calculated FWHM of the

IT band, since its agreement or the disagreement permits one to identify whether the complex is well behaved or not towards the Hush approach. Further, the $E_{op} = E_{IT}$ can be equated with the Franck-Condon term $E_{in}(= \lambda_{in})$ and the solvent term E_{out} $(= \lambda_{out})$.

$$E_{IT} = E_{in} + E_{out} = \quad = \lambda_{in} + \lambda_{out} \qquad ..(14)$$

E_{in} can be obtained from the metal-ligand vibrations around the metal centers. If n is the number of ligands per metal center

$$E_{in} = \lambda_i = \quad n \left(\frac{2 f_p f_q}{f_p + f_q} \right) (d_p^\circ - d_q^\circ) \qquad ..(15)$$

where f_p, d_p° = force constant and equilibrium bond length of the M-L bond when M is in +p oxidation state.

f_q, d_q° = force constant and equilibrium bond length of the M-L bond when M is in +q oxidation state.

Using a dielectric continuum model, Marcus developed an expression for the solvent reorganizational energy

$$E_{out} = \lambda_\circ = (\Delta e)^2 \left(\frac{1}{2a_p} + \frac{1}{2a_q} - \frac{1}{r_{pq}} \right) \left(\frac{1}{D_{op}} - \frac{1}{D_s} \right) \qquad ..(16)$$

where a_p and a_q are the radii of the +p and +q coordination r_{pq} is the distance separating these spheres and D_{op} and

D_s are the optical and static dielectric constants of the medium. The equation (16) suggests that the energy of a mixed-valence IT transition will be solvent dependent. If the IT transition energy, $\bar{\nu}_{IT}$, is plotted against $(\frac{1}{D_{op}} - \frac{1}{D_s})$, the slope provides a measure of E_{out} and the intercept, a measure of E_{in}. However, it should be noted that a class III system shows solvent independence because, both metal centers suffer the same degree of solvation.

The magnitude of H_{AB} is given by

$$H_{AB} = 2.05 \times 10^{-2} \, [\epsilon_{IT} \Delta\bar{\nu}_{IT}/(\bar{\nu}_{IT})]^{1/2} . \bar{\nu}_{IT}/r_{pq} \qquad ..(17)$$

Further, equation (1) can also be written as,

$$\psi_a = (1-\alpha^2)^{1/2}.A_p + \alpha B_q \qquad ..(18)$$

following a LCAO description. Ignoring the overlap integral $S_{ab} = \langle \psi_a | \psi_b \rangle$, the transition moment for the IT transition is given by

$$|M| = e\alpha(r_d - r_a) = e\alpha R \qquad ..(19)$$

where r_a and r_d are the position vectors of acceptor and donor units and R is the donor-acceptor distance. The transition

moment is related to the intensity via the dipole strength, D, the oscillator strenth, f is the molar intensity via:

$$|M| = e\, D^{1/2} \qquad\qquad ..(20)$$

$$f = 1.085 \times 10^{-5}\, \bar{\nu}_{IT}\, D \qquad\qquad ..(21)$$

$$f = 4.6 \times 10^{-9}\, \epsilon_{IT}\, \Delta\bar{\nu}_{1/2} \qquad\qquad ..(22)$$

From these equations one can write the delocalization factor, α^2, as,

$$\alpha^2 = 4.24 \times 10^{-4}\, [(\epsilon_{IT}.\Delta\bar{\nu}_{1/2})/(\bar{\nu}_{IT}.R^2)] \qquad\qquad ..(23)$$

where R is expressed in $\mathring{A}$ units. If α^2, thus calculated, falls below 0.0625 limit, then the compound falls in class II category.

For asymmetric systems for which an energy difference ΔE_o (cf. Fig. 1(a)) exists between the two sites, the following relationships hold good.

$$E_{op} = \lambda + \Delta E_o = 2(\lambda\Delta G_{th}^{*})^{1/2} \qquad\qquad ..(24)$$

$$\Delta G_{th}^{*} = \frac{(\lambda + \Delta E_o)^2}{4\lambda} \qquad\qquad ..(25)$$

$$E_{op} = [16\, kT\, \ln(2)]^{-1}\Delta\bar{\nu}_{1/2} + \Delta E_o \qquad\qquad ..(26)$$

Meyer and coworkers[42] suggested that the rate of electron transfer in a symmetrical complex ($\Delta E_o = 0$) can be obtained by (27) (subjected to a few assumptions),

$$k_{et} = (2\pi/h) \, H_{AB}^2 \, [\pi/(kT \, \overline{\nu}_{IT})]^{1/2} \, \exp \, (-\overline{\nu}_{IT}/4 \, kT) \qquad ..(27)$$

while for a asymmetric complex,

$$k_{et} = (2\pi/h) \, H_{AB}^2 \, [\pi/kT \, (\overline{\nu}_{IT} - \Delta E_o)]^{1/2}$$

$$\exp \, [-\overline{\nu}_{IT}^2/(\overline{\nu}_{IT} - \Delta E_o)/4 \, kT] \qquad ..(28)$$

The localized or delocalized piture of a particular electron transfer event is somewhat arbitrary in the light of the time scale of the physicochemical method used. For example, if an electron transfer event occurring 10^6 times per sec. is 'seen' by electronic spectral studies, (time scale $\sim 10^{-15}$ s) evolves a localized picture. If the rate of ET is faster, viz., 10^{15} times per sec., then electronic spectroscopy 'sees' a delocalized picture, but ESCA (time scale $\sim 10^{-17}$ s) would 'see' a localized picture (cf. Table I.1):

The Hush Model is fundamentally a classical model (high temperature limit) in which both the inner shell and outer shell reorganizational effects are treated.

Table I.1. Electron delocalization in Creutz-Taube complex as "seen" by various physicochemical methods

Experimental Technique	Assignment favored	Ref
UV-Vis spectroscopy	Localized	41
Near-IR, solvent dependence, $\Delta\bar{\nu}_{1/2}$	Delocalized	42, 52a
IR, Raman spectroscopy	Controversial	41, 55
Mössbauer spectroscopy at 4.2 K	Localized	56
ESCA	Controversial	57, 58
^{1}H NMR spectroscopy	Delocalized	59
EPR spectroscopy	Localized	60
Crystal structure	Delocalized	61
Single crystal EPR	Controversial	62
RR spectroscopy	Localized	55
Model calculations	Localized	64
	Borderline case	43

Several other treatments emphasizing the inner shell have appeared; among which the model proposed by Piepho, Krausz and Schatz (PKS) has received maximum attention.[43] In this vibronic coupling model, only symmetric inner shell modes of the couple were treated and the surrounding medium is neglected. The band

maximum, its intensity and shape are iteratively fitted to three parameters, ϵ, an electronic coupling parameter, λ, a vibronic coupling parameter and $\bar{\nu}$, the wave number of the totally symmetric metal ligand stretching vibration (usually fixed as 500 cm^{-1}).

Another treatment has been given by Bukhs.[44] In this model, both the low frequency solvent modes and high frequency inner shell modes have been taken into consideration. For high temperature limit and when $H_{AB} \ll E_{out}$ the Bukhs linewidth reduces to the Hush linewidth. Bukhs has provided model calculations of band shapes, assuming $E_{in} = 1000 \ cm^{-1}$ and $\nu_{M-L} = 500 \ cm^{-1}$, from which E_{out} and H_{AB} for both class II and III systems may be deduced. All these three analyses were applied to the C-T ion as well as several other systems. They are in excellent agreement as far as the delocalized complexes are concerned.[37] Thus "the model described by Bukhs has the virtue of completeness but is intrinsically rather unwieldy. That proposed by PKS is intuitively appealing, but neglects the medium which..... is the major source of the electron transfer barrier for many of the species treated.... Hush treatment remains the most powerful and tractable."

1.4 Stability of the Mixed-Valence Compounds

For the mixed-valence compounds[28a] we deal with of which the C-T ion is an example, the mixed-valence state (23) is always

stable with respect to the isovalent states [(22) + (33)]. The stability of the mixed valence species relative to the isovalent ones is reflected in the equilibrium quotient, K_c, for the comproportionation reaction (29).

$$(33) + (22) \quad \underset{K_c}{\rightleftharpoons} \quad 2 \ (23) \qquad \qquad ..(29)$$

and the stability of the mixed-valence state expressed as the free energy change is given by (30).

$$\Delta G^\circ = -(RT/2) \ \ln \ (K_c/4) \qquad \qquad ..(30)$$

The stability of the mixed valence state when in statistical equilibrium ($K_c = 4$) with respect to the isovalent states should be factored out and the rest of the stability represented by ΔG° in (30) is constituted by several factors (vide supra). However, the important experimental problem is concerning with the evaluation of the K_c values. This can be done using electrochemistry. If E_1° and E_2° represent the two potentials governing the sequential reduction (31):
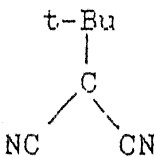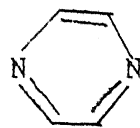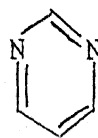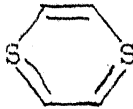
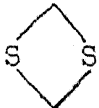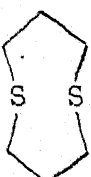$$(33) \xrightarrow{\ E_1^\circ\ } (32) \xrightarrow{\ E_2^\circ\ } (22) \qquad ..(31)$$

then

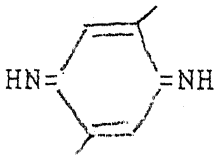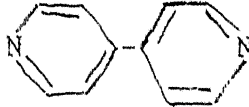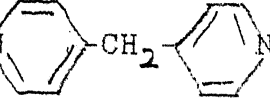$$\log K_c = 16.9 \ (E_1^\circ - E_2^\circ) \qquad \qquad ..(32)$$
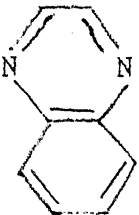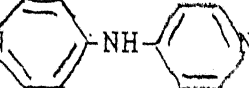
The difference $(E_1^O - E_2^O)$ can be determined accurately using cyclic voltammetric or differential pulse polarographic methods for large values, e.g. $(E_1^O - E_2^O) > 200$ mV. However, the situation is completely different when $K_c \longrightarrow 4$, i.e., statistical value. The separation between the signals of the two sequential steps is too small that they merge together to show a single process. Taube and coworkers[45] have used recently two different methods to evaluate ΔE_n values, especially for the cases where $\Delta E_n < 200$ mV. The K_c values obtained by them were by and large within a 10% error limit. The details of the methods can be found in the original papers. Effect of the bridging ligand structure on the values of K_c for $[(NH)_5Ru-L_b-Ru(NH_3)_5]^{5+}$ is illustrated in Table I.2. The stability of the mixed-valence species after allowance for statistical factors ($K_c = 4$) can be attributed to several factors, the relative contributions of which can not be ascertained quantitatively.[28a,37,45a,46b] These are as follows: (i) stabilization due to the delocalization of the optical electron, (ii) stabilization due to structural changes in going from isolvalent to mixed-valence moieties, (iii) stabilization due to purely electrostatic factors, (iv) variation in the magnetic interaction between two paramagnetic centers via a superexchange pathway could also affect the stability and (v) the inductive effect of the +3 charge discussed by Taube and coworkers[45a,46c]. Thus,

$$\Delta G^o_{tot} = \Delta G^o_{del} + \Delta G^o_{coul} + \Delta G^o_{struct} + \Delta G^o_{mag} + \Delta G^o_{induc} \qquad ..(33)$$

able   1.2:   Effect of Bridging Ligand Structure on Compro-
portionation Constant Values in $[(NH_3)_5 Ru\text{-}BL\text{-}Ru(NH_3)_5]^{5+}$ System.

Bridge	$\bar{\nu}_{IT}$ ϵ_{max} (kK) (M^{-1} cm^{-1})	K_c
$N \equiv N$	9.8 (1400)	$\sim 10^8$
$NC\text{—}CN$	7.0 (410)	10^{13}
t-Bu—C(—CN)(—NC)	8.5 (16000)	$> 10^{10}$
pyrazine	6.4 (5000)	10^6
pyrimidine	7.15 (41)	300
1,4-dithiine	10.3 (6)	~ 40
dithietane	8.2 (86)	890
dithiacyclodecane	8.3 (80)	< 10

Structure		
$\diagdown S \diagup \diagdown S \diagdown$ (methyl methylenedithioether)	10.8 (45)	125
(dibenzo diazepine ring)	5.9(4000)	4×10^{7}
HN= =NH	9.62(–) 7.14(670) 5.65(800)	10^{10}
(4,4'-bipyridine)	9.7(920)	20
—CH$_2$— N (benzylpyridine)	12.3(30)	7
—NH— N (phenylaminopyridine)	10.9(1010)	¨26

The contributions of all of these terms have been evaluated in the past.

1.5   Electron Deloalization in Mixed-Valence Compounds

The mixed-valence molecule is a moldel for the precursor complex of an intramolecular electron transfer reaction and the results of the studies on these could be directly utilized to the understanding of electron transfer processes in general. Large number of investigations, theoretical or experimental, have been devoted to the extent of electron delocalization between metal centers.[28a,37] The delocalization could be explained using the simplest of the known mixed-valence molecules, viz., H_2^+. Eventhough, H_2^+ gains large stabilization due to the electronic delocalization, it differs much from the mixed-valence molecules of our concern in the following ways: (i) there is direct orbital overlap in H_2^+; direct overlap of the metal ion orbitals is not possible as they are separated by large distances by bridging units and (ii) there is no charge trapping by the medium; H_2^+, which is stable only in the gaseous phase and is not stable compared to $[H_3O^+ + H]$ in aqueous solution. Especially, when molecular units of higher dimensions are considered, the medium has a key role to play.

The main concern of the investigators in recent past was to make a quantitative understanding of 'the extent of electron

delocalization in mixed-valence compounds.[28a] Another point that received the maximum attention was how to relate the extent of electron delocalization to the molecular and the electronic structures of the bridging units.[47] In fact, an unambiguous mechanism for the electron transfer via the bridging ligands is not available. Different pathways[28] such as, 'through-space', 'through-bond' and 'superexchange' or a compromise of all these to different degrees have been suggested and each one of these pathways have their evidences.[37]

1.6 Role of Bridging Ligands in Electron Mediation

The delocalization parameter α^2 is determined by E_{ab} and H_{AB} (cf. Eqns. (5) and (8)). E_{ab} is presumed to be related to the difference in the site potentials around the sites of different valencies and hence to the structure of the species. The other term, H_{AB}, in the light of the bridging ligands is considered in this section. The problem of the role played by the bridging ligands[48] has been addressed by Day and coworkers as early as 1974.[38] The following is the treatment given by Mayoh and Day.

Two metal centers A and B with orbitals χ_A and χ_B are separated by a bridging ligand BL with a HOMO and LUMO, ϕ_L and ϕ_L^*, respectively. Assuming non-degeneracy of the orbitals, the ground state configuration $\chi_A^1 \phi_L^2 \chi_B^2$ could be expressed in determinental form as

$$\Psi_o = \left| \chi_A \bar{\chi}_A \phi_L \bar{\phi}_L \chi_B \right| \qquad \qquad \cdots (34)$$

and the IT charge transfer configuration, $\chi_A^2 \phi_L^2 \chi_B^1$ has a wave function

$$\Psi_1 = \left| \chi_A \phi_L \bar{\phi}_L \chi_B \bar{\chi}_B \right| \qquad \cdots (35)$$

They can interact to generate new ground and excited states given by

$$\Psi_G = (1 - \alpha^2)^{1/2} \, \Psi_o + \alpha \Psi_1 \qquad \qquad \cdots (36)$$

$$\Psi_E = (1 - \beta^2)^{1/2} \, \Psi_o + \beta \Psi_1 \qquad \qquad \cdots (37)$$

As the IT bands have appreciable intensity, there has to be an interaction betwen χ_A and χ_B, eventhough they are far apart, viz. >5 Å. Hence 'local charge transfer states' can be invoked, in which electrons are transferred to and from the bridging ligand. Thus, the transitions, $\chi_A \dashrightarrow \phi_L^*$ and $\phi_L \dashrightarrow \chi_B$ with determinental wave functions,

$$\Psi_2 = \left| \chi_A \phi_L \bar{\phi}_L \phi_L^* \chi_B \right| \qquad \cdots (38)$$

$$\Psi_3 = \left| \chi_A \bar{\chi}_A \phi_L \chi_B \bar{\chi}_B \right| \qquad \cdots (39)$$

could mix with the ground- and excited-state wave functions.

Using a second-order perturbation treatment

$$\alpha = \sum_{i=2,3} \frac{\langle \psi_0 | H | \psi_i \rangle \langle \psi_1 | H | \psi_i \rangle}{(E_1 - E_0)(E_i - E_0)} \qquad \text{.. (40)}$$

$$\beta = \sum_{i=2,3} \frac{\langle \psi_0 | H | \psi_i \rangle \langle \psi_1 | H | \psi_i \rangle}{(E_1 - E_0)(E_i - E_0)} \qquad \text{.. (41)}$$

where $E_n = \langle \psi_n | H | \psi_n \rangle$ and thus one could calculate α or β, which is a measure of the electron delocalization, from these equations. Calculations of this kind yielded values of α^2 which is in good agreement with the observed intensity of the IT band.[37,38]
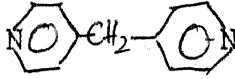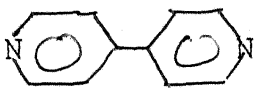
Recently, Ondrechen and coworkers[49] have developed a three site model, which explicitly involves the bridging ligand. This treatment, while assuming the coupling between the electronic states of the metal centers and that (π^* orbital) of the bridging ligand, omits the direct overlap of the orbitals of the metal centers. A Hamiltonian is presumed, using which the Schrödinger equation solved yields different conditions for class II and III systems in terms of J, the coupling integral between metal and bridging ligand. Though this model is undoubtedly an improvement over all the models discussed thusfar, it too is inadequate in explaining several of the experimental observations.[28a]

Despite the inadequacies of the theoretical models, there seem to evolve a few generalizations from the experimental approach in understanding the role of the bridging ligands in the

mediation of the optical electron. Most of these are based on the studies on Ru(II)/Ru(III) ammines with a variety of bridging ligands.[28a]

(i) The electronic interaction decreases exponentially with the increase in number of atoms in the bridging ligands.

(ii) Smaller bridging ligands with π- donor/acceptor capabilities generally mediate strong interaction, e,g. O^{2-} ion, N_2, $(CN)_2$ and etc. However, in the case of larger ligands such as, and etc., the extended configuration though facilitates interaction, is insufficient to couple the metal d-orbitals strongly.

(iii) Saturated σ-bonds between the coordinating sites of organic ligands couple the metal centers weakly, e.g., mediates a stronger interaction between metal orbitals than that of and interaction via is less than that via

(iv) For disubstituted aromatic bridging groups (e.g., dicyanobenzenes, diazabenzenes) the stronger electronic interaction occurs with <u>ortho-</u> and <u>para-</u> isomers.

Qualitative and quantitative explanations for the above generalizations have also been offered. Table I.3 summarizes

Table 1.3: Parameters obtained for some of the representative compounds.

No.	Ion	$\tilde{\nu}_{IT}$ (cm^{-1})	ϵ(max) (M^{-1}cm^{-1})	$\Delta\tilde{\nu}_{1/2(cal)}$ (cm^{-1})	$\Delta\tilde{\nu}_{1/2(exp)}$ (cm^{-1})	α^2	K_{com}	H_{AB} (cm^{-1})
1.	$[(NH_3)_5Ru\,pyz\,Ru(NH_3)_5]^{5+}$	6370	5000	3830	650	a	10^6	3150
2.	$[(CN)_5Fe\,pyz\,Fe(CN)_5]^{5-}$	8300	2200	4400	4800	10^{-2}	50	900
3.	$[(CN)_5Fe\,pyz\,Ru(NH_3)_5]$	6060	1550	3700	4300	9.8×10^{-3}	10^4	---
4.	$[(bpy)_2Ru\,pym\,Ru(bpy)_2]^{5+}$	5060	---	---	---	---	$10^{2.6}$	---
5.	$[(bpy)_2Ru\,pym\,Os(bpy)_2]^{5+}$	8080	330	4400	3400	2.4×10^{-3}	10^{10}	---
6.	$[(NH_3)_5Ru\,NCCN\,Ru(NH_3)_5]^{5+}$	7000	410	4000	1610	---	10^{13}	3550
7.	$[(CN)_5Fe\,CN\,Fe(CN)_5]^{6-}$	7700	32	4220	5100	---	---	---
8.	$[(CN)_5Fe\,CN\,Ru(NH_3)_5]$	10400		4900	4600	---	---	---
9.	$[(CN)_5Os\,NC\,Ru(NH_3)_5]$	12600	---	5400	6500	---	---	---
10.	$[(NH_3)_5Ru\,N\equiv N\,Ru(NH_3)_5]^{5+}$	9800	1400	4760	2600	a	$\sim10^8$	4920

a, the delocalization is maximum, i.e., 100 /

some of the results obtained for different mixed-valence systems.

1.7 Chalcogenocyanate Ions and Electron Transfer

Though several small molecules such as CN^- [27,50] and Cl^- [51] ions, N_2 [52] and $(CN)_2$ [53] moieties and O^{2-} [7-9,54] ions have been used as bridging ligands in mixed-valence compounds, thiocyanate ion and in general the chalcogenocyanate ions do not find a place in this list, despite its crusading role in solving many of the mechanistic problems of inorganic chemistry. [19]

The problem, thus, defined was approached with (i) the systematic synthesis of a few thiocyanate and selenocyanate bridged mixed-valence complexes with mainly $[(NH_3)_5Ru]^{n+}$, $[(CN)_5Fe]^{n-}$ and $[(bpy)_2Ru]^{n+}$ building blocks and (ii) physical characterization of these new compounds and the electron transfer studies on them using the intervalence transfer band (IT) and the Hush model.

SECTION II. EXPERIMENTAL DETAILS

2.1 Introduction

In this section the different experimental methods are discussed. Materials, solvents, synthetic methodologies for pentaammine-, pentacyano- and bis(bipyridine)ruthenium compounds and the details of the physicochemical methods used for characterization of these compounds are discussed.

2.2 Materials

2.2a. Chemicals

All the chemicals used were of chemically pure or analaR grade. $[(NH_3)_5RuN_2]Br_2$ and $[(NH_3)_5RuX]X_2$ ($X^- = Cl^-$ or Br^-) were prepared by the published procedures.[66] Sodium salt of the amminepentacyanoferrate(II) trihydrate was prepared by the standard procedure,[67] purified[68] and dried to constant weight over KOH, which absorbs alcohol but not ammonia.[69] A strong and sharp signal in the infrared spectrum at 1245 cm$^-$, due to the $\delta_s(NH_3)$, was used as a diagnostic for the presence of ammonia molecule in the compound.[70] The starting complexes for the synthesis of the chalcogenocyanate bridged Ru-2,2'-bipyridine complexes, viz., cis-$[(bpy)_2RuCl_2].2H_2O$,[71,72] $[(bpy)_2RuNOCl]-(PF_6)_2$[71,72] and $[(bpy)_2Ru(NO)(NO_2)](PF_6)_2$,[71] were prepared

using the methods described by Fergusson and cowork-
ers[72] and Meyer and coworkers.[71] These compounds were purified
as described in the literature.

Commercial grade sodium-, potassium- and ammonium
thiocyanate, potassium selenocyanate (Fluka AG), potassium
azide (AR grade), ammonium hexafluorophosphate (LR grade,
Janssen Chimica), sodium tetraphenylborate (Sisco), sodium
perchlorate (Riedel), tetraphenylphosphonium chloride (Aldrich)
and rubidium chloride (S.D. Chemicals) were procured and used as
such. Hexafluorophosphoric acid, 60 weight % solution in water
(Janssen Chimica) was used wherever mentioned. Ion exchange
resins Dowex 1-X8 (100-200 mesh) in the chloride form and Dowex
50W-X8 (200-400 mesh) in the H^+ form were procured from Bio-Rad.
Sephadex G-10 (40-120 μ), Sephadex G-25 (20-50 μ) and Sephadex
LH-20 resins for gel filtration and neutral alumina for
adsorption chromatography were obtained from Pharmacia
Fine Chemicals and S. D. Chemicals, respectively.
Tris(bipyridine)iron(III) hexafluorophosphate was prepared as
described earlier.[82] Ce(IV) perchlorate solution was prepared
from Ce(IV) hydroxide and 6M perchloric acid[76a] and analysed
spectrophotometrically. Cr(II) solutions in perchloric or
hydrochloric acid were generated by the reduction Cr(III)
solutions using zinc.

2.2b   Solvents

Doubly distilled water was used for the synthetic purposes and spectroscopic measurements were carried out using triply distilled water.   All the other organic solvents were dried by the standard procedures[73] and distilled before use.

2.3   Physicochemical Methods

2.3a   Chromatography

Chromatographic separation was used as the primary purification procedure.   Gel filtration, using the difference in the molecular weights of the compounds, in aqueous medium was carried out on Sephadex G-10 or Sephadex G-25 column (50x1.5 cm).   Sephadex LH-20 resin with appropriate organic solvents was used for the purification of the compounds, which are soluble in organic solvents.   The column preparation[74] was carried out as follows: An approximately weighed amount of the appropriate resin was allowed to swell overnight in appropriate solvent.   The swollen resin is transferred to the column (50x1.5 cm), which was washed well with the solvent.

The ion exhange columns were **regenerated** using dilute hydrochloric acid or 1M sodium hydroxide solution.   After **regeneration** the column was washed extensively with water for the absence of the acid or base.

Adsorption chromatography using neutral alumina[73] was used for the purification of the ruthenium bipyridine complexes. The column dimension was 50x3 cm.

2.3b Microanalysis

Carbon, hydrogen and nitrogen present in the samples were analysed by the Microanalytical Section, I.I.T., Kanpur. Halogen and sulfur present in the samples were analysed as silver halide and barium sulfate, respectively after decomposing the known amount of the sample using 1:8 mixture of sodium nitrate and sodium hydroxide.[75] Selenium was estimated by oxidizing to selenate, followed by reducing it to selenite by boiling with concentrated hydrochloric acid and finally to selenium powder by hydroxylammonium chloride.[76]

2.3c Vibrational Spectroscopy

Infrared spectra were obtained by using Perkin-Elmer Model-580 or Model-1320 spectrophotometer. Samples were prepared as potassium bromide pellets. Spectra for some of the compounds having pentacyanoferrate moiety were recorded in a nujol mull. Vibrational spectra in the region 600-200 cm^{-1} were obtained using cesium iodide pellets. The resonance Raman spectra were obtained using the Spex spectrometer described earlier.[77] Samples were taken in 1 mm i.d. capillary tubes.

The scattered radiation observed at right angles was dispersed in a Spex 1403 double monochromator equipped with a cooled photomultiplier tube (C-31034) and a Spex digital photon counting system, DPC-2. Slitwidths used were in the range of 3-10 cm^{-1}. The relative intensities of the vibrational bands were obtained by comparing the intensities of the bands with that of the ν(CN) band of the acetonitrile solvent at 2249 cm^{-1}.[78]

2.3d Electronic Absorption and Emission Spectra

Absorption spectra in the UV-vis region were recorded using Shimadzu Model UV-190 double beam spectrophotometer. Near infrared region of the spectra were probed using Cary Model-17D or Hitachi Model MU-3400 spectrophotometer. Sample solution and reference solvent were taken in 1 cm matched quartz cells. The extinction coefficients were calculated by recording the absorbance for atleast two different cocentrations of the solution.

The emission spectra for the $[(NH_3)_5RuNCS]^{2+}$, $[(NH_3)_5RuSCN]^{2+}$ ions and the 2,2'-bipyridine ruthenium complexes were recorded, at the first instance, on an indegenously assembled scanning spectrofluorimeter described earlier by Dogra and coworkers.[79] The excitation of the bipyridine-ruthenium complexes using 150 W Xe-Hg lamp at different wave lengths (those overlap with the MLCTs of the compounds) and detection using IP-28 photomultiplier tube did not yield any emission

signal. Thus, the sensitivity of this instrument was taken as the upper limit of ϕ_{em} for the emission, present, if any. However, excitation using Ar^+ ion laser lines (Spectraphysics 165-09) and detection using a cooled PMT (C-31034) of the Spex spectrometer,[77] described earlier, yielded the emission maxima. The values for the quantum yields of the emission could not be evaluated accurately by this technique also, as the samples underwent local burning due to the high power exciting laser.

2.3e Mössbauer Studies

Mössbauer spectra of the iron compounds were obtained using a constant acceleration drive with 15 mCi ^{57}Co source obtained from New England Nuclear Co. The data were stored in a Canberra S-80 multichannel analyser. The experimental spectra were least squares fitted for Lorentzian line shapes using a computer program, MOSFIT, described elsewhere.[80] The spectrometer was calibrated using natural iron.

2.3f Magnetic Measurements

Magnetic moments at room temperature were obtained using a Guoy balance. $Hg[Co(NCS)_4]$ was used as the reference.

2.3g Nuclear Magnetic Resonance Spectral Measurements

^{1}H nmr spectra in DMSO-d$_6$ were recorded using Bruker WP-80 instrument. Trials to observe the ^{13}C resonances for thiocyanate and selenocyanate groups using Bruker WM-400 instrument(^{13}C at 100 MHz) failed due to insufficient solubility of these compounds in solvents such as D$_2$O, DMSO-d$_6$ etc.

2.3h Electrochemical Measurements

The redox potentials of the compounds were determined by cyclic voltammetry. The CV measurements were performed using a three electrode potentiostatic circuit and a MPI Model MP-1042 Voltammetry Controller and Plotamatic MF 715 X-Y recorder. A Beckman Pt-electrode, a Pt-wire counter electrode and saturated calomel electrode constitute the three electrode assembly. Potassium nitrate was used as the supporting electrolyte for measurements in aqueous solution while, tetrabutylammonium perchlorate or tetrafluoborate was used as the supporting electrolyte in non-aqueous medium. Junction potentials were eliminated[34b] by using a salt-bridge constituting the same concentration of the base electrolyte as that of the bulk solution and it was positioned between the bulk test solution and the reference electrode. All the potentials are referenced to SCE.

2.4 Synthesis of Compounds with Pentaammineruthenium(II/III) Units

2.4a $[(NH_3)_5RuSCN]X_2$ and $[(NH_3)_5RuNCS]X_2$ ($X^- = Br^-$, I^- and ClO_4^-

A typical reaction is carried out as follows: An aqueous solution (5-10 mL) of approximately 10 times the stoichiometric excess of ammonium thiocyanate was added to an aqueous solution (15-20 mL) of $[(NH_3)_5RuX]X_2$ (X = Cl^- or Br^-) (0.2 g) maintained at 70-75°C. The solution was stirred until the color of the reaction mixture turned bright red (1-2 h). The resulting solution was cooled to room temperature and filtered into a saturated aqueous solution of the corresponding anion (potassium iodide, sodium perchlorate or sodium bromide). The reddish violet precipitate was filtered and washed several times with ethanol and with ether.

The saturated aqueous solution of this crude product was sorbed on to a column of anion exchanger in Cl^- form (20x2 cm). It was eluted with water. The cationic portion thus collected with the effluent was transferred on to a column of Sephadex G-10 (50x1.5 cm). The compounds were eluted with a very dilute (10^{-5} M) aqueous solution of sodium bromide or potassium iodide. With a very slow elution rate ($\sim$ 5 mL per h) clear separation of three bands was observed. The bands were eluted separately and the effluents were concentrated at room temperature. A saturated solution of the anion was added to the first, second

and third band concentrates to precipitate $[(NH_3)_5RuSCN]X_2$, $[(NH_3)_5RuNCS]X_2$ and $[(NH_3)_4Ru(NCS)_2]X$, respectively.

The same reaction, when carried out at lower or higher temperatures,[14,15] is known to give oligomeric and polymeric products, respectively.

Anal. for $[(NH_3)_5RuSCN]Br_2$ (red):

Calcd. C, 2.97; H, 3.71; N, 21.04; Br, 39.60.

Obsd. C, 3.15; H, 4.09; N, 20.85; Br, 40.00.

$[(NH_3)_5RuSCN]I_2$ (red violet):

Calcd. C, 2.41; H, 3.01; N, 16.87; I, 51.00.

Obsd. C, 2.35; H, 2.85; N, 17.07; I, 50.55.

$[(NH_3)_5RuNCS]Br_2$ (red):

Calcd. C, 2.97; H, 3.71; N, 21.04; Br, 39.60.

Obsd. C, 2.95; H, 4.15; N, 21.44; Br, 39.30.

$[(NH_3)_5RuNCS]I_2$ (red violet):

Calcd. C, 2.41; H, 3.01; N, 16.87; I, 51.00.

Obsd. C, 2.22; H, 3.43; N, 17.20; I, 51.43.

2.4b $[(NH_3)_5RuNCSRu(NH_3)_5]X_5$ ($X^- = Br^-$, I^- and ClO_4^-)

An aqueous solution of 1:1 stoichiometric mixture of $[(NH_3)_5RuSCN]Br_2$ (0.202 g) and $[(NH_3)_5RuCl]Cl_2$ (0.146 g) was

stirred with 2% Zn-Hg amalgam and 10^{-5} M hydrochloric acid under dinitrogen atmosphere. The solution was filtered from the amalgam when it turned light yellow. Air was bubbled into the solution, the color of which immediately changed to bright red. A saturated aqueous solution of the anion (potassium iodide, sodium bromide or sodium perchlorate) was added to precipitate the crude product of the dimer. The deep pink colored crude product, when passed through Sephadex G-10 column (50x1.5 cm) yielded a single band. The effluent of this band was concentrated at room temperature and the pure dimeric compound was precipitated by adding the appropriate anion. The compound was washed with ethanol and ether.

Anal. for $[(NH_3)_5RuNCSRu(NH_3)_5]I_5$ (deep pink):

        Calcd. C, 1.13; H, 2.82; N, 14.46; S, 3.00; I. 59.62.

        Obsd. C, 2.05; H, 3.23; N, 14.70; S, 2.85; I, 60.08.

2.4c $[(NH_3)_5RuNCSRu(NH_3)_5]X_4$ ($X^- = Br^-$ or ClO_4^-)

Aqueous solutions of stoichiometric (1:1) amounts of $[(NH_3)_5RuN_2]Br_2$ (0.187 g) and $[(NH_3)_5RuSCN]Br_2$ (0.202 g) in 15 mL each were mixed. The resulting solution was stirred for about 14-15 h at room temperature ($\sim37^\circ$C), whereby the color of the solution turned from red to reddish yellow. It was filtered and excess of the anion (sodium bromide or sodium perchlorate) was added to the filtrate. The precipitated reddish

brown compound was filtered, washed with ethanol and ether.

Anal. for $[(NH_3)_5RuNCSRu(NH_3)_5]Br_4$:

        Calcd. C, 1.60; H, 4.00; N, 20.53; Br, 42.66; S, 4.27.

        Obsd. C, 1.79; H, 4.44; N, 20.20; Br, 42.65; S, 4.65.


2.4d $[(NH_3)_5RuSeCN]X_2 \cdot 2H_2O$ and $[(NH_3)_5RuNCSe]X_2 \cdot 2H_2O$ ($X^- = I^-$, ClO_4^-, Cl^- or Br^-)

These compounds were prepared by a procedure similar to that described in 2.4a. The following points should also be taken into account while preparing the complexes: (i) potassium selenocyanate was used instead of ammonium thiocyanate; (ii) the reaction mixture was stirred at 55-60°C for 10 min whereby a deep blue solution resulted along with a little Se powder, which was filtered off; (iii) stirring for longer periods deposited Se powder in large amounts; (iv) the solutions were preserved at 0°C, if necessary; (v) the reactions and workup procedures were carried out in a acid free atmosphere as the $SeCN^-$ is decomposed to deposit Se powder; (vi) the first band from the sephadex column yielded the Se-bonded isomer while the closely following second band yielded the N-bonded isomer.
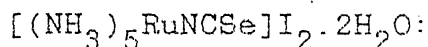
Anal. for $[(NH_3)_5RuSeCN]I_2 \cdot 2H_2O$:

        Calcd. C, 2.06; H, 3.27; N, 14.45; I, 43.72; Se, 13.60.

        Obsd. C, 1.93; H, 2.95; N, 13.95; I, 43.44; Se, 13.55.

$[(NH_3)_5RuSeCN](ClO_4)_2 \cdot 2H_2O$:
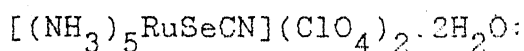
    Calcd. C, 2.30; H, 4.12; N, 16.00; Se, 15.11.

    Obsd. C, 2.26; H, 4.10; N, 16.10; Se, 14.75.

$[(NH_3)_5RuNCSe]I_2 \cdot 2H_2O$:

    Calcd. C, 2.06; H, 3.27; N, 14.45; I, 43.72; Se, 13.60.

    Obsd. C, 1.87; H, 2.84; N, 13.80; I, 43.74; Se, 13.41.

$[(NH_3)_5RuNCSe](ClO_4)_2 \cdot 2H_2O$:
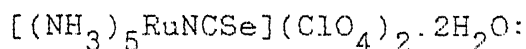
    Calcd. C, 2.30; H, 3.62; N, 16.00; Se, 15.11.

    Obsd. C, 2.59; H, 4.19; N, 15.85; Se, 14.86.

2.5 Synthesis of Compounds with Pentacyanoferrate(II/III) Units

2.5a $[(CN)_5FeNCS]^{3-}$ Ion

The compound was prepared using the procedure reported by Gray and coworkers.[17] Tetra n-butylammonium and tetraphenylphosphonium salts of the compound were prepared. These compounds could not be analysed satisfactorily. However, the infrared spectra exhibited the bands corresponding to the cations and anion.

2.5b $[(CN)_5FeNCSe]^{3-}$ Ion

It was prepared using the procedure reported by Gray and coworkers,[17] with slight modifications. $Na_3[Fe(CN)_5(NH_3)] \cdot 3H_2O$

(0.47 g), PPh_4Cl (1.3 g) and KSeCN (0.24 g) were stirred for 4-5 h in 50 mL of 3:1 acetone and water mixture. The resulting solution was concentrated at reduced prssure at room temperature. The resulting residue was recrystallized from acetone/ether to produce blue violet microcrystalline product. This when passed through Sephadex LH-20 resin yielded a single band.

Anal. for $(PPh_4)_3[(CN)_5FeNCSe]$:

Calcd. C, 71.56; H, 4.59; N, 6.42; Se, 6.04.

Obsd. C, 71.90; H, 5.05; N, 5.98; Se, 6.45.

2.5c $[(CN)_5FeNCXFe(CN)_5]^{5-}$ Ions (X = S or Se)

A typical reaction to prepare the binuclear complexes was carried out as follows: Air was stirred into the solution of sodium amminepentacyanoferrate(II) trihydrate (ca. 2 mmol) in 15 mL of water for 15-20 min followed by the addition of 5 mL aqueous solution of sodium thiocyanate or potassium selenocyanate (ca. 1 mmol). The color of the solution immediately changed to green. Air was bubbled overnight through the reslting mixture effecting the intensification of the green color. The stirring of the solution was continued until dark yellow or red brown components of the solution disappeared. The solution was filtered through a fine porosity sintered crucible and was sorbed on to a column of Sephadex G-10 (40x2 cm). The

compounds were eluted with water. With a slow enough elution rate (0.5 mL per min), clear separation of two bands was noticed. The large greenish yellow first band and the blue second band (in smaller amounts) were eluted separately and concentrated at room temperature. At higher temperatures, the compounds decomposed to give a dark blue, insoluble polymeric product. Excess methanol and acetone mixture (4:1, v/v) was added to the concentrates with stirring. The precipitated $Na_5[(CN)_5FeNCSFe(CN)_5].xH_2O$ and $Na_3[(CN)_5FeNCS].xH_2O$ or the corresponding sodium and potassium salts of the selenocyanate analogs, respectively, from the first and second bands were filtered. They were washed extensively with methanol and acetone and dried over calcium chloride. Yields: 60 and 10-15%, respectively, from the first and second bands for the thiocyanate case and 70-80 and 5-10%, respectively, from the first and second bands for the selenocyanate case.

The acid salts of the compounds $[(NC)_5FeNCXFe(CN)_5]^{5-}$ (X = S or Se) were prepared by passing the respective solutions through the cation exchanger in hydrogen cycle. The deep blue colored acid salt was eluted with water and was neutralized with the appropriate base to pH 7 and on removing the solvent water at low pressure, yielded the salts of the corresponding cations. Thus, neutralization with sodium carbonate, potassium carbonate, tetraethylammonium hydroxide and tetrabutylammonium hydroxide yielded the corresponding sodium, potassium, tetraethylammonium and tetrabutylammonium salts, respectively.

These salts were washed extensively with acetone and dried under vacuum over calcium chloride.

Tetraphenylphosphonium and rubidium salts of the dimeric anions were also prepared. An excess of PPh_4Cl in 20 mL of 1:2 (v/v) water to ethanol was added to an aqueous solution of the sodium salt of the dimer. Slow evaporation over a period of a few days yielded green microcrystalline tetraphenylphosphonium salt of the dimeric compounds. The procedure to prepare the rubidium salt was the same as that given for the PPh_4^+ salt, except that an aqueous solution of RbCl was used in the place of PPh_4Cl. The compounds were washed with acetone and ether and dried over calcium chloride. More of the rubidium salt can be precipitated from the mother liquor by adding excess of methanol and ether mixture with stirring.

Anal. for $(PPh_4)_5[(CN)_5FeNCSFe(CN)_5] \cdot 8H_2O$

      Calcd. C, 69.28; H, 5.11; N, 6.79; S, 1.41; Fe, 4.94.

      Obsd. C, 69.48; H, 5.16; N, 6.06; S, 2.01; Fe, 4.55.

$(PPh_4)_5[(CN)_5FeNCSeFe(CN)_5] \cdot 6H_2O$
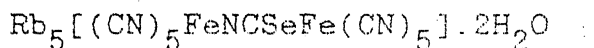
      Calcd. C, 68.95; H, 4.91; N, 6.75; Se, 3.47; Fe, 4.91.

      Obsd. C, 69.10; H, 5.11; N, 6.56; Se, 3.45; Fe, 4.80.

$Rb_5[(CN)_5FeNCSFe(CN)_5] \cdot H_2O$

      Calcd. C, 15.06; H, 0.22; N, 17.58; S, 3.65; Fe, 12.79.

      Obsd. C, 15.04; H, 1.71; N, 17.50; S, 3.60; Fe, 12.45.

$Rb_5[(CN)_5FeNCSeFe(CN)_5] \cdot 2H_2O$

    Calcd. C, 14.03; H, 0.43 N, 16.37; Se, 8.39; Fe, 11.90.

    Obsd.   C, 13.68; H, 1.84; N, 16.41; Se, 8.01; Fe, 11.55.

2.5d $[(NC)_5FeNCXFe(CN)_5]^{7-}$ ions (X = S or Se)

Sodium amminepentacyanoferrate(II) trihydrate (ca. 2 mmol) and sodium thiocyanate or potassium selenocyanate (ca. 1 mmol) were mixed simultaneously in degassed water under dinitrogen atmosphere. The solution was stirred for about 10 h. The resulting pale yellow solution was filtered into an excess of methanol and acetone mixture (4:1, v/v). A bright yellow precipitate obtained, was filtered, washed extensively with acetone and dried under vacuum. The compound when passed through Sephadex G-10 column showed a large yellow band and a small brown band, which was discarded. The yellow compound had a tendency to deliquesce in the atmosphere and probably underwent oxidation to yield a mixture of the mixed-valence (23) and the oxidized (33) products. Satisfactory microanalysis of the compound could not be obtained.

2.5e $[(NC)_5FeNCXFe(CN)_5]^{6-}$ Ion (X = S or Se)

These species were generated in situ by the reduction of $[(NC)_5FeNCXFe(CN)_5]^{5-}$ (X = S or Se) species using stoichiometric amounts of $K_4[Fe(CN)_6]$, hydroquinone or aqueous Cr^{2+} solution. Considerable amounts of solid compounds were also isolated using

Sephadex gel filtation from a solution containing 1:1 stoichiometric mixture of $Na_5[(NC)_5FeNCXFe(CN)_5]$ and the product of the reaction carried out by the procedure 2.4d. The aqueous solution of the mixture was sorbed on to a column of Sephadex G-25 and with a slow enough elution rate 5-10 mL per h using water as the eluent, three bands were seen. The middle one when added to an excess of methanol and acetone mixture (4:1, v/v) yielded the desired products. This was washed with acetone and dried under vacuum. A rubidium salt was also prepared (cf. 2.5c).

Anal. for $Rb_6[(CN)_5FeNCSFe(CN)_5].5H_2O$

          Calcd. C, 12.78; H, 0.97; N, 14.91.

          Obsd. C, 12.36; H, 1.84; N, 14.95.

  $Rb_6[(CN)_5FeNCSeFe(CN)_5].4H_2O$

          Calcd. C, 12.43; H, 0.75; N, 14.50.

          Obsd. C, 12.25; H, 1.69; N, 14.21.

All the compounds having pentacyanoferrate (II/III) units have a tendency to absorb moisture extensively from the atmosphere. Hence, they were generally stored over calcium chloride in a vacuum desiccator.

2.6 Synthesis of Compounds with Bis(bipyridine)ruthenium(II/III) Units

2.6a [Cl(bpy)$_2$Ru(NCS)]

The compound was prepared by two different procedures: (i) The complex $[(bpy)_2Ru(NO)Cl](PF_6)_2$ (0.202 g) was dissolved

in acetone (20-25 mL) and protected from light. An equimolar amount of KN_3 (0.021 g) dissolved in methanol was added dropwise with stirring, producing the purple solvenato complex, $[(bpy)_2Ru(acetone)Cl]^+$ [81]. A saturated methanolic solution of potassium thiocyanate was added to this and the resulting solution was stirred for an hour. The solution was then filtered into an excess of diethyl ether with stirring and the precipitated crude product was filtered and washed extensively with water to remove the unreacted potassium thiocyanate and then with ether. Recrystallization from CH_2Cl_2-ether yielded a dark purple product (yield: 70-80%). It was further purified by gel filtration through Sephadex LH-20 resin as follows. A concentrated solution of the recrystallized product in 5-10 mL acetonitrile was sorbed on to the column top (50x1.5 cm). slowest possible elution (0.5 mL per min) with acetonitrile: CH_2Cl_2 (1:1, v/v) resolved two bands on the column. Based on the retention times, the compound from the major second band was to be the desired monomeric product. This was separated out by precipitation using excess of diethyl ether from the effluent; yield: 60%.

(ii) A suspension of cis-$[(bpy)_2RuCl_2].2H_2O$ (0.1 g) in 15-20 mL of water was refluxed with vigorous stirring for 20-25 min. The resulting red brown $[(bpy)_2Ru(H_2O)Cl]^+$ solution was filtered through a fine porosity glass frit and cooled to room temperature. An aqueous solution (5-10 mL) of potassium thiocyanate (~0.5 g) was added with stirring. A dark colored

crude product which was immediately precipitated was filtered and washed well with water. This was purified as described in 2.6a(i) by gel filtration through Sephadex LH-20 column. The band moved in major amount was eluted with acetonitrile: CH_2Cl_2 or acetonitrile: benzene mixture (1:1, v/v). The compound was precipitated from the concentrated effluent by adding excess of diethyl ether. Yield: 75-85%. Another small band moved through the column was identified to be $[(bpy)_2Ru(SCN)Cl]$ based on the position and integrated intensity of the $\nu(CN)$ band in the vibrational spectrum.

Anal. for $[(bpy)_2Ru(NCS)Cl].2H_2O$

       Calcd. C, 46.41; H, 3.68; N, 12.89; Cl, 6.63; S, 5.89.

       Obsd. C, 46.73; H, 3.74; N, 12.53; Cl, 6.60; S, 5.23.

2.6b $[(bpy)_2Ru(NCSe)Cl]$

The compound has been prepared by the procedures described in 2.6a. Potassium selenocyanate was used instead of potassium thiocyanate, yield: ~75%. The small amount of the compound that was obtained by effective gel filtration on Sephadex LH-20 was identified to be the corresponding Se-bonded isomer, $[(bpy)_2Ru(SeCN)Cl].xH_2O$, based on the position and integrated intensity of the $\nu(CN)$ band of the Se bonded selenocyanate group.

Anal.for [(bpy)$_2$Ru(NCSe)Cl].2H$_2$O

        Calcd. C, 42.71; H, 3.39; N, 11.86.

        Calcd. C, 42.86; H, 3.26; N, 12.11.

2.6c [(bpy)$_2$Ru(NCS)$_2$]

The compound was prepared by the method described by Fergusson and coworkers. Excess of potassium thiocyanate (~1.0 g) with cis-[(bpy)$_2$RuCl$_2$].2H$_2$O (0.2 g) in 20 mL of ethanol and water mixture (1:1, v/v) was refluxed for 2 h. Deep purple crystals deposited after cooling were filtered and washed extensively with water. The dried crude product was recrystallized from CH$_2$Cl$_2$-diethyl ether mixture. Further purifification was carried out by gel filtration through Sephadex LH-20 column.

2.6d [(bpy)$_2$Ru(NCSe)$_2$].2H$_2$O

The compound was synthesized by a procedure analogous to that described in 2.6c. However, unlike in the thiocyanate case, a 5-10 fold molar excess of potassium selenocyanate was added. The crude product was washed with water to remove the unreacted potassium selenocyanate. Further purification was carried out on a Sephadex LH-20 column (50x1.5 cm). The major amount of the compound was eluted in a single band using acetonitrile: CH$_2$Cl$_2$ (1:3, v/v) mixture as eluent. The complex

was separated from the concentrated eluate by adding excess of diethyl ether with stirring; yield: 70-80%.

Anal.for $[(bpy)_2Ru(NCSe)_2] \cdot 2H_2O$

Calcd. C, 40.06; H, 3.03; N, 12.75.

Obsd. C, 40.38; H, 3.81; N, 12.65.

2.6e $[(bpy)_2Ru(NCS)Cl]X$ ($X^- = PF_6^-$ or BPh_4^-)

Oxidation of the corresponding Ru(II) compound was carried out using Ce(IV) perchlorate solution. A stoichiometrically equimolar solution of Ce(IV) was added with stirring to a solution of $[(bpy)_2Ru(NCS)Cl]$ in acetone, kept in dark. The stirring was continued for an hour. Excess of the anion (sodium tetraphenylborate or ammonium hexafluorophosphate) was added to this and the solution was filtered into a large volume of diethyl ether with stirring. The flocculant purple brown to dark brown colored precipitate was filtered and washed extensively with water and then with ether. The compound was recrystallized with acetone/diethyl ether; yield: 85-90%. The compound purity was further checked by passing it through Sephadex LH-20 column, where it showed a single band.

Anal. for $[(bpy)_2Ru(NCS)Cl]BPh_4$

Calcd. C, 65.37; H, 4.36; N, 8.47.

Obsd. C, 65.07; H, 4.05; N, 8.87.

2.6f [(bpy)$_2$Ru(NCSe)X]Y (X$^-$ = Cl$^-$ or SeCN$^-$; Y$^-$ = PF$_6^-$ or BPh$_4^-$)

These compounds were synthesized and purified exactly as described in 2.6e. The dark purpole colored [(bpy)$_2$Ru(NCSe)Cl]Y and red orange colored [(bpy)$_2$Ru(NCSe)$_2$]Y showed satisfactory microanalytical results.

Anal. for [(bpy)$_2$Ru(NCSe)Cl]BPh$_4$:

Calcd. C, 61.86; H, 4.12; N, 8.02.

Obsd. C, 61.50; H, 3.84; N, 7.95.

[(bpy)$_2$Ru(NCSe)$_2$]BPh$_4$:

Calcd. C, 58.60; H, 3.82; N, 8.92.

Obsd. C, 58.22; H, 4.03; N, 8.66.

2.6g [Cl(bpy)$_2$RuNCSRu(bpy)$_2$Cl]X (X$^-$ = BPh$_4^-$, ClO$_4^-$ or PF$_6^-$)

An aqueous solution of [(bpy)$_2$Ru(H$_2$O)Cl]$^+$ was prepared from cis-[(bpy)$_2$RuCl$_2$].2H$_2$O as described in 2.6a(ii). To this, a stoichiometrically equimolar amount of [(bpy)$_2$Ru(NCS)Cl].2H$_2$O (0.1 g) in 15-20 mL of ethanol was added. The resulting mixture was deaerated by bubbling dinitrogen gas (10-15 min) and the solution was refluxed for 2.5 h with a continual stream of dinitrogen over the mixture. The solution was filtered into an aqueous solution of sodium tetraphenylborate, sodium perchlorate or ammonium hexafluorophosphate. The fluocculant red brown

precipitate was filtered, washed with water and dried; yield: 90-95%. Chromatographic purification of the complex was carried out using alumina column (50x3 cm). A concentrated solution of the crude product in acetonitrile was charged on to the column. The elution was carried out using acetonitrile: CH_2Cl_2 or acetonitrile:benzene mixture (1:9, v/v) and slowly enriching acetonitrile in the mixture to 2:3, v/v proportion. The major portion of the compound moved as a single band which was eluted and precipitated using excess of diethyl ether: yield: 80-85%. Minor amount of the monomeric impurities were discarded.

The same compound was also prepared by refluxing 2:1 stoichiometric mixture of cis-$[(bpy)_2RuCl_2]$.$2H_2O$ and potassium thiocyanate in ethanol for 60-72 h. The crude product was purified by adsorption chromatography on alumina column as described in the preceeding paragraph.

Anal. for $[Cl(bpy)_2RuNCSRu(bpy)_2Cl]BPh_4$:

Calcd. C, 61.17; H, 4.09; N, 9.88.

Obsd. C, 61.83; H, 4.00; N, 10.21.

2.6h $[Cl(bpy)_2RuNCSRu(bpy)_2Cl](BPh_4)_3$

An acetone solution (10-15 mL) of $[Cl(bpy)_2RuNCSRu(bpy)_2Cl]BPh_4$ (100 mg) was protected from light. A solution containing a little more than stoichiometrically two equivalents of Ce(IV) was added with stirring and the stirring was continued

for an hour.   To the resulting solution excess of solid sodium
tetraphenylborate was added.   The solution was then filtered
into excess of diethyl ether with stirring whereupon a red
orange precipitate was formed in quantitative yield.   It was
filtered and washed well with water (4x10 mL portions) and
finally with ether.

Anal. for [Cl(bpy)$_2$RuNCSRu(bpy)$_2$Cl](BPh$_4$)$_3$:

          Calcd. C, 70.92; H, 4.81; N, 6.59.

          Obsd. C, 70.58; H, 5.09; N, 7.00.

2.6i [Cl(bpy)$_2$RuNCSRu(bpy)$_2$Cl](BPh$_4$)$_2$

The mixed-valence species was prepared by either oxidizing
the (22) compound with one equivalent of Ce(IV) solution or by
mixing equimolar amounts of (22) and (33) compounds in
acetonitrile.   The tetraphenylborate salt, separated out from
these solutions, was not stable for longer periods and
consistent microanalytical results could not be obtained.

.6j [Cl(bpy)$_2$RuNCSRu(bpy)$_2$(NCS)]BPh$_4$

Fifteen millilitres of an aqueous solution of [(bpy)$_2$-
u(H$_2$O)Cl]$^+$ was prepared from cis-[(bpy)$_2$RuCl$_2$].2H$_2$O (52 mg)
s described in 2.6a(ii). An equimolar amount of cis-[(bpy)$_2$-
u(NCS)$_2$] in ethanol (10 mL) was added and the resulting

solution was refluxed for 2 h. The solution was filtered into an aqueous solution of sodium tetraphenylborate. The red brown precipitate formed in about quantitative yield was filtered, washed successively with water and ether and dried. The purification was carried out as described in 2.6g.

Anal. for $[Cl(bpy)_2RuNCSRu(bpy)_2(NCS)]BPh_4$:

Calcd. C, 61.06; H, 4.01; N, 10.79.

Obsd. C, 60.54; H, 4.20; N, 11.05.

2.6k $[Cl(bpy)_2RuNCSRu(bpy)_2(NO_2)]BPh_4$

The dark brown colored acetonato complex $[(bpy)_2Ru(acetone)-NO_2)]^+$ was prepared from $[(bpy)_2Ru(NO)(NO_2)](PF_6)_2$ (194 mg) as described in 2.6a(i). A stoichiometrically equimolar amount of $[(bpy)_2Ru(NCS)Cl]$ (136 mg) in ethanol/acetone mixture (1:1, v/v) (20-25 mL) was added to this and the solution was refluxed for 2-2.5 h. The resulting solution was processed as described in 2.6j. The major dimeric product was eluted and precipitated using excess of diethyl ether and the minor amounts of unreacted monomeric compounds were discarded.

Anal. for $[Cl(bpy)_2RuNCSRu(bpy)_2(NO_2)]BPh_4$:

Calcd. C, 60.70; H, 4.05; N, 10.90.

Obsd. C, 60.22; H, 3.84; N, 11.09.

Anal. for [Cl(bpy)$_2$RuNCSeRu(bpy)$_2$Cl](BPh$_4$):

        Calcd. C, 59.05; H, 3.94; N, 9.54.

        Obsd. C, 59.64; H, 4.33; N, 9.02.

2.6o [Cl(bpy)$_2$RuNCSeRu(bpy)$_2$Cl](BPh$_4$)$_3$

It was prepared by a similar procedure as that described in 2.6h. The red orange colored compound was washed well with water and ether.

Anal. for [Cl(bpy)$_2$RuNCSeRu(bpy)$_2$Cl](BPh$_4$)$_3$:

        Calcd. C, 69.22; H, 4.70; N, 6.43.

        Obsd. C, 69.70; H, 5.05; N, 6.95.

2.6p [Cl(bpy)$_2$RuNCSeRu(bpy)$_2$Cl]$^{2+}$

The mixed-valence compound was prepared by mixing the stoichiometrically equimolar solutions of the complexes (22) and (33) in acetonitrile. The tetraphenylborate salt, separated out from this solution, showed an almost similar near infrared band with slightly reduced intensity to that of the (23) compound generated in situ by the oxidation of (22) using [Fe(bpy)$_3$]$^{3+}$ in acetonitrile.

2.6q [Cl(bpy)$_2$RuNCSeRu(bpy)$_2$(NCSe)]BPh$_4$

This compound was prepared by a procedure similar to that described for the synthesis of the analogous thiocyanate

compound (2.6j). [(bpy)$_2$Ru(NCSe)$_2$].2H$_2$O was used instead of cis-[(bpy)$_2$Ru(NCS)$_2$].

Anal. for [Cl(bpy)$_2$RuNCSeRu(bpy)$_2$(NCSe)](BPh$_4$):

        Calcd. C, 56.94; H, 3.74; N, 10.06.

        Obsd. C, 57.25; H, 4.11; N, 10.50.

2.6r [Cl(bpy)$_2$RuNCSeRu(bpy)$_2$(NO$_2$)]BPh$_4$

It was prepared by the procedure described in 2.6k; [(bpy)$_2$Ru(NCSe)Cl] was used in the place of [(bpy)$_2$Ru(NCS)Cl].

Anal. for [Cl(bpy)$_2$RuNCSeRu(bpy)$_2$(NO$_2$)]BPh$_4$:

        Calcd. C, 58.56; H, 3.90; N, 10.51.

        Obsd. C, 58.76; H, 3.54; N, 10.75.

2.6s [Cl(bpy)$_2$RuNCSeRu(bpy)$_2$X](BPh$_4$)$_3$ (X$^-$ = NO$_2^-$ or SeCN$^-$)

The oxidation of the (22) asymmetric dimers were carried out as described in 2.6l. The products were obtained in almost quantitative yield.

2.6t [Cl(bpy)$_2$RuNCSeRu(bpy)$_2$X]$^{2+}$ (X$^-$ = NO$_2^-$ o SeCN$^-$)

The mixed-valence compounds were genrated _in_ _situ_ using Ce(IV) or [Fe(bpy)$_3$]$^{3+}$ oxidation in acetonitrile.

SECTION III : LINKAGE ISOMERISM

3.1 Introduction:

This section deals with the results on the various linkage isomers synthesized in our study.

3.2 Synthetic Aspects:

N- and S/Se-bonded linkage isomers of thiocyanato-/seleno-cyanato complexes of almost all of the transition metals have been synthesized[10] and characterized by various physicochemical techniques such as, IR, electronic and multinuclear n.m.r. spectral (^{13}C and ^{15}N), ESCA studies and dipole moment measurements, etc. Despite this, certain aspects of the chalcogenocyanate linkage isomerism still remains unanswered.[11,19]

Although the simple and the classical substitution reactions of $[(NH_3)_5RuX]X_2$ (X = Cl, Br, I) with thiocyanate/selenocyanate ions simultaneously generate two linkage isomers, viz., $[(NH_3)_5RuNCX]^{2+}$ and $[(NH_3)_5RuXCN]^{2+}$ (X = S or Se) with a relatively large yield of S or Se-isomers.[14c,15c] The reaction of $[(NH_3)_5RuN_2]X_2$ with thiocyanate ion gives higher yield of N-isomer (N-/S-bonded isomer yield ratio, ~ 2). Similar reaction of $[(NH_3)_5RuX]X_2$ with selenocyanate ion also yielded both the link-

age isomers. The ratio of N-/Se-bonded isomers in the latter case was approximately, 5. Recently, Jackson and coworkers[13] have repoted that the SCN⁻ anation reaction of $[(NH_3)_5Co(OH_2)]^{3+}$ involves the heretofore unrecognized formation of the unstable S-bonded $[(NH_3)_5CoSCN]^{2+}$, produced parallely with the N-bonded complex $[(NH_3)_5CoNCS]^{2+}$. The kinetically formed N-/S-isomer ratio was found to be ca. 2.8. The formation of the S-isomer and its subsequent decomposition went undetected in several previous studies. These results emphasize the generality of the formation of both the linkage isomers in the NCX⁻ substitution reactions of the metal ion complexes. It appears that these reactions are kinetically controlled and the thermodynamically unstable linkage isomers, thus, formed during the reaction, subsequently decomposes to the thermodynamically stable isomer.[19]

The $[Fe(CN)_5]^{2-}$ and $[(bpy)_2Ru]^{2+}$ systems form the thermodynamically stable N-bonded isomers, as characterized by the various physicochemical methods. The reaction between $[(bpy)_2ClRu(OH_2)]^+$ and NCX⁻ ions though yielded both N- and S/Se-bonded isomer, the S or Se-bonded isomer was formed in low yields compared to the N-bonded one.

3.3 Infrared Spectral Studies:

Vibrational spectroscopy provides a fairly conclusive way of identifying the linkage isomerism of chalcogenocyanate complexes.[10] The positions of the $\nu(CN)$, $\nu(CX)$ and $\delta(NCX)$ of the

coordinated chalcogenocyanates along with the integrated intensity of the ν(CN) band are used to determine the nature of linkage isomer. The data for these bands are given in Tables 4.1 to 4.4 and fall in the expected regions for the linkage isomers derived therefrom. The integrated intensity of the ν(CN) band of all the isomers have been determined quantitatively.

It has been observed that the intensity of ν(CN) band of $[(NH_3)_5RuXCN]^{2+}$ ion is much less than that of the $[(NH_3)_5RuNCX]^{2+}$ ion. This is due to the increased contribution of the $N\equiv C-X^-$ forms of all the resonating structures of the NCX^- ions, when coordinated through the sulfur/selenium end (cf. Table 3.1),

Table 3.1: Resonance Structures of the NCX^- ions

(X = S/Se)	Percentage		
	$C\equiv N-X^-$	$^-N=C=X$	$^{2-}N-C\equiv X^+$
X = S	76	5	19
X = Se	88	0	12

which results in a decrease of the dipole moment of the ion. Conversely, coordination through the nitrogen end of the NCX^- ion favors an increase in the contributions of the other two

forms, resulting in an increase in the dipole moment of the ion. Assuming that a change in the magnititude of the dipole moment causes a corresponding change in the rate of change of the dipole moment during vibration, the difference in the intensity of the bands is understandable. Further, among the two isomers, $[(NH_3)_5RuSCN]^{2+}$ and $[(NH_3)_5RuSeCN]^{2+}$ the latter showed a much weaker $\nu(CN)$ band compared to that of the former. This is due to the larger contribution of $N\equiv C-X^-$ form (cf. Table 3.1) in the case of X=Se than in the case of X=S.

The integrated intensity values for the $\nu(CN)$ band for the $[(bpy)_2ClRuNCX]$ moieties have been determined using Ramsay's method.[10] They are found to be in agreement with the previously reported values for N-bonded isomers (cf. Tables 4.3 and 4.4). The resonance Raman spectral studies of the compounds also confirmed these results (cf. Section 4.6).

3.4 Electronic Spectral Studies :

The electronic spectral data of the linkage isomers are presented in Tables 4.1, 4.6, 4.7, 4.9 and 4.11. The spectra of the complexes, $[(NH_3)_5RuNCSe]^{2+}$ and $[(NH_3)_5RuSeCN]^{2+}$ showed strong intraligand bands of the coordinated selenocyanate group at around 220, 260 and 325 nm. The spectra for the corresponding thiocyanate analogs have been reported earlier.[14b] The bands having maxima at 255 and 269 nm in Se- and N-isomers, respectively can be attributed to the $^1\Sigma^+ \text{---} ^1\Sigma^-$ transition of

the SeCN$^-$ ion, which is forbidden in the free ligand but may become allowed when bonded to the metal ion. Besides these bands, the Se-isomer showed additional bands with absorption maxima at 827, 555, 570(sh) and 395 nm while the other isomer showed bands at 535 and 382 nm. The bands at 555 and 535 nm in Se- and N-bonded complexes, respectively, can be assigned to the charge transfer transition, $2\pi(NCSe) -- d\pi(Ru)$, because of their high intensity (cf. Table 4.1). The red shift in the position of this LMCT band of the $[(NH_3)_5RuSeCN]^{2+}$ ion compared to that of the $[(NH_3)_5RuSCN]^{2+}$ ion, (555 and 515 nm) could be due to the increasing case of oxidation of the SeCN$^-$ ion. Also, the shapes of these bands are of interest. The Se-isomer exhibited a comparatively broad and unsymmetrical band while the N-isomer almost Gaussian shape. In the case of the $[(NH_3)_5RuNCSe]^{2+}$ ion, the microsymmetry around the metal center is closer to O_h while in the Se-isomer it is C_{4v}. Hence, the magnitude of removal of degeneracies of various energy levels in the N-isomer is less than that in the Se-isomer[16,83] and the band for the Se-isomer might even show a shoulder at around 570 nm.

Though the d-d transition in Ru(III) complexes are often obscured due to the large ligand field parameters, the two spin-forbidden transitions $^4t_{1g} --- {}^2T_{2g}$ and $^4T_{2g} --- {}^2T_{2g}$ are often observed as shoulders.[84] Due to the low intensities of the bands at 382 and 395 nm for N- and Se-bonded isomers, these bands may tentatively be assigned to ligand field transitions. Further, the difference in the absorption maxima for the linkage isomers

of thiocyanate complex was found to be small, i.e., $[(NH_3)_5Ru-NCS]^{2+}$ ion, 495 nm; $[(NH_3)_5RuSCN]^{2+}$ ion, 515 nm. A similar trend has been observed for the N- and Se-bonded isomers of the selenocyanato complex (N-isomer, 535 nm and Se-isomer, 555 nm). This suggests that the π-bonding characteristics of both the ends of the chalcogenocyanates are almost similar. Similar observation has been made earlier using electrochemical methods.[24]

Further, the excitation of the pentaamminethiocyanato-ruthenium(III) compounds using the 514.5 nm line of the Ar^+ ion laser, yielded weak emission, the quantum yield of which could not be determined due to the local burning of the samples, even when the spinning technique was used to record the spectrum. The N- and S-isomers (absorption maxima 495 and 515 nm, respectively) showed the emission at around 666 and 700 nm. The results of the electrochemical measurements of the linkage isomers of the thio-cyanato- and selenocyanatobis(bipyridine)ruthenium(II) complexes are discussed in Section 4.8.
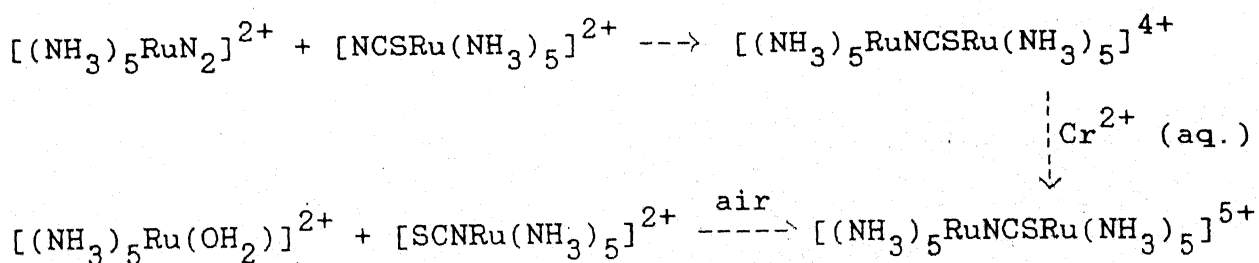
SECTION IV :   ELECTRON TRANSFER PROPERTIES OF THE

BINUCLEAR MIXED-VALENCE COMPOUNDS

4.1   Introduction

The characterization of the thiocyanato- and selenocyanato bridged binuclear mixed-valence complexes using various physicochemical methods are discussed in this section. Further, the electron mediation across the chalcogenocyanate bridges, as obtained from the Hush model calculations on these compounds, is discussed in details.

4.2   Synthetic Aspects

Pentaamminethiocyanatoruthenium(III) ion was reacted with $[(NH_3)_5RuN_2]^{2+}$ at 35-45°C, whereby the binuclear complex was formed.[14c]   The same compound was also prepared by the reduction of the (33) dimer, using aqueous Cr^{2+} solution, which in turn was prepared from $[(NH_3)_5Ru(OH_2)]^{2+}$ and $[(NH_3)_5RuNCS]^{2+}$.   The preparative routes are shown below:

$$[(NH_3)_5RuN_2]^{2+} + [NCSRu(NH_3)_5]^{2+} \longrightarrow [(NH_3)_5RuNCSRu(NH_3)_5]^{4+}$$

$$\downarrow Cr^{2+} \text{ (aq.)}$$

$$[(NH_3)_5Ru(OH_2)]^{2+} + [SCNRu(NH_3)_5]^{2+} \xrightarrow{\text{air}} [(NH_3)_5RuNCSRu(NH_3)_5]^{5+}$$

The completely reduced species $[(NH_3)_5RuNCSRu(NH_3)_5]^{3+}$ ion could not be prepared despite several attempts. This compound seems to be unstable and undergo decomposition to monomeric thiocyanate complex. The probable reason for this intrinsic instability of the (22) ion could be the weak π-bonding in the $[Ru^{II}-NCS-Ru^{II}]$ unit. Ru(II) being a good π-donor[85] probably does not find a match in the weakly π-accepting thiocyanate group,[24] while the "spectator ligands," viz., NH_3, are also σ-donor. Electrochemical studies provide a conclusive evidence to the instability of (22) dimer. The cyclic voltammogram of the (33) dimer showed reduction waves for the successive reductions, (33) $\rightarrow$ (23) and (23) $\rightarrow$ (22). The species, though, seems to be stable in the cyclic voltammetric time scale, undergoes decomposition to $[Ru(NH_3)_5SCN]^{2+}$ in the second and third scans, whereby a new wave at round +0.2 V appeared at the expense of the signal due to (22). The wave at +0.2 V has been attributed to $[Ru(NH_3)_5SCN]^{+} \dashrightarrow [Ru(NH_3)_5SCN]^{2+}$ oxidation. Another corroborative evidence to this effect is from the higher stability of the $[(CN)_5FeNCXFe(CN)_5]^{7-}$ and $[Cl(bpy)_2RuNCXRu(bpy)_2Cl]^{+}$ which were separated (vide supra).

The completely reduced pentacyanoferrate (22) dimer, $[(CN)_5FeNCXFe(CN)_5]^{7-}$ was obtained when the reactants, $Na_3[Fe(CN)_5NH_3].3H_2O$ and NCX^-, were mixed simultaneously in aqueous solution. In fact, this was an exclusive product when the reaction was carried out in degassed water under a dinitrogen atmosphere. If air was bubbled instead of dinitrogen,[69] the

reaction yielded all three of the (22), (23) and (33) species. The (22) species that is formed believed to be partially oxidized to (23) and (33) species. Also, remaining (22) might have reacted with (33) in solution to give the mixed-valence (23) species according to $(22) + (33) \rightleftharpoons 2 \ (23)$. A delay of 10-20 min in the addition of NCX^- ion to the aerated aqueous solution of $Na_3[Fe(CN)_5NH_3]$ yielded exclusively the oxidized species (33) with a small amount of monomeric $[(CN)_5FeNCS]^{3-}$, which was identified by its electronic spectrum.[17]

Aging of the (22) solution in the atmosphere led to the properties of the (33) species to a considerable extent. A deformed band in the near IR region having somewhat lower intensity was observed. Hence, it was concluded that (22) compounds are unstable and are oxidized to (23) and (33) species in the course of time. The instability of (22) species can be attributed to the smaller π-acidities of NCX^- ions compared to those of cyanide ion or pyrazine. Due to the intrinsic instability of the (22) dimer, the reduction of the (33) species seems to be a better pathway to synthesize the mixed-valence ions rather than the oxidation of the (22) species. Reduction of the (33) species with hydroquinone, $K_4[Fe(CN)_6]$ and aq Cr^{2+} as reducing agents yielded the mixed-valence species. It was found to have two steps of reduction corresponding to molar stoichiometries 1:1 and 1:2 of (33) species and the reducing agent, resulting in blue and light yellow solutions. The pale yellow solution showed an electronic spectrum, which resembled

that of the (22) species in the case of selenocyanate and for thiocyanate the resemblance was not complete, suggesting partial decomposition.

The composition of the (33) species in the cases of both thiocyanate and selenocyanate were established by Job's method[86] using aqueous solutions of the reactants $Na_3[(CN)_5FeNH_3] \cdot 3H_2O$ and NCX^- ion. The reaction was very slow at a 10^{-4} M concentration level of the reactants. Hence, solution of 10^{-1} M concentration were used. The mixture was allowed to equilibrate in the dark under air. Portions of these solutions diluted to 10^{-4} M concentration were scanned from time to time, and the limiting values of absorption at appropriate wave lengths were obtained. Limiting values of absorption were plotted as function of F[41] ($F = [Fe(II)]_{init}/([Fe(II)]_{init} + [NCX^-]_{init})$), Fe(II) denoting $[(CN)_5Fe(NH_3)]^{3-}$). The plots displayed a sharp maximum at $F = 0.66$ for the SCN^- ion and $F = 0.68$ for the $SeCN^-$ ion suggesting that the species absorbing at 740 and 690 nm (for the $SeCN^-$ ion) contains $[Fe(CN)_5]^{2-}$ and NCX^- ion in 2:1 molar ratio.

All the compounds except the Rb salts showed a strong tendency to absorb atmospheric moisture and deliquesce with probable decomposition. As a result, it was very difficult to obtain consistent microanalytical results and especially in the case of the (22) dimer satisfactorily reproducible results could not be obtained. However, the microanalytical data for the compounds those were obtained were consistent with the compositions.

In the case of bis(2,2'-bipyridine)ruthenium complexes the (22) dimer was prepared by reacting $[(bpy)_2Ru(OH_2)Cl]^+$ or the solvenato $[(bpy)_2Ru(acetone)Cl]^+$ species with the monomeric $[(bpy)_2RuNCXCl]$ complex. The (22) species formed was separated out using different anions such as PF_6^-, BPh_4^-, ClO_4^-, Cl^- and p-toluene sulfonate. These were stable contrary to both the earlier cases. The mixed-valence compound prepared by the mixing of the (22) and (33) species (cf. Experimental Section) contained considerable amounts of the unreacted (22) and (33) compounds. This is understandable as the comproportionation constant, K_{com}, for the reaction $(22) + (33) \rightleftharpoons 2(23)$ is low (vide supra). Hence, the in situ genration of the (23) species by the oxidation of (22) moiety using Ce(IV) was preferred. A tetraphenylborate salt was also separated out from these solutions. The extinction coefficient values calculated for the different bands in the electronic spectra are based on the molecular weight corresponding to $[Cl(bpy)_2RuNCXRu(bpy)_2Cl]-(BPh_4)_2$.

The oxidations of the (22) compounds in acetone was carried out using a tetraphenylborate salt, whereby the difficulty of the interconversion of hexafluorophosphate salts into chloride form before and after the oxidation which was necessary, was averted in this study. This was due to solubility problems caused by the hexafluorophosphate anion in acetonitrile solution.[87]

4.3 Infrared Spectral Studies

IR spectra of the dimeric compounds $[(NH_3)_5RuNCSRu-(NH_3)_5]^{n+}$ (n = 4 or 5) are similar to the ones reported earlier[14b] for the monomeric complexes, viz., $[(NH_3)_5RuNCS]^{2+}$ and $[(NH_3)_5RuSCN]^{2+}$ (cf. Tab 4.1) except for a slight broadening of the $\nu(CN)$ band in the (33) dimer, suggesting a bridging thiocyanate group.[10] However, the mixed-valence (23) dimer showed a shift in the position along with the broadening of the $\nu(CN)$ band from that of the monomeric complexes. The (23) dimer exhibited an intense $\nu(CN)$ band at 2060 cm^{-1} with a shoulder at around 2090 cm^{-1} the monomer exhibited the band at 2073 cm^{-1}. The broadness of this band ($\Delta\bar{\nu}_{1/2}$ = 120 cm^{-1}) was characteristic of the bridging thiocyanate group. Besides, all the characteristic bands due to coordinated ammonia were observed at around 3400, 3200, 1600, 1300, 800 and 450 cm^{-1}.[88]

The $\delta_s(NH_3)$ band at around 1300 cm^{-1} has been utilized by earlier workers[55,89] as a diagonostic for the oxidation state of the metal centers, in the case of $[(NH_3)_5Ru]^{n+}$ (n = 2 or 3) complexes. This band, in general, has been observed below 1290 cm^{-1} for $[Ru(II)(NH)_5]$ complexes while the Ru(III) analogs showed this at above 1320 cm^{-1}. The observation of this band at 1300 cm^{-1} in (23) dimer, viz., $[(NH_3)_5RuNCSRu(NH_3)_5]^{4+}$ suggests a delocalized limit for the oxidation states with a average valency of 2.5+ on each metal center, rather than a trapped 2+ and 3+ heme.

Table 4.1:   Vibrational and Electronic Spectral Data

Compound	Infrared Data(cm^{-1})[a]			Electronic Spectral Data in nm($M^{-1}cm^{-1}$)
	ν(CN)	ν(CX)	δ(NCX) (X=S or Se)	
1.[$(NH_3)_5$ Ru SeCN]$^{2+}$	2100w	535540	375380	827(154);555(2200); 570(sh);395(w);327(3900) 255(12575);223(s)
2.[$(NH_3)_5$ Ru NCSe]$^{2+}$	2060s 2035sh	640		535(1450);382(121); 322(3086);269(9010); 215(s)
3.[$(NH_3)_5$ Ru SCN]$^{2+b}$	2073	790	420	515(2450)
4.[$(NH_3)_5$ Ru NCS]$^{2+b}$	2057	783	460	495(3000)
5.[$(NH_3)_5$ RuNCS- Ru($NH_3)_5$]$^{4+c}$	2060 2093sh			1710(330);490(1700); 395(1300);330(540); 265(900)

a. Vibrational bands for coordinated NH and various anions are not given

b. Values taken from ref. 14c : c. s(NH) appeared at 1300 cm (see text)

Further, the marking of the relatively weak band due to the $\nu(CS)$ of the SCN^- group in the region 820-750 cm^{-1} by the broad and moderately intense band due to the rocking mode of NH_3 around 800 cm^{-1} left some uncertainty in the assignment of the $\nu(CS)$ band. Although, due to the intrinsic asymmetry of the bridging thiocyanate group, the IR studies are not strongly evidential as in the cases of μ-pyz[87] and μ-$(CN)_2$ complexes, the slight shift in the position of the $\nu(CN)$ bands of the monomer and dimer does help. This shift can be attributed to the nitrogen end coordination of the $[Ru^{III}-SCN]$ unit on Ru(II) and is understandable as the π-acceptor ability of the S-bonded thiocynate is only slightly higher than that of the N-bonded one.

Unlike in the case of $[(NH_3)_5Ru]^{n+}$ complexes, IR spectroscopy provides a simpler and concrete method to establish the oxidation states of the pentacyanoferrate moieties. The $\nu(CN)$ frequencies of Fe(II) cyanides fall in the range 2070-2030 cm^{-1} whereas the range for Fe(III) cyanides in 2130-2090 cm^{-1}. The (33) and (22) compounds of the pentacyanoferrate exhibited two bands in the cyanide stretching region corresponding to the bridging NCX^- and pentacyanoferrate moities. $\nu(CN)$ of the NCX^- bridge for (22) species were observed at markedly lower energy compared to that of the (33) species (cf. Table 4.2). This might be due to larger π-donation in (22) species to the LUMO of the NCX^- ion, a π^* orbital, which is antibonding with respect to both C-N and C-X bonds.

Table 4.2: Infrared spectral data in cm^{-1} and their assignments for some of the compounds, $[Fe(CN)_5NCXFe(CN)_5]^{n-}$ᵍ

	$[Fe(CN)_5NCXFe(CN)_5]^{5-}$		$[Fe(CN)_5NCXFe(CN)_5]^{6-}$		$[Fe(CN)_5NCXFe(CN)_5]^{7-}$		Assignments
	X = S^c	X = Se^d	X = S^e	X = Se^e	X = S^f	X = Se^f	
	2125(s)	2140(s)	2130(s)	2120(s)	2075(s)	2060(s)	$\nu(CN)$ of NCX$^-$
	2100(vs)	2090(vs)	2090(vs)	2085(vs)	–	–	$\nu(CN)$ of $[Fe^{III}(CN)_5]^{n-}$
	–	–	2055(s,sh)	2050(s,sh)	2050(vs)	2050(vs)	$\nu(CN)$ of $[Fe^{II}(CN)_5]^{n-}$
	730	580	750	575	730	–	$\nu(CX)$ of NCX$^-$
	460	420	460	415	–	–	$\delta(NCX)$ of NCX$^-$
	530	520	590 / 530(s,sh)	575 / 525(s,sh)	620	–	$\delta(FeCN)$
	385	380	405	405	410	–	$\nu(FeC)$
						–	

74

a, Unless otherwise stated the spectra were recorded in KBr and CsI disks

b, Recorded in nujol mull.

c, Tetraphenylphosphonium salt

d, Tetraethylammonium salt

e, Rubidium salts

f, Sodium salts

g, Water of crystallization appeared as two characteristic peaks at around 3450 and 1640 cm^{-1}. Peaks due to various cations as PPh_4^+, NEt_4^+, NBu_4^+ etc were obtained at their characteristic positions and are not given here.

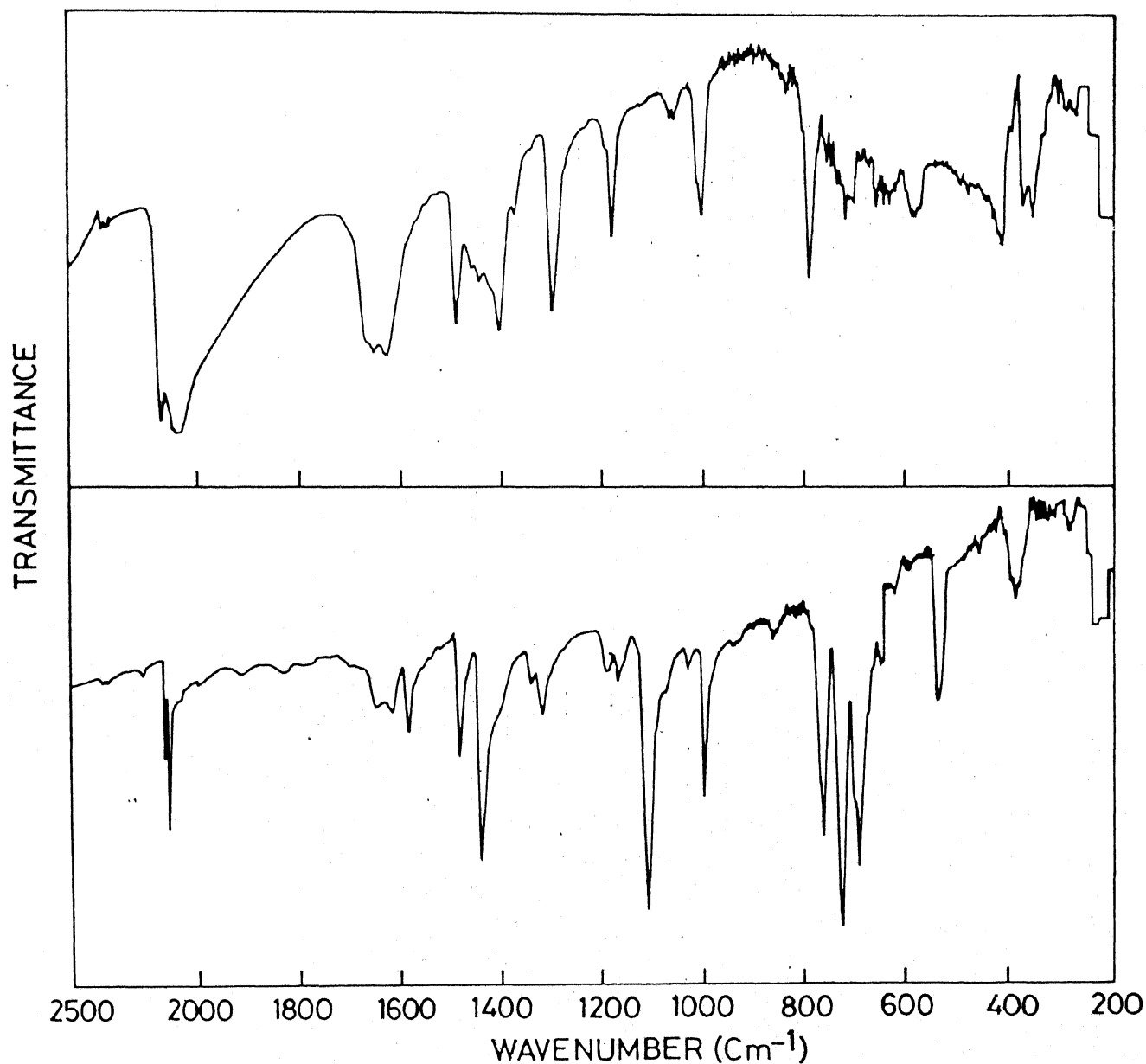Fig. 4.1 Infrared spectra of the representative compounds.

(a) $(PPh_4)_5$ $[Fe(CN)_5NCSFe(CN)_5].xH_2O$ (below) and

(b) $[(C_2H_5)_4N]_6[Fe(CN)_5NCSFe(CN)_5].xH_2O$ (above).

The (23) pentacyanoferrate dimer exhibited ν(CN) bands corresponding to the bridged NCX$^-$ moiety and pentacyanoferrates in +2 and +3 oxidation states. The bands due to ν(CN) of the NCX$^-$ moiety and $[Fe^{II}(CN)_5]^{3-}$ were observed as overlapping bands whose halfwidth was abnormally high and could be resolved into two bands having absorbances at around 2050 and 2085 cm^{-1}. Similarly the band due to δ(FeCN) was observed at two different frequencies charactreristic of $[Fe^{II}(CN)_5]^{3-}$ and $[Fe^{III}(CN)_5]^{2-}$ units (Figure 4.1). The bands due to ν(CX), δ(NCX), δ(FeCN) and ν(FeC) modes of vibrations were also obtained in their charactreristic frequency ranges and are given in Table 4.2. IR spectra of the compounds with different cations did not show any marked difference (± 5 cm^{-1}) in the positions of the various bands thus far discussed.

IR spectra of the bis(2,2'-bipyridine)ruthenium complexes showed characteristic bands for the coordinated 2,2'-bipyridine and chalcogenocyanate ions. For dinuclear complexes a shift in the position and broadening of the ν(CN) mode of vibration (compared to the chalcogenocyanato monomeric complexes) were observed. A shift of ~30 cm^{-1} in the case of NCS$^-$ bridging and of ~10 cm^{-1} for SeCN$^-$ bridging have been observed for the (22) dimers. The integrated intensity of the ν(CN) bands exhibited a 3-5 fold increase in its values, compared to those of the monomeric complexes. The dithiocyanato compound $[Cl(bpy)_2RuNCSRu(bpy)_2NCS]BPh_4$ exhibited two bands at around 2160 and 2110 cm^{-1} in the CN-strething region confirming the presence

of bridging and N-bonded thiocyanate groups. All the compounds exhibited the characteristic bands for the different anions and coligands like NO_2^- ion (Tables 4.3 and 4.4).

The positions of the ν(CN) band in the (22) dimers do give a clue about the structure of the [Ru-NCX-Ru] bridge. Among the three possibilities of the chalcogenocyanate bridging, viz.,

$$
\begin{array}{ccc}
M \diagdown \diagup M, & M \diagdown \diagup M & \text{and} \quad M\text{-NCX-M,} \\
N & N & \\
C & C & \\
X & N &
\end{array}
$$
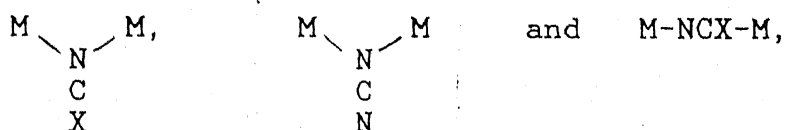
the last possibility is the most probable one. The first and second possibilities could be ruled out because it should give a considerably low value for ν(CN) mode, as there will be extensive π-backdonation from both the metal centers. The second possibility is especially unfavorable in the cases of pentacyanoferrates and bis(2,2'-bipyridine)ruthenium complexes as the "spectrator ligands" are strongly π-acidic and under such circumstances the X-bonded compounds are highly unfavored. Thus, the positions of ν(CN) at somewhat higher frequencies viz. > 2110 cm^{-1} in all these compounds conforms well with the linear bridged structure. All the other characteristic bands due to ν(CX) and δ(NCX) modes were observed at their respective positions and are given in Tables 4.3 and 4.4.

4.4 Absorption Spectral Studies

The essential features of the thiocyanato and selenocyanato- complexes of the pentaammineruthenium(II/III)

Table 4.3 : Infrared Spectral Data in cm^{-1} [a,c,d]

[(bpy)$_2$Ru(NCS)Cl].2H$_2$O [b]	[Cl(bpy)$_2$RuNCSRu(bpy)$_2$Cl]BPh$_4$
2120(vs)[e]	2150(vs)[f]
810(w)	777[g]
660(w)	665(w)
485(vw)	500(w)
430(br)	470(vw)
380(m)	435(br)
360(w)	365(w)
330(br)	330(br)
285(m)	290(m)
265(m)	260(m)

a, Unless otherwise stated the spectra were recorded in KBr and CsI disk.

b, Water of recrystallization appeared as two characteristic peaks at around 3450 and 1640 cm^{-1}.

c, Peaks characteristic of the coordinated 2,2'-bipyridine and the anion BPh$_4^-$ were observed in their charercteristic positions and are not given here.

d, The various peaks at low energies are assigned to the ν(M-S), ν(M-N) and ν(M-Cl) modes of thiocyanate and 2,2-bipyridine and chloro ligands.

e, The integrated intensity A$_{(CN)}$ of the ν(CN) band was calculated using the Ramsay's method;[10] A$_{(CN)}$ = 12x10^4 M^{-1} cm^{-2}. A$_{(CN)}$ value for [(bpy)$_2$Ru(NCS)$_2$] is 10.1 x 10^4 M^{-1} cm^{-2} [30] which is comparable with our value.

f, A$_{(CN)}$ = 25x10^4 M^{-1} cm^{-2}.

g, The 740-800 cm^{-1} region is masked by intense bands due to phenyl ring vibrational modes. The value was obtained from the Raman spectrum.

Table 44 : Infrared Spectral Data in cm^{-1} [a]

Complex	Bands
$[(bpy)_2Ru(NCSe)_2].2H_2O$	2120sh, 2083(s), 660, 485, 430, 360, 290. 3380-3500,[b] 1650.[b]
$[(bpy)_2Ru(NCSe)Cl].2H_2O$	2123(vs), 630(w), 445(w), 430, 375, 355, 335, 300, 290. 3450,[b] 1640.[b]
$[\{Cl(bpy)_2Ru\}_2NCSe]BPh_4$	2130(s), 627(m), 510, 485, 430, 370, 345, 320, 290.
$[\{Cl(bpy)_2Ru\}_2NCSe](Bph_4)_3$	2095(s)
$[\{Cl(bpy)_2Ru\}_2NCSe](BPh_4)_2$	2085(s)

---

a, Spectra were recorded using KBr/CsI pellets; characteristic peaks due to anions and coordinated 2,2'-bipyridine are not given here.

b, Water of crystallization.

system are presented in Table 4.1. Apart from the intraligand band of the thiocyanate and selenocyanate ions, these compounds exhibited moderately intense charge transfer bands in the visible region of their spectra.

Analogous to most of the other mixed-valence systems, the thiocyanate bridged binuclear complex exhibited a near-IR transition at around 1690 nm which can be attributed to the intervalence transfer (Fig. 4.2). The position of the absorption maximum of this band was found to be independent of the solvent parameters, as had been observed for other delocalized systems (Table 4.5). Ignoring the asymmetry (vide supra) of the bridge,

Table 4.5: Solvent Independent Near IR Spectral Data for $[(NH_3)_5RuNCSRu(NH_3)_5]^{4+}$ ion

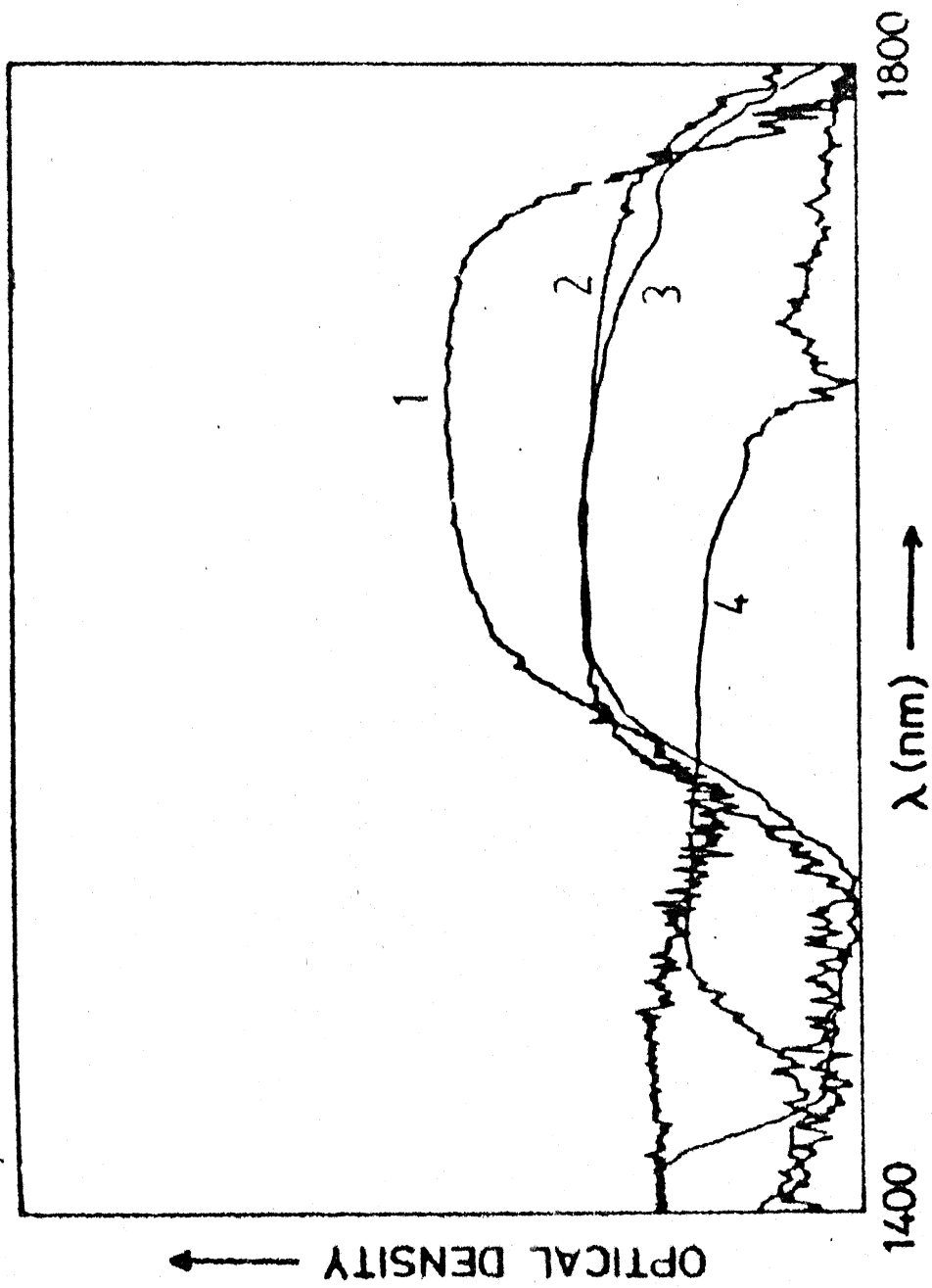| Solvent	$(1/n^2 - 1/D)$[65]	λ_{max} (nm)	ϵ_{max} $(M^{-1} cm^{-1})$
H_2O	0.551	1690	
DMF	0.464	1610	
Chlorobenzene	0.254	1600	331
Formamide	0.468	1640	

82

Fig. 4.2   Near IR spectra for $[(NH_3)_5RuNCSRu(NH_3)_5]^{4+}$ in diffe-

rent solvents.   1. Water; 2. Chlorobenzene; 3. Forma-

mide; 4. N,N -Dimethylformamide.

$[(NH_3)_5 Ru-SCN-Ru(NH_3)_5]Br_4$
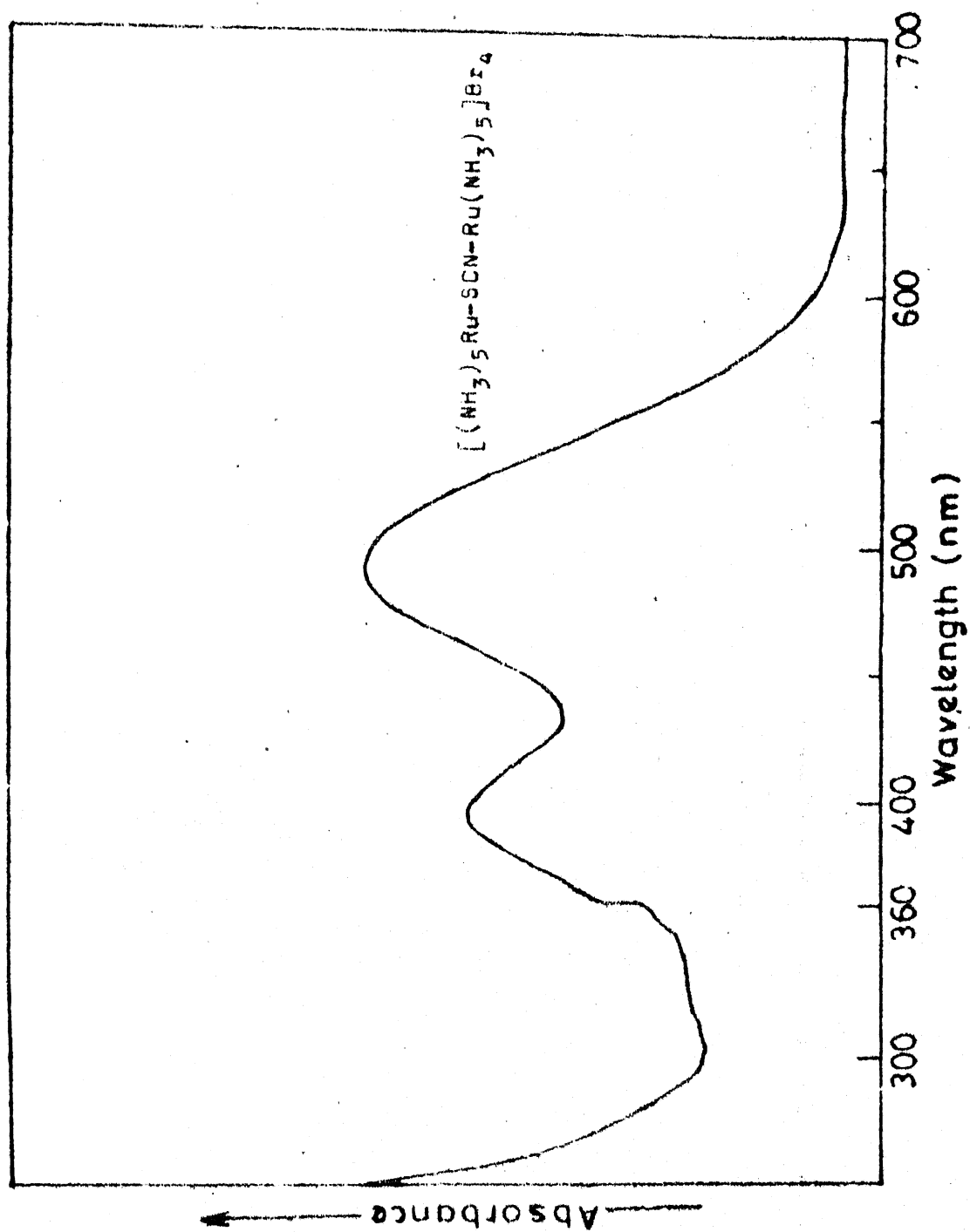
Absorbance

Wavelength (nm)

Fig. 4.3   Electronic spectrum

the IT bandwidth can be calculated using Hush model and the values are given in Table 4.13. The experimental bandwidth is much less than that of the calculated band (cf. Table 4.13). The weak intensity, narrowness compared to the bands of other systems having largely trapped valences and the solvent independence of the absorption maximum of the band are attributred to a delocalized limit[37] rather than to trapped integral valences; i.e., in Robin and Day sense, the dimer can be designated as a class III system.[39]

The d-levels for the dimer can be best described by molecular orbitals delocalized over both the metal centers as have been assumed for the $[(NH_3)_5Ru(N_2)Ru(NH_3)_5]^{5+}$ dimer.[91] Assuming the linearity of the bridge, i.e., SCN^-, the tentative ordering of the molecular orbitals of the dimer in C_{4v} symmetry can be given as

$$E\ (XZ_1 + XZ_2,\ YZ_1 + YZ_2) < B_2\ (XY_1 + XY_2)$$
$$\sim B_2\ (XY_1 - XY_2) < E\ (XZ_1 - XZ_2,\ YZ_1 - YZ_2) < 3\pi(SCN^-)$$

with an unpaired electron in the $E\ (XZ_1 - XZ_2,\ YZ_1 - YZ_2)$ level. From the above ordering the two transitions $(XZ_1 - XZ_2,\ YZ_1 - YZ_2)$ $E \leftarrow B_2$ and $3\pi(SCN^-) \leftarrow B_2$ may be attributed to the near-IR and the 490 nm CT bands, respectively (cf. Fig. 4.3)

Tables 4.6 and 4.7 give the electronic spectral data for the pentacyanoferrate(II/III) complexes with their probable assignments. The electronic spectra of the binuclear

Table 4.6 : Electronic Spectral Data[a] for Thiocyanato-bridged compounds $[Fe(CN)_5NCSFe(CN)_5]^{n-}$

Compound	λ_{max} (ϵ_{max}) ($M^{-1}cm^{-1}$)	Assignment	Ref.
n = 7	395sh	–	This work
	325sh	–	
	285sh	–	
	225vs	–	
n = 6[b]	1300 (670)	IT	This work
	770sh	–	
	393 (1420)	LF, π(NCS) -- $d\pi$(Fe)	
	355 (1420)	σ(CN) -- $d\pi$(Fe)	
	325 (1700)	–	
	280 (2150)	π(CN) -- $d\pi$(Fe)	
	245 (2375)	π(CN) -- $d\pi$(Fe)	
	210 (10160)	IL, NCS^- ion	
n = 5[c]	715 (1600)	2π(NCS) -- $d\pi$(Fe)	This work
	412sh (1700)	LF, π(CN) -- $d\pi$(Fe)	
	405 (1800)	π(NCS) -- $d\pi$(Fe)	
	320sh	LF	
	295 (4430)	IL, NCS^-	
	280 (4210)	π(CN) -- $d\pi$(Fe)	
	250 (5400)	π(CN) -- $d\pi$(Fe)	
	215vs	IL, NCS^- ion	
$[Fe(CN)_5NCS]^{3-}$	521 (3600)	2π(NCS) -- $d\pi$(Fe)	17
	395 (520)	LF	
	350 (995)	π(CN) -- $d\pi$(Fe)	
	323 (1090)	π(CN) -- $d\pi$(Fe)	
	300 (1360)	LF	
	270 (2130)	π(CN) -- $d\pi$(Fe)	
	260 (2280)		

a, Spectra were recorded in water solutions;
b, Rubidium salt;
c, Tetrabutylammonium salt.

Table 4.7 :   Electronic Spectral Data[a] for Selenocyanato-bridged

compounds $[Fe(CN)_5NCSeFe(CN)_5]^{n-}$

Compound	λ_{max} (ϵ_{max}) $(M^{-1}cm^{-1})$	Assignment	Ref.
n = 7	420(s)sh	—	This work
	330sh	—	
	285(-)	—	
	245(-)	—	
n = 6[b]	1264 (730)	IT	This work
	730sh	—	
	398 (1380)	LF, π(NCSe) -- dπ(Fe)	
	318 (1640)	σ(CN) -- dπ(Fe)	
	295 (2180)		
	275 (2520)	π(CN) -- dπ(Fe)	
	240 (3330)		
	213 (12650)	IL, NCSe$^-$ ion	
n = 5[c]	690 (1750)	2π(NCSe) -- dπ(Fe)	This work
	410sh	LF, π(CN) -- dπ(Fe)	
	396 (2250)	π(NCSe) -- dπ(Fe)	
	320sh	LF	
	290 (4100)	IL, NCSe$^-$	
	248 (4510)	π(CN) -- dπ(Fe)	
	220vs	IL, NCSe$^-$ ion	
$[Fe(CN)_5NCSe]^{3-}$	598 (2180)	2π(NCSe) -- dπ(Fe)	17
	397 (595)	LF	
	353 (870)	π(CN) -- dπ(Fe)	
	323 (1150)	π(CN) == dπ(Fe)	
	275 (3226)	π(CN) == dπ(Fe)	
$[Fe(CN)_5CN-$ $Fe(CN)_4NH_3]^{4-}$	625(-)		69

a, Spectra were recorded in water solutions;
b, Rubidium salt;
c, Sodium salt.

pentacyanoferrate complexes obtained by dissolving the solid in aqueous solution were identical with those recorded for the species generated directly in solution.

The electronic spectra of the pale yellow aqueous solution of the (22) species exhibited a number of shoulders below 400 nm (Fig. 4.4) and accurate values for their extinction coefficients could not be determined. The spectra of the (33) species exhibited bands at around 715 nm and 690 nm for thiocyanate and selenocyanate bridged complexes, respectively. This low energy band showed marked dependence with the counter cation. Another band was observed at around 400 nm which exhibitd a low energy shoulder of almost equal intensity. This band, arising due to a LF transition in the corresponding mononuclear complex (cf. Tables 4.6 and 4.7) showed a marked increase in intensity, the reason for which could not be ascertained as similar higher intensity bands were observed in other pentacyanoferrate dimers with various bridging ligands.[69,92] A tentative explanation could be that this band might involve contributiosn from other CT transitions, such as $\sigma(CN) \text{---} t_{2g} (Fe)$.[69] The bands at around 700 nm in the (33) species can be attributed to $2 \pi(NCX) \text{---} t_{2g} (Fe)(LMCT)$ charge transfer. The energies of the HOMO orbitals of NCS^-, $NCSe^-$ and CN^- vary as $NCS^- > NCSe^- > CN^-$ (the HOMO of $NCSe^-$ ion has been assumed to follow the trend observed for NCO^- and NCS^- ions in energy as well as symmetry).[25] Assuming that the $t_{2g} (Fe)$ acceptor orbitals are not perturbed very much by the π-donation from the ligands, the energies of the CT band should
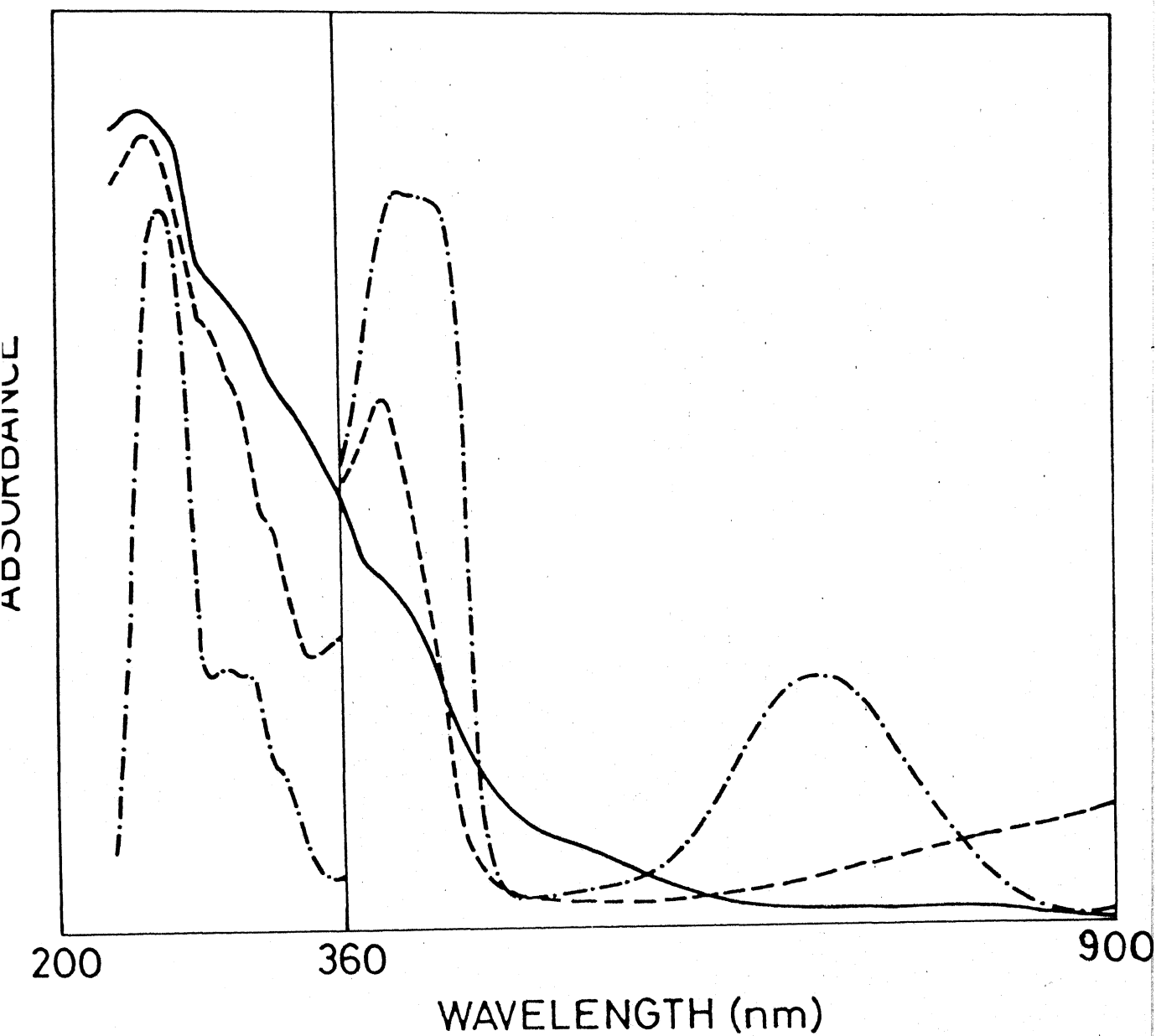
Fig. 4.4 Electronic spectra of the selenocyanato bridged
pentacyanoferrate dimers. (a) (22) dimer (———);
(b) (23) dimer (————); (c) (33) dimer (- - -).

vary as $NCS^- < NCSe^- < CN^-$. The observed behavior parallels this (cf. Tables 4.6 and 4.7). Also, the intensity of this band is reduced approximately by half in the case of dimers compared to that of the monomers. This is a corroborative observation for the nature of the assigned band i.e LMCT.

The mixed-valence (23) compounds exhibited a broad, fairly intense and asymmetric intervalence transfer (IT) band in the near-IR at around 1300 and 1264 nm for the thiocyanato and selenocyanato bridged dimers respectively (Fig. 4.5). The FWHM of these bands calculated using Hush model and the experimentally observed FWHM agreed well (cf. Table 4.13). The position of the absorption maxima of the IT bands showed a linear correlation with the solvent parameters as suggested by Hush (Table 4.8).

Table 4.8: Solvent-Dependent Near IR Spectral Data for $[Fe(CN)_5NCSeFe(CN)_5]^{6-}$ ion

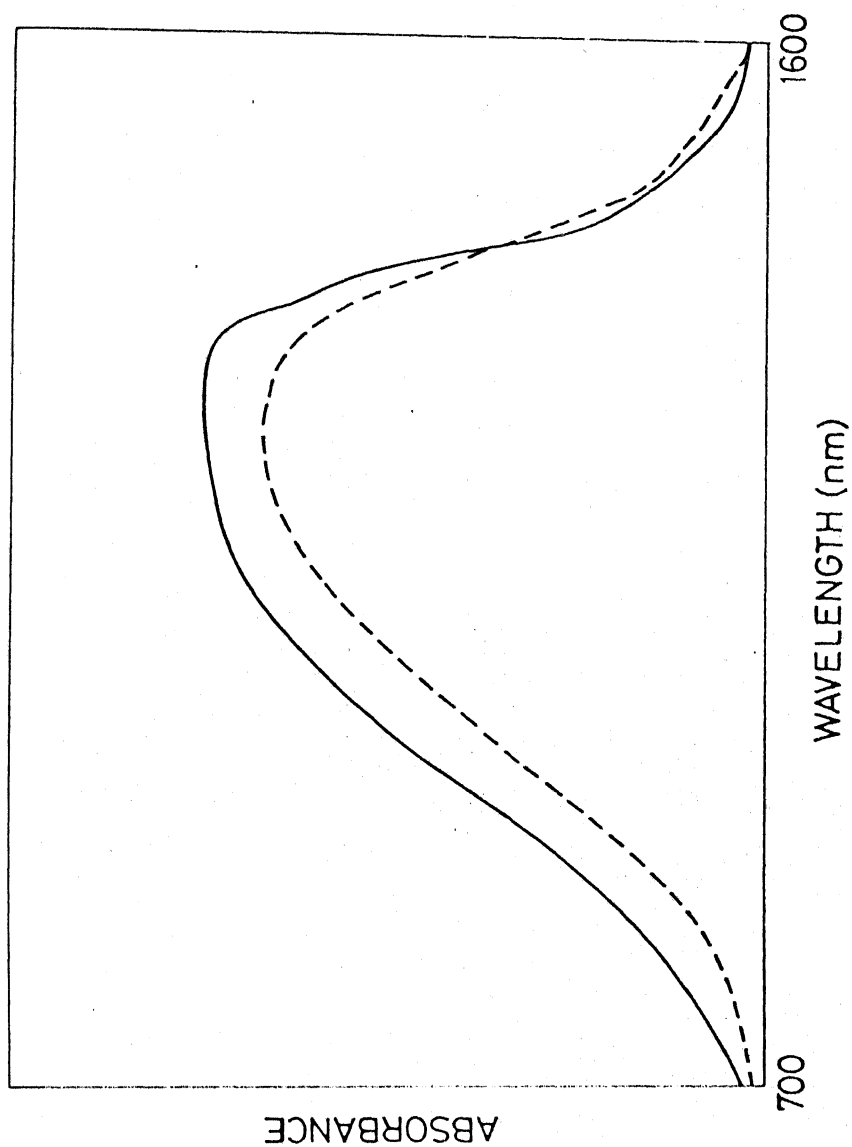| Solvent	$(1/n^2 - 1/D)$	λ_{max} (nm)	ϵ_{max} $(M^{-1}\ cm^{-1})$
Water	0.551	1264	730
Dimethylformamide	0.464	1278	
Dimethylsulfoxide	0.437	1290	
Potassium bromide disk	–	1340	
Perchloric acid (60%)	–	decomposed	

Fig. 4.5 NIR spectra of the mixed-valence pentacyano-
ferrate dimers.   (a) Thiocyanato bridged dimer
(————); (b) selenocyanato bridged dimer (– – – –).

Values of the oscillator strength of the IT band (f), the dipole strength (D), the transition dipole moment ($|M|$) and the mixing coefficient (α) were calculated by using Hush formulas (cf. Section 1.5) and are given in Table 4.13. A value of 7 Å has been worked out for the distance separating the metal centers in the [FeNCSeFe] unit, while the value for the [FeNCSFe] is 6.85 Å and these values are flexible by 10-20%.[10]

The electronic spectral data for the thiocyanato- and selenocyanato complexes of bis(2,2'-bipyridine)ruthenium(II/III) are given in Tables 4.9 and 4.10. All these compounds exhibited bands due to intraligand π--π^* transitions of the coordinated 2,2'-bipyridine at around 290 and 240 nm. The extinction coefficient of the band at around 290 nm has been found to be 25000-35000 $M^{-1} cm^{-1}$ for mononuclear bis(2,2'-bipyridine)ruthenium(II) complexes and the value doubled and tripled, respectively for dinuclear and trinuclear complexes. The intensity of this band, in fact, has been used as a criterion for differentiating between mono-, bi- and trinuclear complexes. A value of 40000-60000 $M^{-1} cm^{-1}$ for the extinction coefficient of the 290 nm band has been observed for the dinuclear complexes synthesized in this study. Besides, all these compounds showed a strong band at the region 210-225 nm, which could involve the contribution from the intraligand transition of the coordinated thiocyanate or selenocyanate ion.

Table 4.9: Electronic Spectral Data for the Monomeric and Dimeric bis(bipyridine)ruthenium(II)/(III) Complexes[a]

| [(bpy)$_2$Ru(NCS)Cl] | | [(bpy)$_2$Ru(NCS)$_2$] | | [Cl(bpy)$_2$RuNCSRu(bpy)$_2$Cl]$^{n+1}$ [c,d] | | |
Ru(II)	Ru(III)	Ru(II)	Ru(III)[b]	(22)	(23)	(33)
502 (4400)		597(sh)	505(sh)	525(sh)	940 (411)	
460(sh)	470 (6300)	515 (5700)	454 (4440)	455 (11365)	470 (13775)	428 (20510)
		440(sh)	420(sh)		460(sh) (13700)	
330 (10200)	322(sh)(10225)	375 (5700)	340(sh)(6940)	330 (991)		325(sh)
294 (42400)	292 (45450)	295 (37500)	289 (35160)	285 (58330)		285 (106300)
290 (39600)						
239 (32800)	242 (25300)	245 (32250)	243 (23640)	250(sh)		242 (64200)
				240 (31580)		
215(s)	217 (29250)	220(s)	220 (25260)	212 (43000)		215 (80650)
λ_{em} ^{g}				λ_{em} ^{h}		
715^e, 703^f				692^e, 680^f		

a, Wave lengths are in nm and the extinction coefficients in M^{-1} cm^{-1} are given in parentheses; spectral data in acetonitrile solutions. b, The perchlorate salt of the oxidized species. c, Tetra-phenylborate salt. d, Data in UV region for the (23) compound was not obtained. e, λ_{ex} = 514.5 nm, f, λ_{ex} = 457.9 nm. g, $\Delta\bar{\nu}_{1/2}$ (FWHM) = 2350 cm^{-1}. h, $\Delta\bar{\nu}_{1/2}$ (FWHM) = 2750 cm^{-1}.

Table 4.10: Electronic Spectral Data for the Monomeric and Dimeric Bis(bipyridine)ruthenium(II)/(III) Complexes[a]

[(bpy)$_2$Ru(NCSe)$_2$]·2H$_2$O		[(bpy)$_2$Ru(NCSe)Cl]·2H$_2$O	[Cl(bpy)$_2$RuNCSeRu(bpy)$_2$Cl]$^{n+}$ [b,c]		
Ru(II)	Ru(III)[b]	Ru(II)	(22)	(23)	(33)
				945 (450)	
493 (6350)		478 (5110)	540sh (~3000)	550sh	
440sh (3850)	421 (7540)	430sh (~4000)	469 (9000)	459 (15760)	456 (16200)
	385sh (5000)				
343 (5720)	315sh	339 (5830)	342 (10520)	337 (18000)	334 (18000)
292 (27740)	285 (46350)	286 (15800)	288 (44235)		287 (91000)
245 (21665)		244 (15230)	237 (44120)		232 (93200)
214 (30380)	220 (53350)	225 (14960)	220 (46000)		222 (103900)

a. Wavelengths are in nm; extinction coefficients in M^{-1} cm^{-1} are given in parentheses; spectral data in acetonitrile solutions.

b. Tetraphenylborate salts of the oxidized species.

c. Data in UV region for (23) was not obtained.

The bands due to the metal to 2,2'-bipyridine charge transfer transition (MLCT) $d\pi(Ru) -- \pi_1(bpy)$ and $d\pi(Ru) -- \pi_2(bpy)$ were observed at around 500 and 340 nm, respectively, for the thiocyanate complexes and at around 540 and 340 nm, for the selenocyanate ones. The interesting observation, however, is that the lowest energy MLCT in the visible region ($d\pi(Ru) --- \pi_1^*(bpy)$) is generally broader and exhibited invariably a shoulder of almost equal intensity. These shoulders were genrally observed towards the higher energy side of the prominent band in monomeric complexes, while in dimers towards the lower energy side (Figs. 4.6 and 4.7). These shoulders were attributed to the $d\pi(Ru) --- 3\pi(NCX^-)$ MLCT transition. Further, the prominent band corresonding to the $d\pi(Ru) -- \pi_1^*(bpy)$ transition showed a solvatochromisom, as would have been expected for these compounds. A blue shift of about 600 cm^{-1} has been observed in going from methylene chloride to acetonitrile. Also, this band was found to be blue shifted in going from a monomer to dimer. The second MLCT band due to $d\pi(Ru) -- \pi_2^*(bpy)$ at around 340 nm is, however, non-solvatochromic. Assignments for these various MLCT bands are further justified by the resonance Raman studies (cf. Section 4.6).

The completely oxidized (33) dimers showed a largely blue shifted band as expected and values for the extinction coefficients of the various bands increased by 2-3 folds (cf. Table 4.9 and 4.10).
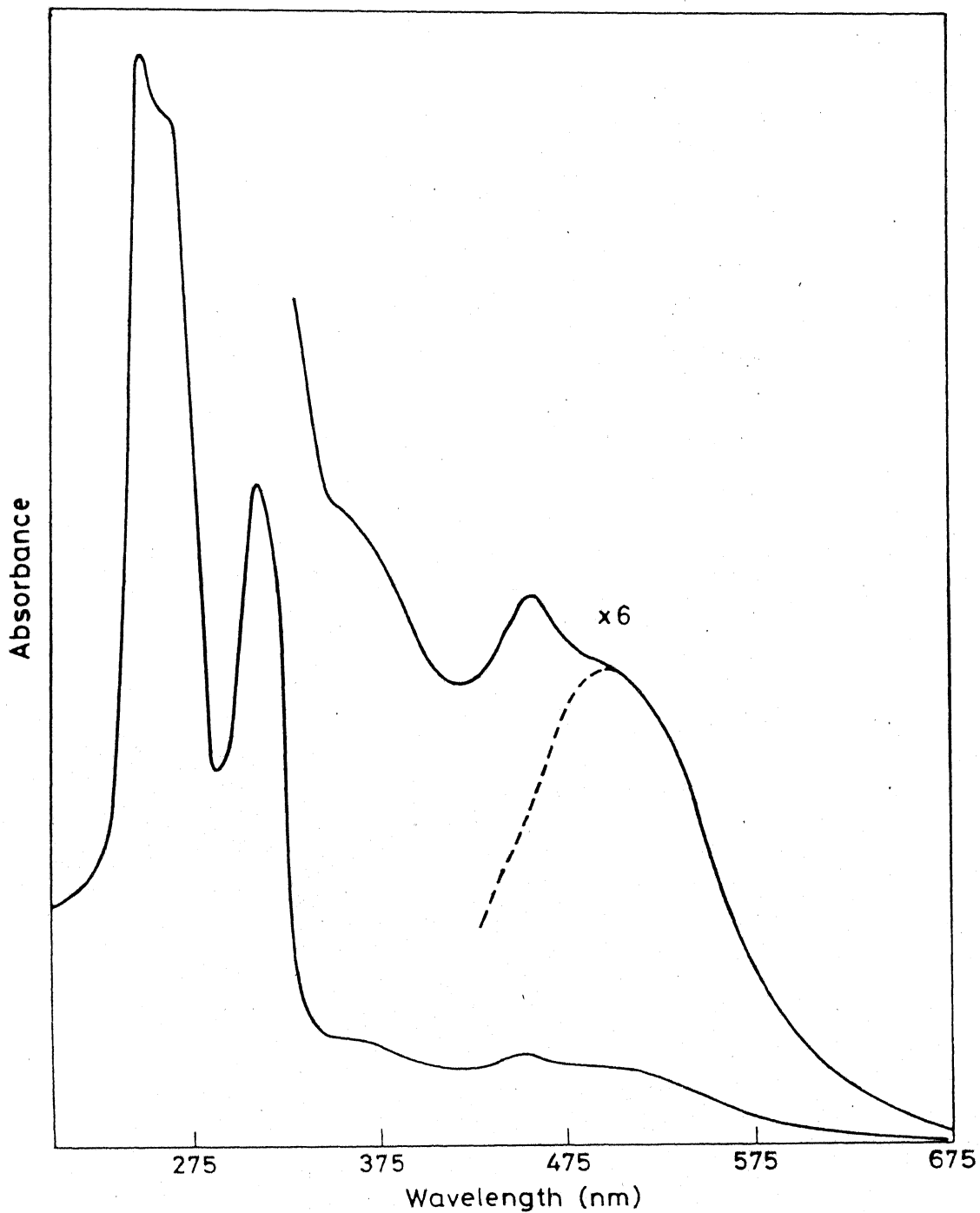
Fig. 4.7   Electronic spectrum of $[Cl(bpy)_2RuNCSRu(bpy)_2(NCS)]$-
BPh_4 in acetonitrile.   The shoulder towards the lower
energy side is prominent and the dashed line shows the
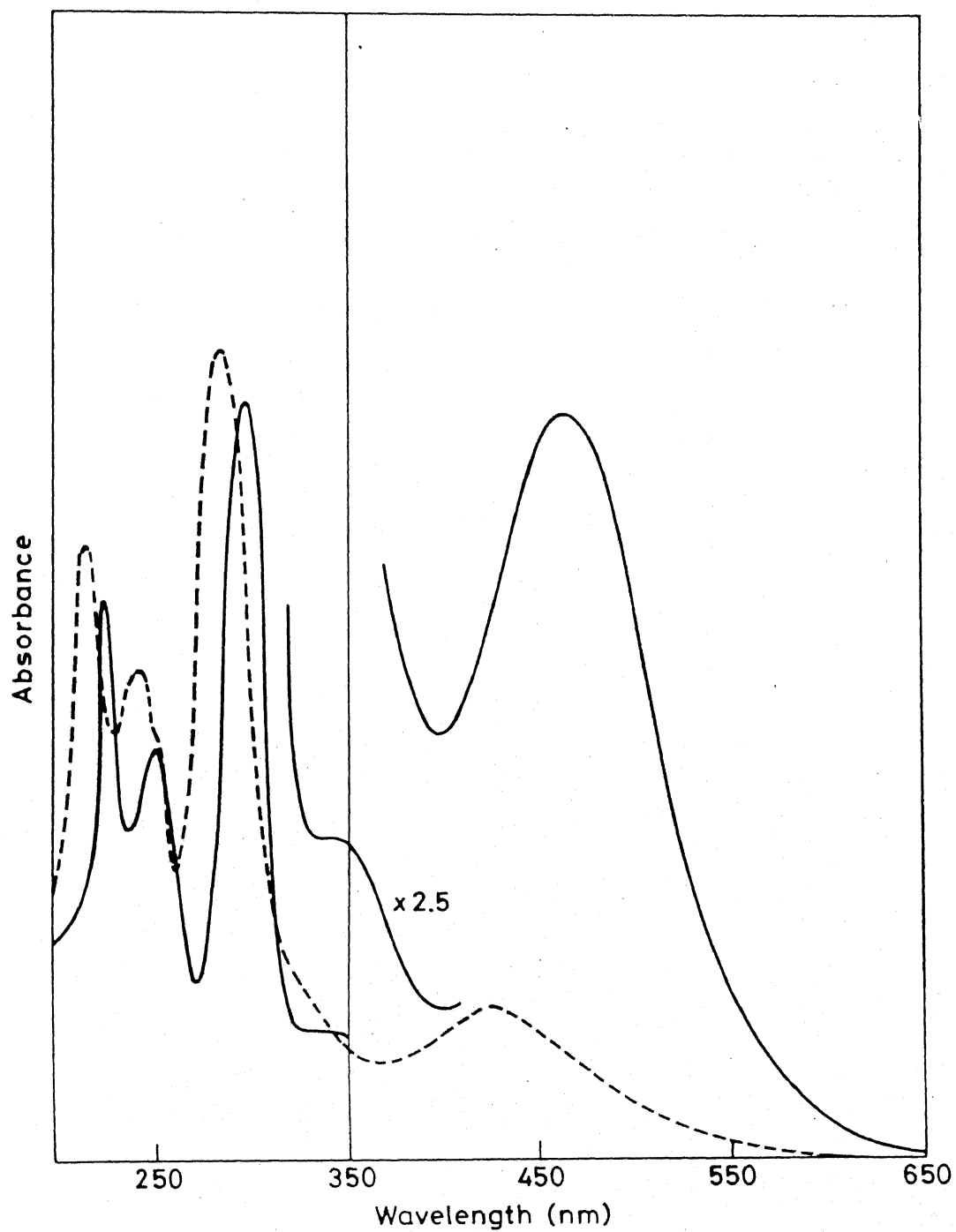band profile assuming a guassian shape.

Fig. 4.8 Electronic spectra of (22) (———) and (33) (----) compounds of $[Cl(bpy)_2RuNCSRu(bpy)_2Cl]^{n+}$ in aceto-nitrile.

The IT bands for (23) complexes in acetonitrile were located at around 950 and 945 nm, respectively for the thiocyanato- and selenocyanato bridged compounds (Figs. 4.9 and 4.10). The experimentally observed FWHM of these bands were in good agreement with the Hush model calculated FWHM (cf. Table 4.13). The solvatochromism associated with these bands conformed well with the dielectric continuum model (cf. Tables 4.11 and 4.12). A linear correlation of the E_{op} with $(1/n^2 - 1/D)$ of the solvents has been obtained for both these compounds, from which the E_{in} and E_{out} values were calculated (Figs. 4.11 and 4.12). As discussed earlier, the different parameters, such as f, D, $|M|$ and α have been calculated and are presented in Table 4.13. A value of ~7 Å have been chosen for the distance separating the metal centers in the [RuNCXRu] unit.[10]

4.5 Emission Spectral Studies

The emission characteristics of linkage isomers of penta-amminethiocyanatoruthenium(III) have been discussed in Section 3.4. Emission properties of the 2,2'-bipyridine complexes are discussed herein. Eversince the excited state redox properties of the simple compound $[(bpy)_3Ru]^{2+}$ have been understood and have been utilized in photoreduction of water,[7c-e] there is an expanding interest in the emission properties of the transition metal -2,2'-bipyridine complexes.[93] Hence, an investigation of the emission properties of the 2,2'-bipyridine complexes
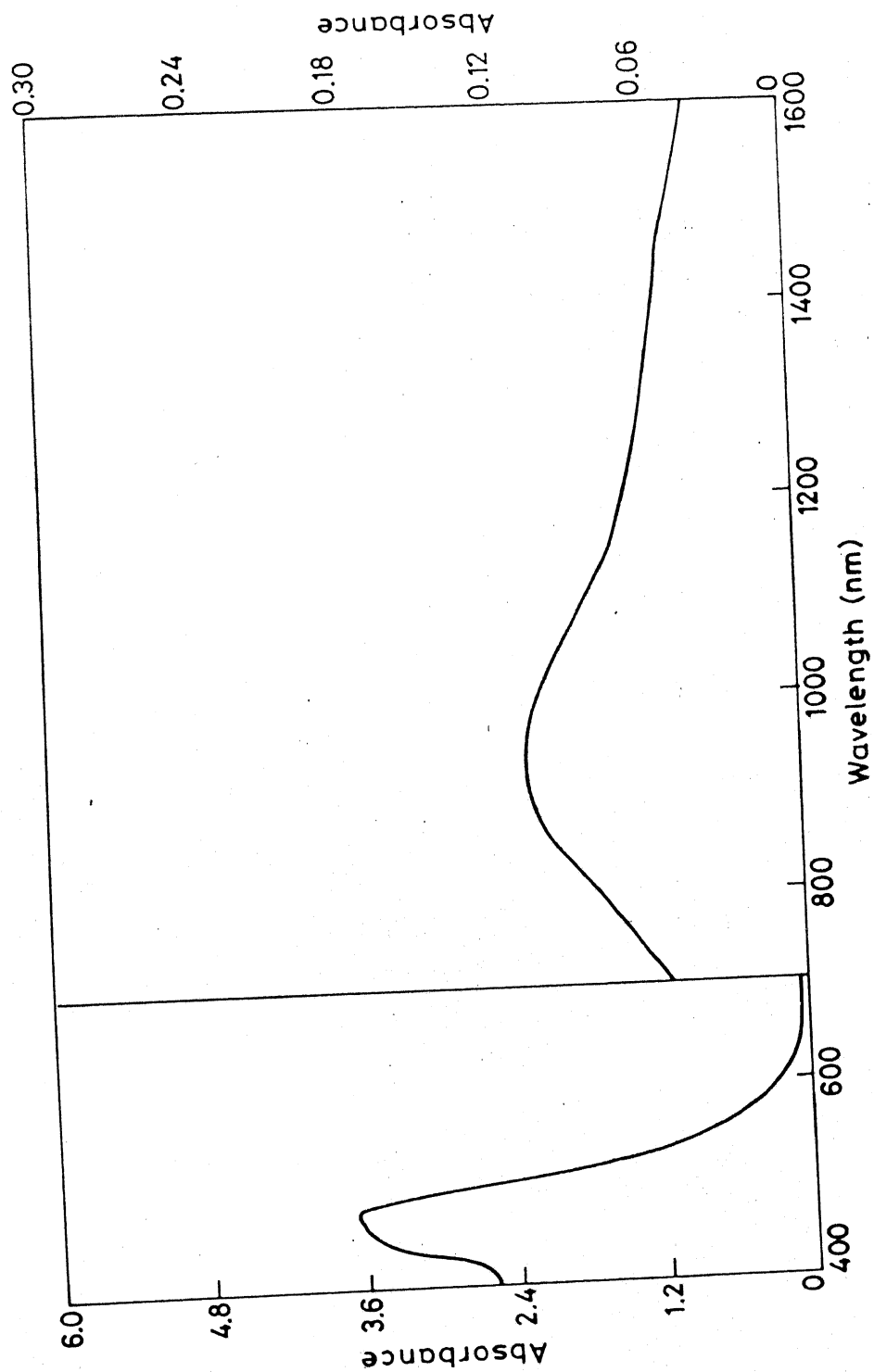
Fig. 4.9   NIR and Visible spectrum of   [Cl(bpy)$_2$RuNCSRu(bpy)$_2$ Cl]$^{2+}$ in acetonitrile.   The concentration was 10^{-3} M.
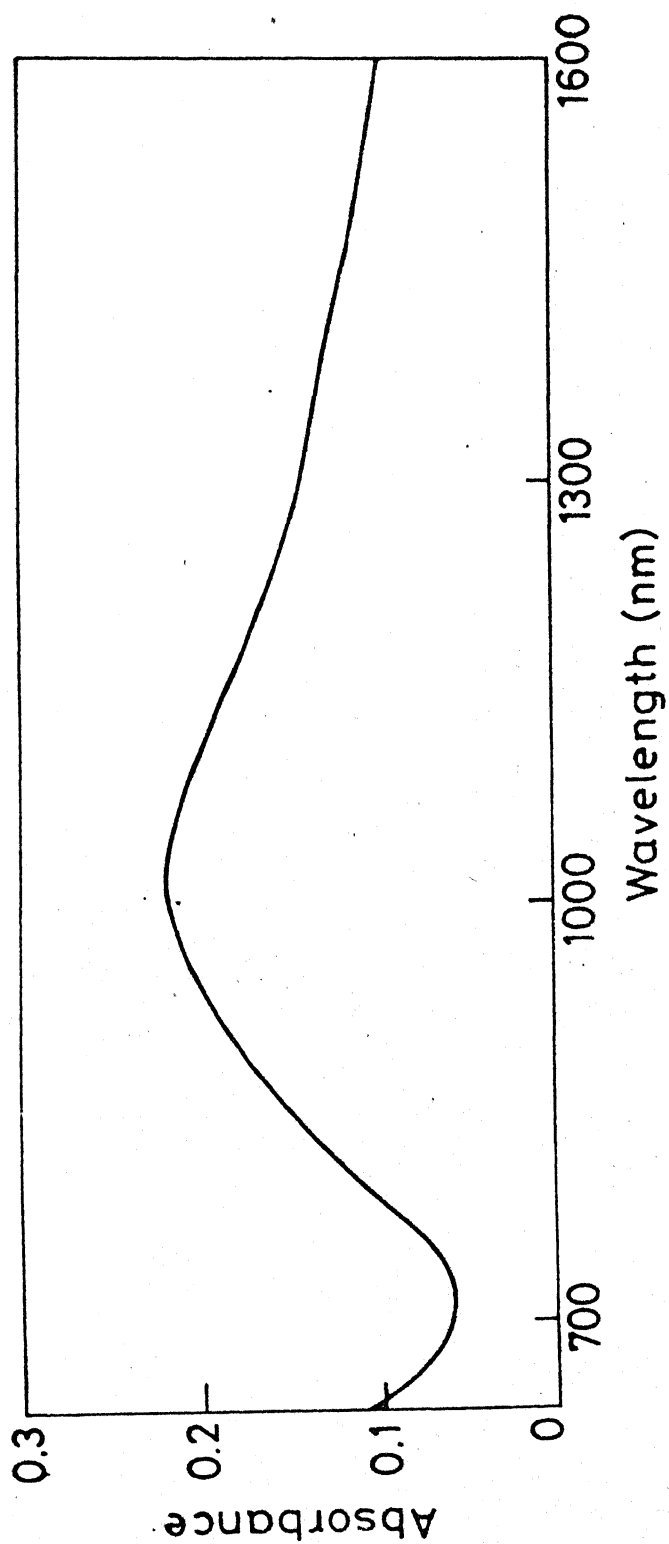
Fig. 4.10 NIR spectrum of $[Cl(bpy)_2RuNCSeRu(bpy)_2Cl]^{2+}$ in acetonitrile. The concentration used is 5×10^{-4} M.
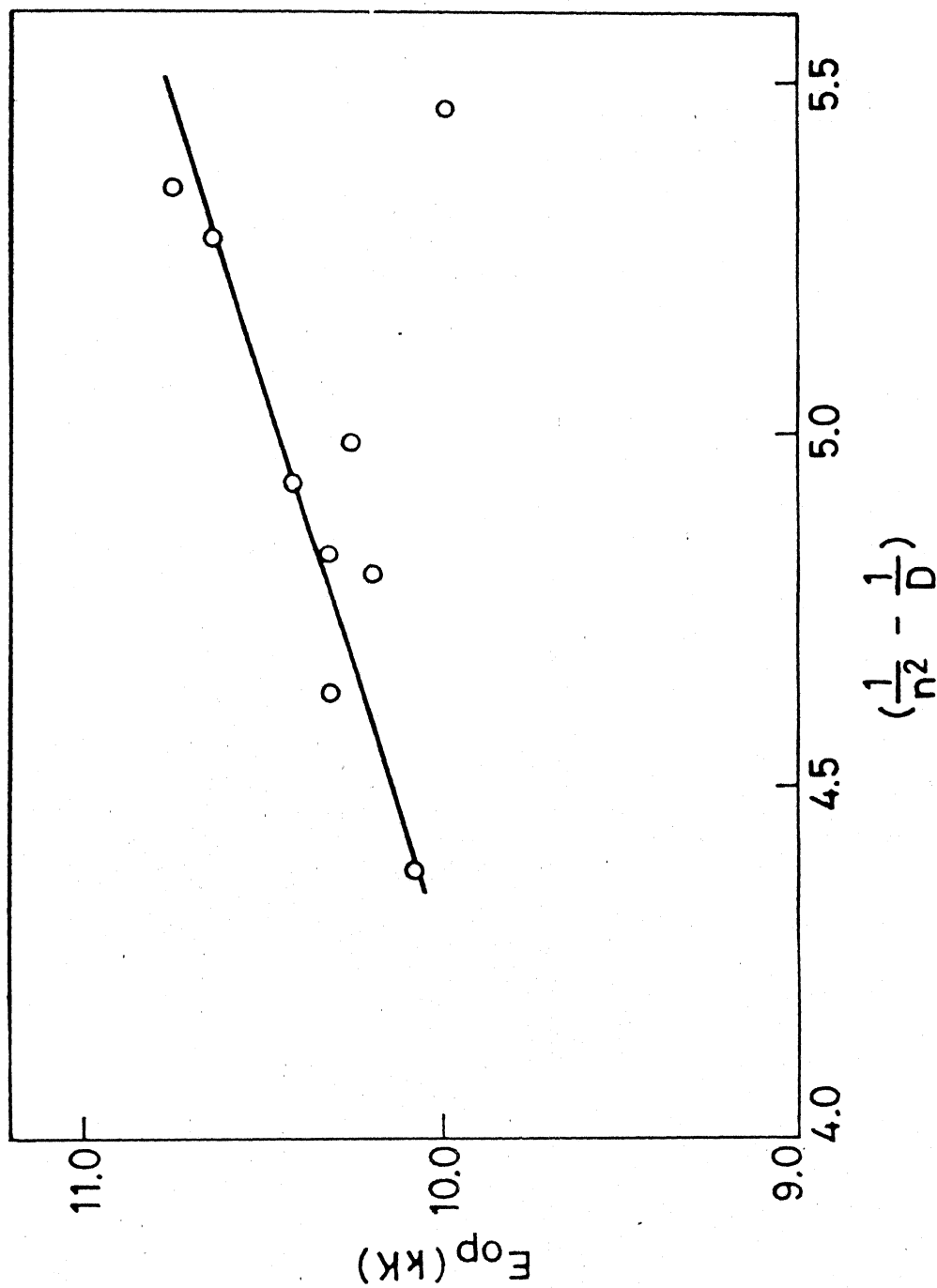
Fig. 4.11 Plot of $(1/n^2 - 1/D)$ vs. E_{op} for the IT transition of $[Cl(bpy)_2RuNCSRu(bpy)_2Cl]^{2+}$ ion. $E_{in} = 7265$ cm^{-1}; $E_{out} = 3490$ cm^{-1} in CH_3CN.
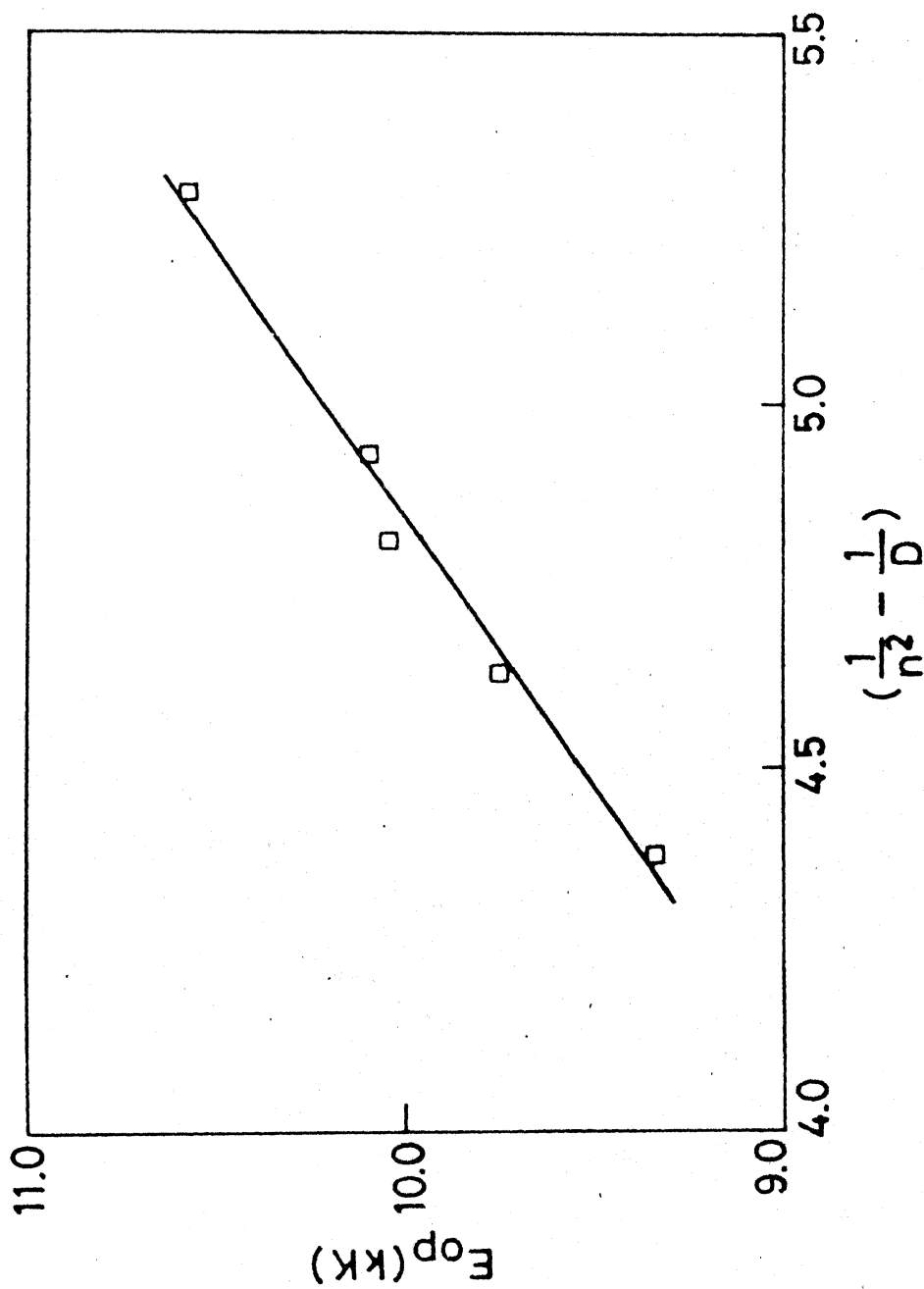
Fig. 4.12 Plot of $(1/n^2 - 1/D)$ vs. E_{op} for the IT transition of $[Cl(bpy)_2RuNCSeRu(bpy)_2Cl]^{2+}$ ion. E_{in} = 3750 cm^{-1}; E_{out} = 7110 cm^{-1} in CH_3CN

Table 4.11 :   Solvent Dependent NIR Spectral Data for

$[Cl(bpy)_2RuNCSRu(bpy)_2Cl]^{2+}$ [a]
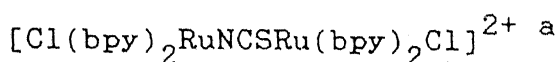
Solvent	$(1/n^2 - 1/D)$ [b]	$\bar{\nu}_{IT}$ (cm^{-1})	ϵ_{IT} (M^{-1} cm^{-1})
Water	0.546	10000	
Methanol	0.535	10753	
Acetonitrile	0.528	10638	411
Ethanol	0.499	10256	
Acetone	0.493	10417	387
N-Methyl formamide	0.483	10309	
Propylene carbonate	0.481	10204	
N,N-Dimethyl formamide	0.463	10309[c]	185
Dimethyl sulfoxide	0.438	10080	

a, Tetraphenylborate salt; the spectra obtained for the solid in acetonitrile was identical with that for species generated in situ by $[Fe(bpy)_3]^{3+}$ oxidation in acetonitrile; Typical concentration ~5 x 10^{-3} M.

b, Taken from ref. 65.

c, The compound decomposes in DMF solution as seen from the extinction coefficient value viz., 185 M^{-1} cm^{-1}.

Table 4.12 : Solvent Dependent NIR Spectral Data for

$$[Cl(bpy)_2RuNCSeRu(bpy)_2Cl]^{2+ \; a}$$
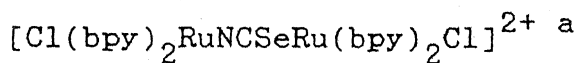
Solvent	$(1/n^2 - 1/D)^b$	$\bar{\nu}_{IT}$ (cm^{-1})	ϵ_{IT} (M^{-1} cm^{-1})
Acetonitrile	0.528	10582	450
Acetone	0.493	10101	493
Propylene carbonate	0.481	10050	
N,N-Dimethyl formamide	0.463	9756	
Dimethyl sulfoxde	0.438	9346	

a, Tetraphenylborate salt; the spectra obtained for the solid in acetonitrile was identical with that for species generated in situ by [Fe(bpy)$_3$]$^{3+}$ oxidation in acetonitrile except for a slight decrease in the extinction coefficient.

b, Taken from ref.65.

Fig. 4.13 Absorption (a) and emission (c) spectra of
(bpy)$_2$Ru(NCS) Cl and absorption (b) and
emission (d) spectra of Cl(bpy)$_2$RuNCSRu-
(bpy)$_2$Cl BPh$_4$ in acetonitrile . The $_{ex}$ for
emission spectra is 457.9nm.

synthesized in this study was undertaken and the results are presented in the following paragraphs.

Emission spectra for [(bpy)$_2$Ru(NCX)Cl] and [Cl(bpy)$_2$Ru-NCXRu(bpy)$_2$Cl]BPh$_4$ were obtained in the solid state and in solutions at room temperature and they are illustrated in Figs. 4.13 and 4.14. The relevant data are presented in Table 4.14. The excitation sources used were Ar$^+$ ion laser lines. The spectra were uncorrected for instrumental factors. Due to the local burning of the samples by the high power laser, the evaluation of emission quantum yields presented difficulties. However, an upper limit of ϕ_{em} << 0.01 was obtained (cf. Experimental Section). Hence, these compounds seem to be weak emitters. A few of the observations emerged from these studies are the following:

(a) The (22) dimer emission is approximately 5-10 folds less than that of the monomer, i.e., the dimer emission is quenched considerably as compared to that of the monomer. This could be due to the coordination of the second [(bpy)$_2$Ru]$^{n+}$ unit in the dimeric complex. The situation is somewhat similar to the quenching of the fluorescence observed in the tris(4-nitro-2,2'-bipyridine)ruthenium(II) complex. The tris(2,2'-bipyridine)-ruthenium(II) is luminescent and when a strongly electron withdrawing group, such as NO$_2^-$ is substitued at the 4-position of 2,2'-bipyridine, the π^* orbital has been found to be stabilized by ~3750 cm^{-1}. Resonance Raman studies of this
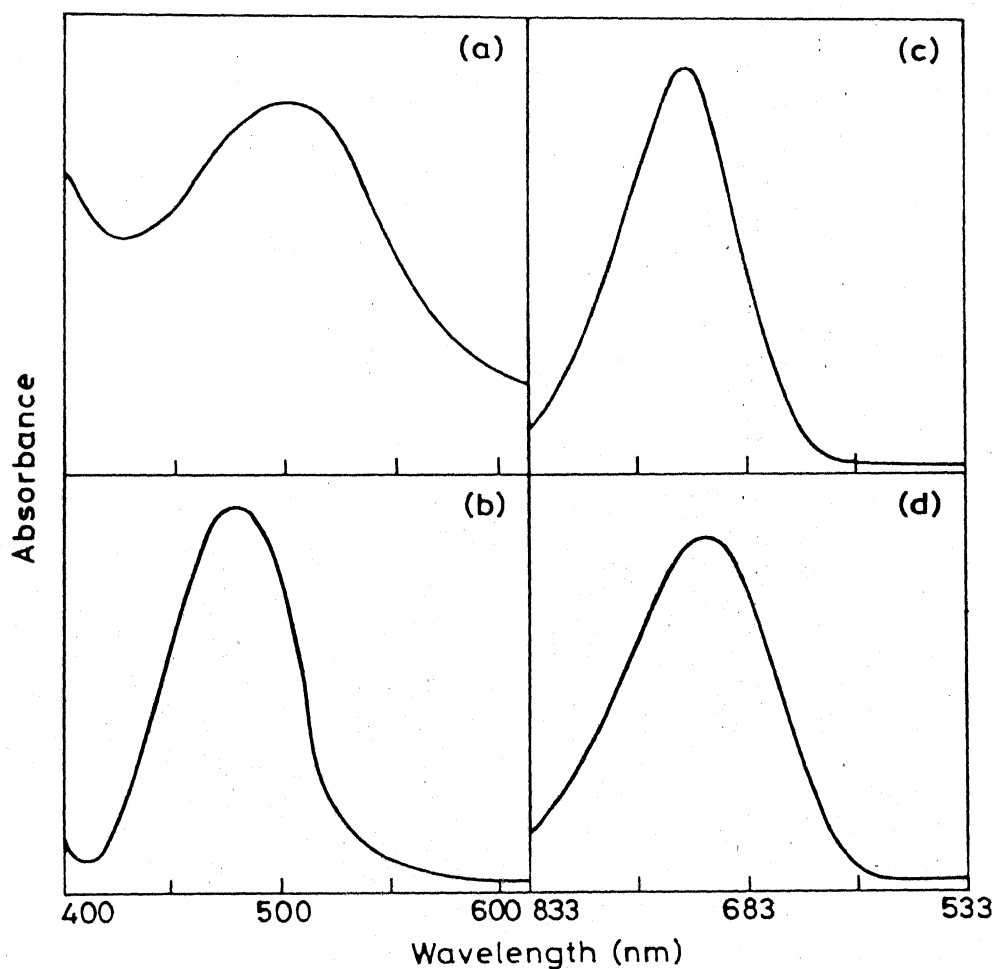
107
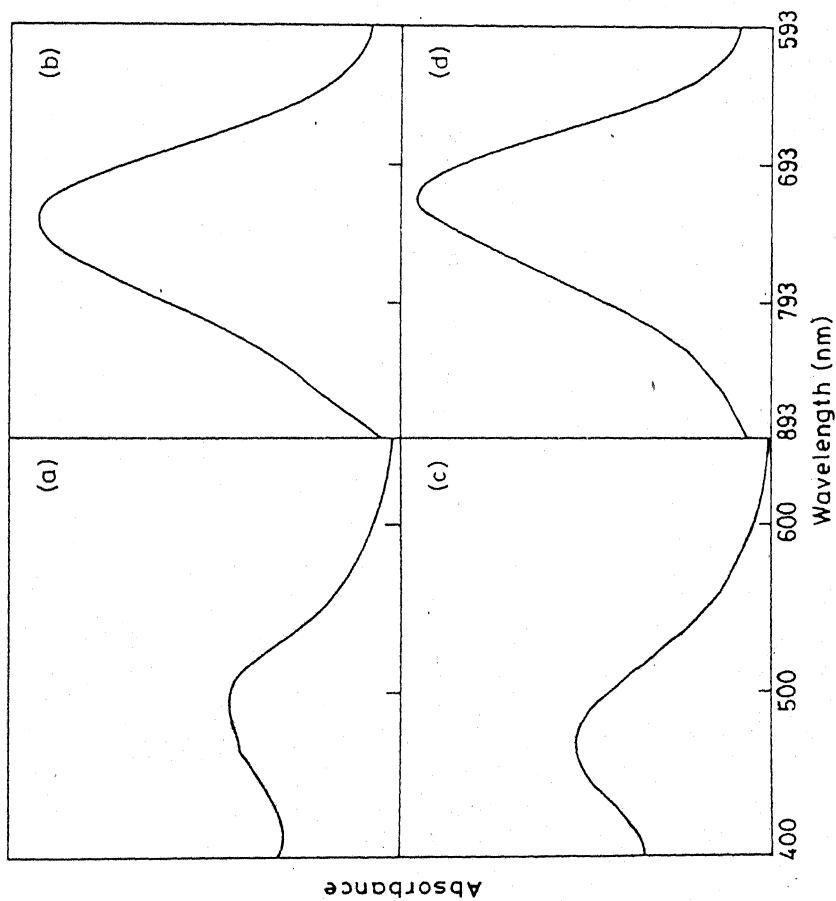
Fig. 4.14 Absorption (a) and emission (b) spectra of [(bpy)$_2$Ru(NCSe)Cl].2H$_2$O and absorption (c) and emission (d) spectra of [Cl(bpy)$_2$RuNCSeRu(bpy)$_2$-Cl]BPh$_4$ in acetonitrile. The λ_{ex} for emission spectra is 524.5 nm.

Table 4.13. Characteristic Parameters Calculated from IT Bands and Hush Formulas.

Compound	Solvent	$\tilde{\nu}_{IT}$ (cm⁻¹)	ϵ_{IT} (M⁻¹ cm⁻¹)	$\Delta\tilde{\nu}_{1/2(exp)}$ (cm⁻¹)	$\Delta\tilde{\nu}_{1/2(calc)}$ (cm⁻¹)	$10^2 \cdot f$	D (Å)	$10^{10} \cdot |M|$ (Å esu)	H_{AB} (cm⁻¹)	$10^3 \cdot \alpha^2$
$[(NH_3)_5RuNCSRu(NH_3)_5]^{4+}$	water	5920	331	929	3800	-	-	-	-	Delocalized
$[(CN)_5FeNCSFe(CN)_5]^{6-}$	water	7692	670	3553	4215	1.10	0.36	1.74	396	5.3
$[(CN)_5FeNCSFe(CN)_5]^{6-}$	water	7911	730	3086	4275	1.04	0.35	1.67	391	5.0
$[Cl(bpy)_2RuNCSRu(bpy)_2Cl]^{2+}$	aceto nitrile	10638	411	5464	4959	1.03	0.30	1.44	453	1.85
	acetone	10417	387	6286	4905	1.12	0.32	1.51	466	2.02
$[Cl(bpy)_2RuNCSeRu(bpy)_2Cl]^{2+}$	aceto nitrile	10582	450	5445	4994	1.13	0.31	1.51	465	1.90
	acetone	10101	493	4463	4830	1.01	0.30	1.46	425	1.76

Table 4.14: Emission Spectral Data[a]

λ_{ex} (nm)	$[(bpy)_2Ru(NCSe)Cl] \cdot 2H_2O$		$[Cl(bpy)_2RuNCSeRu(bpy)_2Cl]BPh_4$	
	λ_{em} (cm^{-1})	$\Delta\bar{\nu}_{1/2}$ (cm^{-1})[b]	λ_{em} (cm^{-1})	$\Delta\bar{\nu}_{1/2}$ (cm^{-1})[b]
457.9	14240	2360	13560	2440
476.5	14280[c]	2500[c]	14775[c]	3220[c]
			~16300sh	
514.5	14425	2220	13380	2500
			(14100)[c]	(2500)[c]

a, Spectra were recorded using solid samples; error ±50 cm^{-1}.

b, FWHM.

c, Spectra recorded in acetonitrile solution.

nitroderivatized complex suggest that the excited state of the MLCT has a significant portion of the charge localized on the nitro group. Since the nitro groups are strongly coupled to the solvent molecules, the fluorescence of the tris(nitrobipyridine)-ruthenium(II) is quenched by an efficient radiationless deactivation of the excited state.[94] In a binuclear complex, the second metal center can act[93] similarly and depending on the extent of coupling between the metal centers the emissive state can be partially or fully deactivated. Such an effect of the coordination of the second $[(bpy)_2Ru]^{n+}$ unit has been reported recently by several workers.[93] Thus, the withdrawal of electron density by the second $[(bpy)_2Ru]^{n+}$ unit from the first metal center and thereby providing pathway for an efficient nonradiative deactivation of the emissive state is suggested to be the reason for the quenching of emission for the dimers.

(b) The emission maxima for the dimeric compounds are red shifted by approximately 1000 cm^{-1} from those of the monomeric compounds. This red shift is a strong evidence for the interaction between the metal centers via the chalcogenocyanate bridges.

(c) Excitation spectra of these emissions for monomers and dimers suggest that within the excitation interval employed, i.e. 514.5-457.7 nm, the excitation leads to the population of the same emissive state. The excitation of the selenocyanate bridged (22) dimer (λ_{max} = 469 nm) at 476.5 nm yielded an emission

spectrum at room temperature, which exhibited a clear shoulder (Fig. 4.15). The separation of the shoulder from the prominent emission maximum viz., 1500 cm^{-1} suggests that this might be a vibrational structure. The vibrational mode of the 2,2'-bipyridine ring observed at around 1480 cm^{-1} seems to be strongly coupled with the MLCT excited state and thus, it seems that the emissive state is localized mainly on the 2,2'-bipyridine coligands. This is borne out by the solvatochromism (Table 4.14) associated with the emission maxima of these bands and resonance Raman Studies (vide supra).

(d) The luminescence of the selenocyanate compounds are quenched by approximately 10 folds as compared to their thiocyanate analogs. This must be due to larger -interaction in selenocyanate complexes as compared to the thiocyante compounds (cf. Section 4.9).

(e) The solvatochromism associated with the dimer emission was considerably larger than that of the monomer emission.

4.6 Resonance Raman Spectral Studies

Earlier studies[93-96] show that the laser excitation in the intense visible absorption bands of bis- and tris(polypyridyl)-ruthenium(II) complexes yield detailed resonance Raman Spectra above 1000 cm^{-1}, characteristic of the coordinated polypyridyl units. Excitation of $[(bpy)_3Ru]^{2+}$ using different Ar$^+$ ion laser

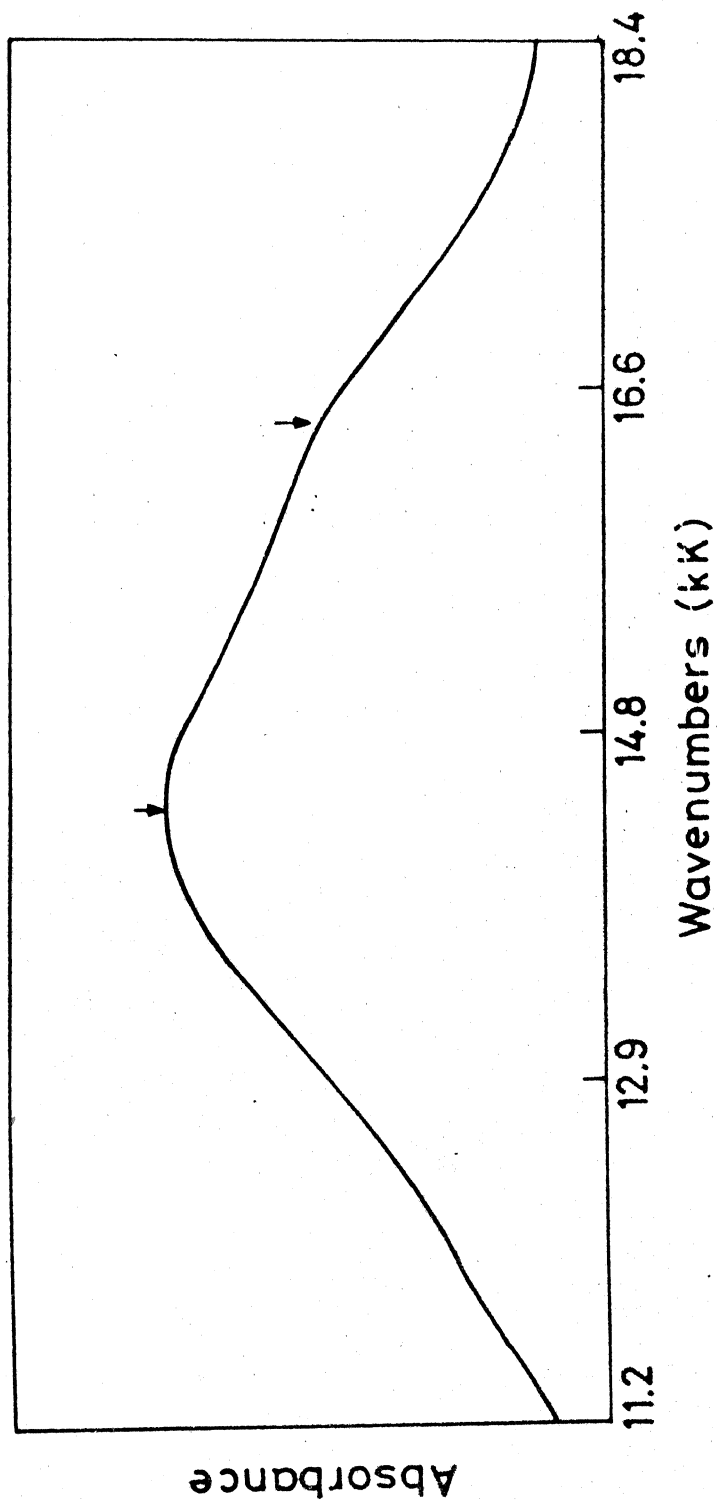Fig. 4.15 Emission spectrum of the dimer , [Cl(bpy)$_2$RuNCSe Ru(bpy)$_2$Cl]BPh$_4$ in acetonitrile (λ_{max} = 469 nm).

The λ_{ex} for emission spectra is 476 nm.

lines in the interval 457.9-514.5 nm that overlap the MLCT bands to different degrees yielded an excitation independent seven line characteristic pattern for the coordinated 2,2'-bipyridine ligand.[96] In contrast, detailed resonance Raman spectral studies, on a few bis(bipyridyl)ruthenium(II) complexes having various diimine bridging ligands showed marked dependence on the excitation wave lengths. Depending on the excitation within the two different MLCT terminating at the π^* orbitals of the "spectator" 2,2'-bipyridine ligands and the bridging diimine the corresponding modes were found to be enhanced in intensity. Thus, an unambiguous assignment of the visible absorption bands in these complexes was possible.[93a]

Such an exercise was not possible in our study, as the MLCT transitions associated with the 2,2'-bipyridine and the bridging thiocyanate and selenocyanate groups are overlapping to a large extent. However, excitation of the monomeric and dimeric 2,2'-bipyridine complexes, atleast, in two different wavelength within the Ar^+ ion laser lines yielded convincing results. Excitation of [(bpy)$_2$Ru(NCS)Cl] at 514.5 nm ($\nu_o - \nu_e = 485$ cm^{-1}; cf. Table 4.15) yielded the enhancement in the intensities of the 2,2'-bipyridine vibrational modes along with a few low frequency modes attributable to ν(Ru-N) of the 2,2-bipyridine unit. When the exciting wave length was changed to 457.9 nm ($\nu_o - \nu_e = 1920$ cm^{-1}), the RR spectrum obtained showed bands at 2120 and 810 cm^{-1} (w,br) along with the characteristic vibrations of 2,2'-bipyridine, which were somewhat reduced in intensity. These bands at 2120
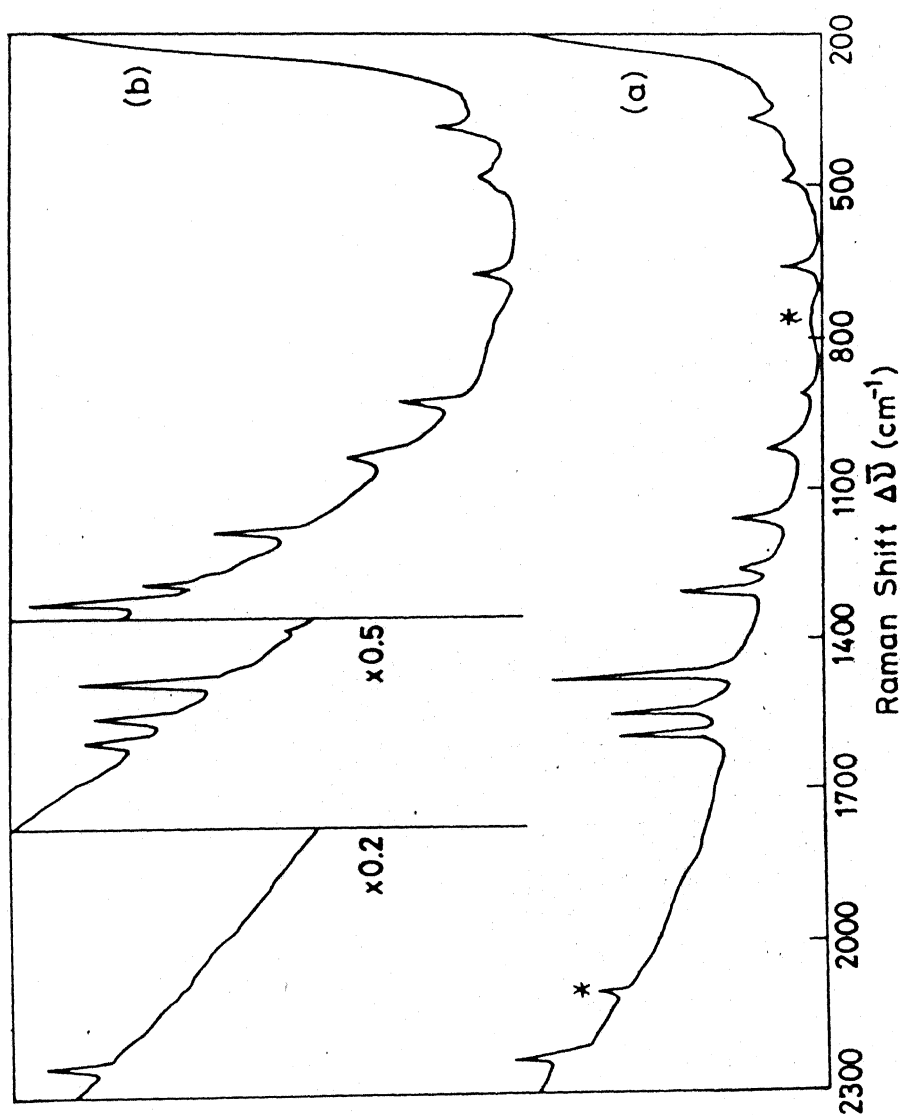
Fig. 4.16 Resonance Raman spectra of [Cl(bpy)$_2$RuNCSRu(bpy)$_2$Cl]-BPh$_4$ in acetonitrile with (a) 457.9 and (b) 514.5 nm excitation wave lengths. Intensity reference is the 2249 cm^{-1} (ν(CN)) band of the acetonitrile solvent. Spectral slitwidth (a) 6 cm^{-1} and (b) 8 cm^{-1}. Laser power: 100 mW. The peaks marked with asterisks are

Table 4.15 : Resonance Raman Spectral Data[a] in cm^{-1}

| [Ru(bpy)$_2$(NCS)Cl].2H$_2$O | | [Cl(bpy)$_2$RuNCSRu(bpy)$_2$Cl]BPh$_4$ | |
λ_{ex} = 514.5 nm	λ_{ex} = 457.9 nm	λ_{ex} = 514.5 nm	λ_{ex} = 457.9 nm
379 (0.8)	378 (0.6)	373 (3.4)	375 (3.5)
489 (0.8)[b]	485 (1.3)[b]	487 (0.6)[b]	486 (0.6)[b]
661 (0.7)	661 (0.7)	660 (0.6)	663 (0.7)
	*808 (1.0)	*777(br)	-
1021 (0.7)	1020 (0.4)	1035 (1.8)	1035 (2.3)
1035 (0.6)			
1163 (1.7)	1160 (0.8)	1157 (2.3)	1159 (3.3)
1265 (0.8)	1265 (0.4)	1279 (2.0)	1280 (3.0)
1307 (2.1)	1310 (1.1)	1321 (3.3)	1320 (5.4)
1486 (6.1)	1485 (3.9)	1482 (6.8)	1480 (9.2)
1560 (3.5)	1558 (2.4)	1554 (2.9)	1555 (3.9)
1606 (2.2)	1603 (1.1)	1598 (3.1)	1600 (4.9)
	*2120 (1.2)	*2146(w)	-

a, Spectra recorded using acetonitrile solutions in capillaries. relative intensity values in parentheses were calculated with reference to the ν(CN) band of acetonitrile. The peaks denoted by asterisks are due to coordinated thiocyanate ions.

b, The peak at around 485 cm^{-1} is very broad.

Table 4.16 :   Resonance Raman Spectral Data[a] in cm^{-1}

| [Ru(bpy)$_2$(NCSe)Cl].2H$_2$O | | [Cl(bpy)$_2$RuNCSeRu(bpy)$_2$Cl]BPh$_4$ | |
λ_{ex} = 476.5 nm	λ_{ex} = 457.9 nm	λ_{ex} = 476.5 nm	λ_{ex} = 514.5 nm
302	-	-	326
374 (10)	373 (3.0)	373 (3.3)	376 (1.7)
494 (6)[b]	489 (2.5)[b]	489 (4.0)[b]	468 (1.0)[b]
			496 (1.0)
1022 (15)	1021 (4.1)	1021 (4.3)	1020 (1.7)sh
			1036 (2.2)
1166 (20)	1166 (6.0)	1161 (7.0)	1160 (4.0)
1266 (13)	1265 (5.0)	1261 (4.3)	1264 (1.6)
1310 (38)	1309 (10)	1305 (11)	1307 (3.2)
1478 (78)	1480 (21)	1477 (26)	1480 (9.9)
1550 (55)	1550 (17)	1553 (17)	1556 (5.6)
1594 (53)	1593 (15)	1597 (15)	1600 (5.0)
	*2120 (2.0)		*2128 (1.0)(w)
2249 (10)	2250 (10)	2251 (10)	2250 (10)

a, Spectra were recorded using acetonitrile solutions in 1 mm i.d. capillary tubes; the relative intensity values in parentheses were calculated using the ν(CN) of CH$_3$CN as the reference; the peaks denoted by asterisks are due to coordinated selenocyanate ions.

b, Broad bands.

and 810 cm^{-1} were attributed to the ν(CN) & ν(CS) mode of vibrations of the coordinated thiocyanate group. The same effect was observed with analogous selenocyanate compound. [(bpy)$_2$Ru(NCSe)Cl], when excited with laser lines at 457.9 and 476.5 nm showed enhancement in the intensity of the vibrational modes corresponding to the coordinated 2,2'-bipyridine to different degrees. However, the exitation of this compound with 457.9 nm line showed the vibrational bands corresponding to ν(CN) and ν(CSe). These observations suggest that in these compounds the lowest energy CT band in the visible region corresponds to the dπ(Ru)-π_1^* (bpy) CT while, the higher energy shoulder to this prominent band should have considerable contributions from the dπ(Ru) --- 3π(NCX$^-$) CT.

Similarly, excitation at 457.9 nm ($\nu_o - \nu_e = 147$ cm^{-1}) and 514.5 nm ($\nu_o - \nu_e = 2545$ cm^{-1}) of the thiocyanato bridged (22) dimer, [Cl(bpy)$_2$RuNCSRu(bpy)$_2$Cl]BPh$_4$ yielded the enhancement in intensities of the vibrational modes of the coordinated 2,2'-bipyridine and thiocyanate groups. The excitation at 514.5 nm of the dimer showed weak band due to ν(CN) at 2146 cm^{-1} and a broad and weak band due to ν(CS) at around 777 cm^{-1}. Analogous results were obtained for the selenocyanate bridged dimer, [(bpy)$_2$RuNCSeRu(bpy)$_2$Cl]BPh$_4$ with excitations at 476.5 and 514.5 nm. These results suggest that the dπ(Ru) --- 3π(NCX$^-$) CT lies towards the lower energy side of the prominent band in the dimeric complexes, i.e., the Ru --- NCX$^-$ CT is red-shifted when going from a monomer to a NCX$^-$ bridged (22) dimer (cf. section

4.4). This suggests that the $3\pi(NCX^-)$ acceptor orbitals are stabilized in the dimer.[93a] This stabilization is a direct outcome of the interaction of the 3π-acceptor orbitals of the chalcogenocyanate with the $d\pi$-donor orbitals of the second metal center in the dimeric complex.

Lack of facilities to excite these compounds at further higher and lower frequencies of the MLCT bands did not allow us to clarify this point categorically.

4.7 Mössbauer Spectral Studies

The less frequently[69,97] available Mössbauer data for the ligand-bridged pentacyanoferrate dimers prompted us to carry out Mössbauer studies on the pentacyanoferrate dimers synthesized in this study. The Mössbauer (^{57}Fe) spectra for the (33) and (23) compounds were recorded at room temperature using polycrystalline samples. The values for the isomer shift (δ) quadrupole splitting parameter (ΔE_Q) and line width (Γ) were obtained by a least-squares fit of the experimental spectrum for Lorentzian line shapes. The numerical values are presented in Table 4.17. Though the isomer shift values of the iron centers in different oxidation states are in an acceptable range with the previously reported values,[97b,c] there seems to be a discrepancy in the values for quadrupole splitting parameters, especially in (33) species. These (33) compounds exhibited markedly lower values for ΔE_Q. A tentative explanation is that the electric field gradient (q) created by the NCX^- on the two iron centers might be

Table 4.17: Mössbauer Data

Compound	δ mm s^{-1}	ΔE_Q mm s^{-1}	Γ mm s^{-1}
Fe^{III}NCSFe^{III}	-0.126	0.134	0.142
Fe^{III}NCSeFe^{III}	-0.122	0.0^b	0.176
Fe^{III}NCSFe^{II}	-0.121	0.0	-
	-0.061	1.017	0.168
	-0.120	2.024	0.231
Fe^{III}NCSeFe^{II}	-0.120	0.0	-
	-0.041	1.999	0.136
	-0.093	0.636	0.317

a, Values with respect to natural iron;

b, The line could not be resolved.

symmetric and approximately equal, resulting in a near equivalence of the iron centers and hence lowering the ΔE_Q values.[98] The (23) compounds exhibited a pair of doublets corresponding to different iron centers in the +2 and +3 oxidation states. The samples underwent decomposition after the irradiation as seen from the spurious signal at around $\delta = -0.121$ mm s^{-1} which appeared and grew in intensity in the course of time. The lower intensity of this signal in the SeCN$^-$ bridged dimer compared to that of the SCN$^-$ bridged dimer may be understood in terms of the lesser stability of the SCN$^-$ bridged (23) species as evident from the K_c values (cf. Table 4.20).

4.8 Electrochemical Studies

(a) $[(NH_3)_5Ru]^{n+}$ System:

The cyclic voltammogram of the $[(NH_3)_5RuSCNRu(NH_3)_5]^{n+}$ species showed two one-electron reduction waves (Fig. 4.17) one having a maximum at around 0.325 V and the other around 0.575 V with practically no anodic peaks in the first scan (scan rate, 120 mV s^{-1}). The cathodic maximum around 0.575 V exhibited the anodic counterpart around 0.5 V after the second scan, suggesting quasiirreversibility of the process ($E_{1/2}$ = 0.538 V; ΔE_p = 75 mV). After third scan, the cathodic peak around 0.325 V started disappearing with the appearance of a new peak around 0.2 V. It suggested the formation of an intermediate which was possibly disproportionating, with one of the disproportionation products having ruthenium in the +3 oxidation state. The aquation of the electrogenerated intermediate may lead to the formation of $[(NH_3)_5RuSCN]^{2+}$. This inference is understandable by the fact that after the third scan the system was showing the same redox behavior as that of $[(NH_3)_5RuSCN]^{2+}$.

The equilibrium between the mixed-valence (23), completely oxidized (33) and completedly reduced (22) moieties is also a possibility if the half-wave potentials of the two one-electron redox processes are close enough.[99] Such an equilibrium between mixed-valence and (33) moities can explain the following tentative scheme.
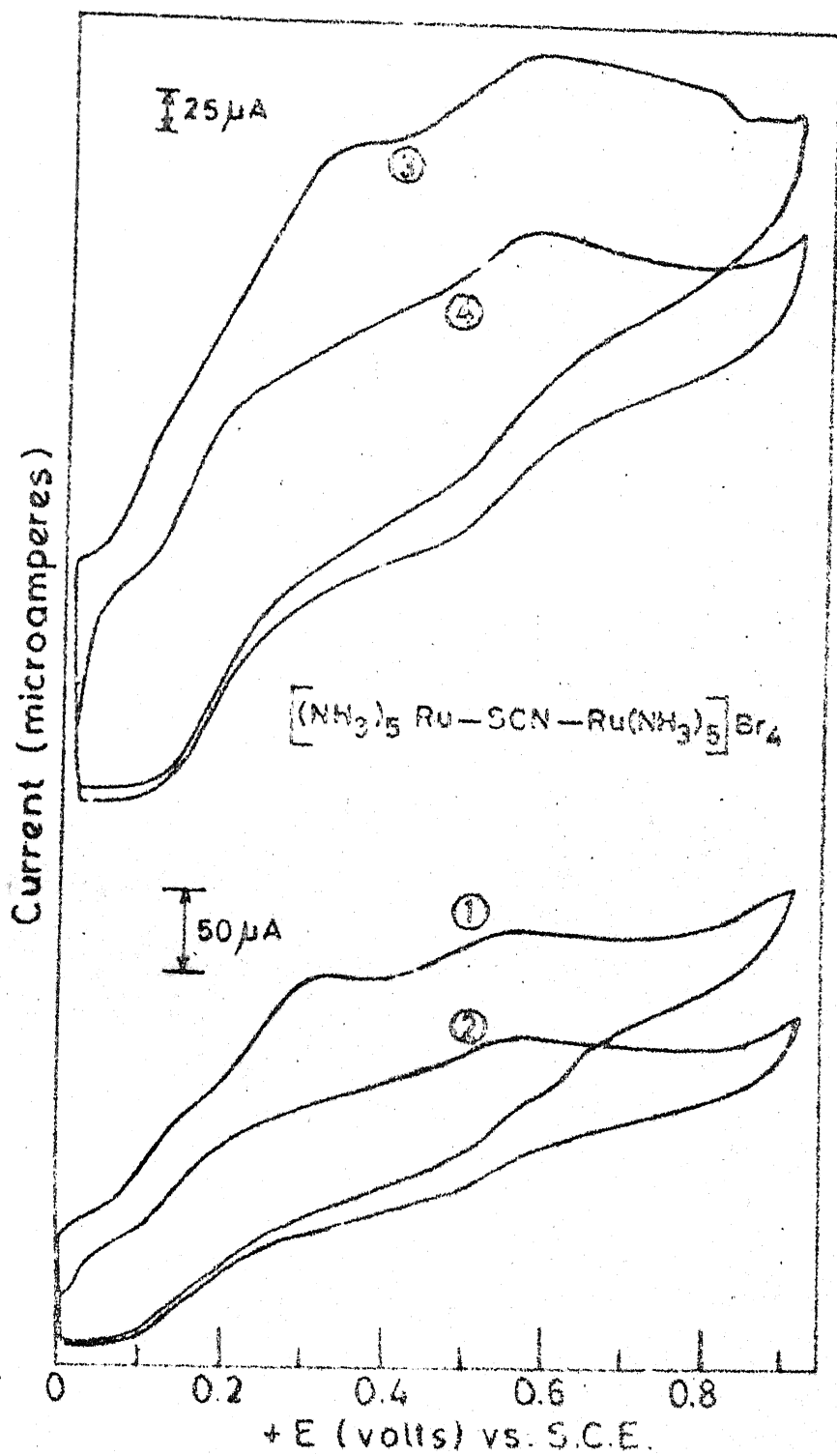
Fig. 4.17 Cyclic voltammograms for $[(NH_3)_5RuNCSRu(NH_3)_5]^{4+}$ ion.

$$\text{Ru(III)-SCN-Ru(III)} \xrightarrow{0.325 \text{ V}} \text{Ru(II)-SCN-Ru(III)}$$

$$\text{Ru(II)-SCN-Ru(III)} \xrightarrow{0.575 \text{ V}} \text{Ru(II)-SCN-Ru(II)}$$

$$\text{Ru(II)-SCN-Ru(II)} \xrightarrow{\text{Disp.}} \text{Ru(III)-SCN}$$

$$\text{Ru(III)-SCN} \xrightarrow{0.2 \text{ V}} \text{Ru(II)-SCN}$$
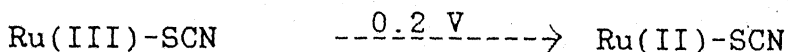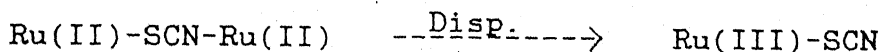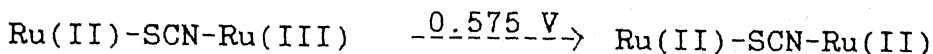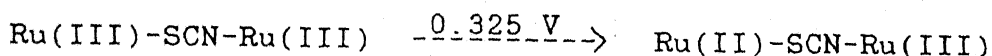
The confirmation of such a scheme was not possible because of the lack of the coulometric data. Besides, the efforts to synthesize the (22) moiety failed and the product invariably decomposed to $[(NH_3)_5RuSCN]^{2+}$. The instability of (22) species is tentatively attributed to the comparatively weaker π-acidities of the nitrogen and sulfur ends of the thiocyanate group (vide infra).

(b) $[CN)_5Fe]^{n-}$ Systems:

The cyclic voltammograms of the NCX bridged dimers (Fig. 4.18) were recorded in water using potassium nitrate as the supporting electrolyte. The results are given in Table 4.20. The compounds exhibited two waves corresponding to the two step oxidation of (22) species. The comproportionation quotients (cf. Section 1.4) and the stability per mol of the mixed-valence species with respect to the isovalent ones were also calculated. The interesting feature to note is the separation of the two redox stages by 0.188 and 0.2 V for the thiocyanate and selenocyanate bridged dimers, respectively.
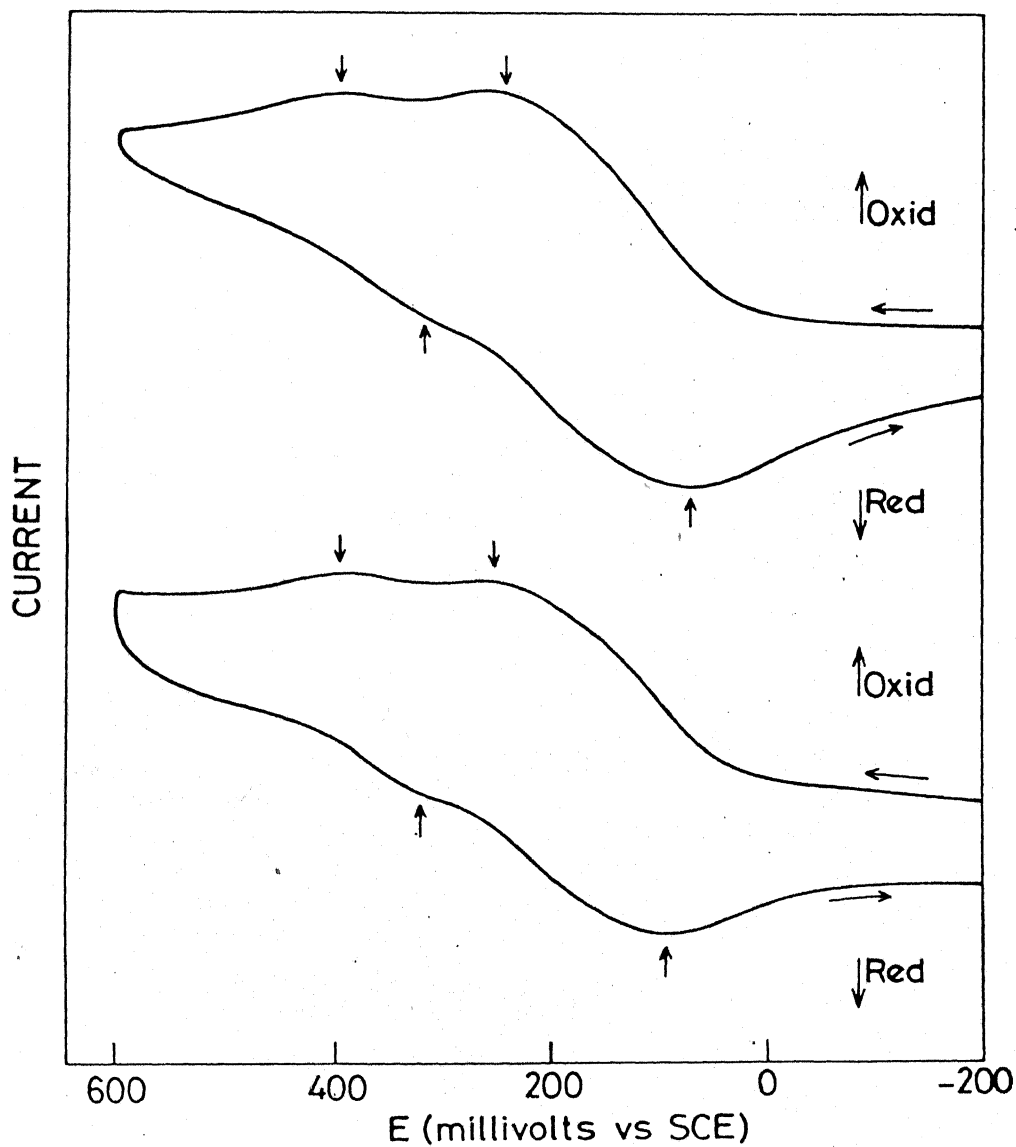
Fig. 4.18 Cyclic voltammograms of the pentacyanoferrate
(23) dimers in water solution. (a) thiocyanato
bridged dimer (below) and (b) selneocyanato bridg-
ed dimer (above). Scan rate is 100 mV s^{-1}.
Values of $E_{1/2}$ and ΔE for $K_4[Fe(CN)_6]$ under the
same conditions are 237.5 and 75 mV,

(c) $[(bpy)_2Ru]^{n+}$ Systems:

The essential electrochemical redox properties of thiocyanate-bipyridine complexes are given in Tables 4.18 and 4.19. The monomeric complexes, apart from the Ru(II/III) couples yielded a second oxidation wave and the corresponding cathodic part (cf. Fig. 4.19 and 4.20; Tables 4.18 and 4.19). Since, the ligands could not be oxidized at these potentials (0.9-1.0 V), this second oxidation is assigned to the oxidation of Ru(III) to Ru(IV). Efforts to separate this Ru(IV) species by chemical oxidation are underway.

The peak potentials are scane rate (ν) dependent. Plots of ΔE_p versus $\nu^{1/2}$ were found to be linear with intercept values ranging from 60-85 mV slightly larger than the theoretical values, 59 mV.[100] Although there seem to be certain quasiirreversibility in some of the processes ($i_{pa}/i_{pc} \neq 1$), all the redox processes conform to one electron change.

The thiocyanate bridged dimeric (22) compound showed two overlapping waves with a single maximum (Fig. 4.19) for both the oxidation and the reduction processes, the other appearing as clear shoulders. The first step is reversible while the successive oxidation of (23) $\rightarrow$ (33) seems to be quasi-reversible. The K_c value calculated using the separation between the two redox stages is 343.

The data for the selenocyanate complexes are given in Table 4.19. Representative voltammograms are illustrated in Fig. 4.20.
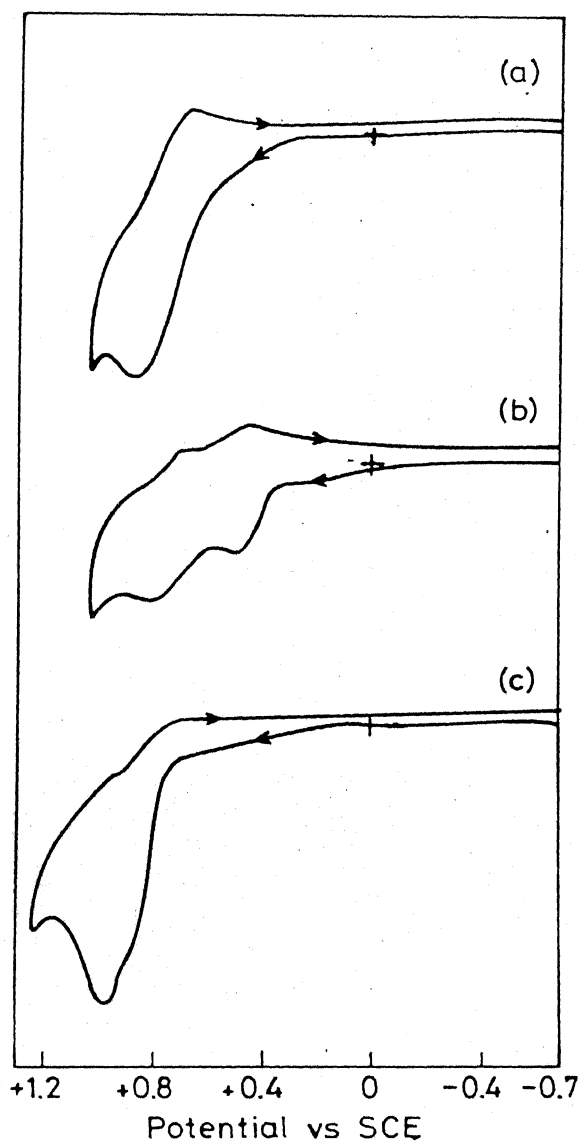
Fig. 4.19 Cyclic voltammograms for the oxidations of
monometic and dimeric compounds in methylene
chloride. Supporting electrolyte, TBAP. (a)
$[(bpy)_2 Ru(NCS)Cl]$, (b) $[(bpy)_2Ru(NCS)_2]$
(scan rate = 200 mV s^{-1} and (c) $[Cl(bpy)_2Ru-$
$NCSRu(bpy)_2Cl] BPh_4$ (scan rate: 100 mV s^{-1}).
The shoulders in the case of (c) are clearly
visible in higher scan rates.

Table 4.18 : Electrochemical Data for the Bis(bipyridine)ruthenium(II/III)
Complexes in Methylene Chloride

Complex	Oxidations [a,b]		Reductions [a,b,c]	
	$E_{1/2}^{(1)}$	$E_{1/2}^{(2)}$	$E_{1/2}^{(3)}$	$E_{1/2}^{(4)}$
[Ru(bpy)$_2$(NCS)Cl]	+0.80(84)	+1.07)84)	-1.41(83)	-1.69(63)
[Ru(bpy)$_2$(NCS)$_2$	+0.51(61)	+0.77(75)	-1.41[d]	-0.60[d]
[Cl(bpy)$_2$RuNCSRu(bpy)$_2$Cl]- BPh$_4$	+0.82[d]	+0.97[d]	-1.42[d]	-1.66[d]

a, The potential values in volts are referred to SCE at room temperature.

The error is ± 0.02 V.

b, ΔE_p values are given in parentheses and were extrapolated from the intercepts of the plots of ΔE_p versus $\nu^{1/2}$, where ν is scanrate

c, The reduction waves are due to the 2,2'-bipyridine ligands.

d, Overlapping waves.
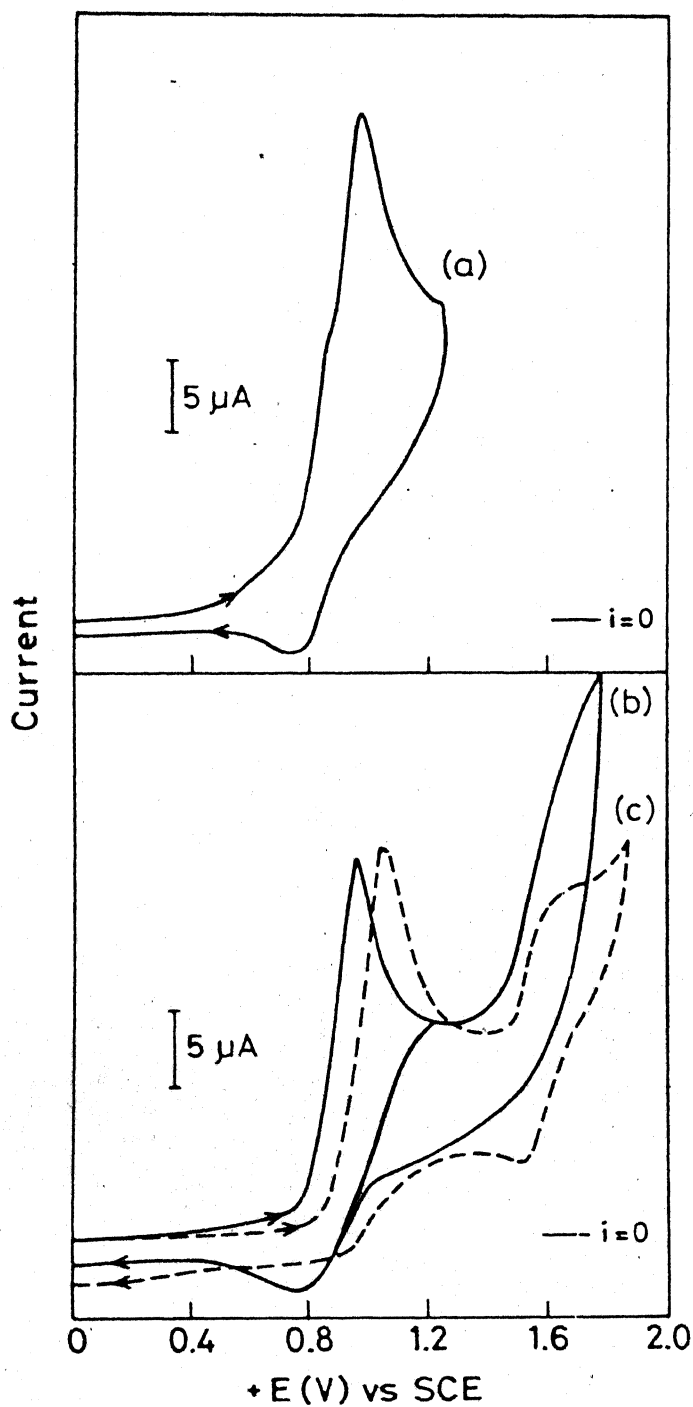
Fig. 4.20 Cyclic voltammograms (oxidative scan) of mono-
meric, $[(bpy)_2Ru(NCSe)Cl].2H_2O$ (a) and the
dimeric $[Cl(bpy)_2RuNCSeRu(bpy)_2Cl]BPh_4$ (b) and
$[Cl(bpy)_2RuNCSRu(bpy)_2Cl]BPh_4$ (c).   Supporting
electrolyte 0.1 M TBAP. (a) scan rate 100 mV s^{-1};
in methylene chloride. (b) scan rate 100 mV s^{-1};
in acetonitrile. (c) scan rate: 200 mV s^{-1}; in
acetonitrile.   The shoulder is clearly visible
in (a).

Table 4.19 : Electrochemical Data for the Bis(bpyridine)ruthenium(II/III) complexes in Methylene Chloride[a]

Complex	Oxidations			Reductions		
	$E_{1/2}$	$E_{1/2}$	$E_{1/2}$	$E_{1/2}$	$E_{1/2}$	$E_{1/2}$
$[(bpy)_2Ru(NCSe)_2]\cdot2H_2O$	+0.32(60)	+0.98(115)	–		-1.36[b]	–
$[(bpy)_2Ru(NCSe)Cl]\cdot2H_2O$	+0.59(74)	+0.92(111)	–		-1.52(166)[b]	-1.97(74)
$[Cl(bpy)_2RuNCSeRu-$	+0.89(85)[b]			-1.26((80))	-1.50(80)	
$(bpy)_2Cl]BPh_4$	{+0.87(116)}[b,c]		+1.55[d]			{-1.36(100)}[b,c]

a, The potential values in volts are referred to SCE at room temperature; error is ±0.02 V; ΔE_p values given in the parentheses were obtained from the intercept values of the $i^{1/2}$ versus plots by extrapolation (see text).

b, Overlapping waves;   c, In acetonitrile;   d, Poorly defined irreversible wave.

The monomeric complexes $[(bpy)_2Ru(NCSe)_2].2H_2O$ and $[(bpy)_2Ru-NCSeCl].2H_2O$ exhibited Ru(II)/Ru(III) couple at 0.32 and 0.50 V, respectively. Apart from this, these compounds exhibited another wave at slightly more positive potentials, as have been observed with the corresponding thiocyanate complexes due to the Ru(III) to Ru(IV) oxidation.

The peak potentials for the redox processes are scan rate dependent and a plot of ΔE_p versus $v^{1/2}$ is linear with intercept values in the range 60-80 mV.[100] Further, the ratio of the peak currents for anodic and cathodic parts of these waves i_{pc}/i_{pa} is close to unity (~0.9), suggesting the reversible one-electron nature of these redox processes.

The electrochemistry of the dimer is interesting. It showed two waves corresponding to the successive (22) $\rightarrow$ (23) and (23 $\rightarrow$ (33) oxidations that are poorly separated. The separation between the anodic wave corresponding to (23) -- (33) oxidation and the cathodic wave corresponding to (23) -- (22) reduction, varied between 160-290 mV in the range of scan rates employed, viz., 50-400 mV s^{-1}. The variation was, linear with respect to $v^{1/2}$. The addition of the two successive one-electron reversible steps, which are poorly separated, could show such a behavior. The variation of the peak current i_p with respect to the scan rate, was also examined. A plot of ln (v) versus ln (i_p) was linear with slope values suggesting a diffusion controlled process. The current function $i_{pc}/v^{1/2}$ was also invariant, as is

observed for reversible redox processes.[100]

However, due to the poor resolution of the two peaks, an accurate value for the comproportionation constant, K_c, could not be obtained and only an upper limt $K_c < 350$ could be predicted. Further, the dimer showed another two-electron wave at more positive potentials (E_{pa} = +1.6 V). This peak is irreversible as evident from the absence of the cathodic part of this wave. However, the anologous thiocyanate compound exhibited a more defined wave ($E_{1/2}$ = 1.55 V), corresponding to a two-electron change (cf. Fig. 4.20). Chemical oxidations of the NCX^- bridged (22) species using four equivalents of Ce(IV) yielded a compound, which has probably NCX^- bridged Ru(IV) moiety. However, a more careful study is necessary to clarify this point.

The electrochemical studies indicate that the binuclear complexes undergo successive two one-electron oxidation, with the two oxidations occurring within a very short potential range. One would then expect that longer chain polymers to exhibit multielectron redox propeties within a relatively shorted span of potentials. This may be a desirable property for utilization of these compounds as catalysts for multielectron transfer processes. As the thiocyanate ion has a larger potential as the bridging ligand in several linear chain and three dimensional polymeric transition metal complexes,[101] the synthesis of appropriate thiocyanate bridged compounds, those can be used as multielectron transfer catalysts, could be planned in future.

Table 4.19 : Electrochemical Data[a] for the NCX⁻ Bridged Dimers

Compound	E_1/mV	ΔE_1/mV [b,c]	E_2/mV	ΔE_2/mV [c]	K_c	ΔG°_{tot}/kcal mol⁻¹ [d]	ΔE
$[Fe(CN)_5NCSFe(CN)_5]^{n-}$	175.0	150	362.5	75	1474	1.773	18
$[Fe(CN)_5NCSeFe(CN)_5]^{n-}$	162.5	175	362.5	75	2399	1.919	20
$[Ru(NH_3)_5NCSRu(NH_3)_5]^{n+}$	325.0	–	538.0	75	3978	2.071	21
$[Cl(bpy)_2RuNCSRu(bpy)_2Cl]^{n+}$	820.0[f]	–	970.0[f]	–	343	1.335	15
$[Cl(bpy)_2RuNCSeRu(bpy)_2Cl]^{n+}$	870(116)[f]	–	890(85)[f]	–	–	–	

a, Potentials are referred to SCE;   b, Irereversible process;

c, ΔE_1 or $2 = E_{p,a} - E_{p,c}$

d, ΔG°_{tot} were calculated using the Equation $\Delta G^\circ = -RT$ in $(K_c/4)$ where 4 is the statistical
    contribution; T = 300 K

e, Separation between two redox stages; $\Delta E = E_2 - E_1$

f, Overlapping waves

4.9 Electron Delocalization in Chalcogenocyanate Bridged Binuclear Complexes

(a) (22) complexes:

As shown from the electrochemical studies (cf. section 4.8) the pentaammine ruthenium (22) dimer seems to be unstable and efforts to synthesize this compound failed and the product invariably decomposed to $[(NH_3)_5RuSCN]^{2+}$. The instability of the $[(NH_3)_5RuNCSRu(NH_3)_5]^{3+}$ species is tentatively attributed to the comparatively weaker π-acidities of the nitrogen and sulfur ends of the thiocyanate group which are severely mismatched with the strong -basicity[85] of the $[(NH_3)_5Ru]^{2+}$ unit, thereby imparting the intrinsic instability to the system. However, the pentacyannoferrate (22) dimer seems to be more stabilized, which might be due to the -interactions in the $[Fe(CN)_5]^{3-}$ unit. Here again the (22) dimer undergoes atmospheric oxidation in the course of time to yield (23) and (33) dimers.

The bis(2,2'-bipyridine)ruthenium complexes showed some of the interesting electronic spectral features. In going from the monomeric $[(bpy)_2Ru(NCX)Cl]$ to the dimeric $[Cl(bpy)_2RuNCXRu(bpy)_2Cl]^+$ a red shift of about 3000 cm^{-1} (for X = S) and 3500 cm^{-1}) (for X = Se) have been observed for the $d\pi(Ru)$--- $3\pi(NCX^-)$ MLCT band. This is attributed to the stabilization of the 3π-acceptor orbital of the chalcogenocyanate ligands due to the coordination of the second $[(bpy)_2Ru]^{2+}$ unit on the free sulfur or selenium end of $[(bpy)_2RuCl(NCX)]$ unit. Inspite, a large stabilization of around 7000-8000 cm^{-1}, due to greater inter-

chalcogenocyanate CT depletes the charge on the metal center and as a result all the other M-ligand units will receive lower charge and vice-versa. This can cause a RR effect for all of the symmetric vibrational modes of the other ligands even when the excitation was done within a particular CT band. The closeness of the acceptor orbital energies of 2,2'-bipyridine and chalcogenocyanate could augment this phenomenon and thereby giving observed RR spectra.

(b) (23) complexes:

The IT band characteristics of the ligand-bridged binuclear mixed-valence compounds in combination with the Hush model can be used to evaluate the interaction between the metal centers in these compounds. The observed IT band for the $[(NH_3)_5RuNCSRu(NH_3)_5]^{4+}$ dimer is much narrower (cf. Table.4.13) compared to the calculated band using Hush model. This narrowness of the IT band and the solvent independence suggest a class III picture for this compound. However, a solvent-dependent IT band which was ~25% narrower than the calculated one was observed for the $[(CN)_5FeNCXFe(CN)_5]^{6-}$ dimers. Bands narrower than the calculated ones have been observed earlier for strongly interacting systems.[41,52,53] Bands broader than the calculated ones were observed for weakly interacting systems.[45] Based on this, the narrowness and solvent-dependence of the IT bands for the chalcogenocyanate bridges pentacyanoferrate dimers suggests a class II picture with a considerably larger delocalization of the

optical electron for the pentacyanoferrate dimers. The IT bands for $[Cl(bpy)_2RuNCXRu(bpy)_2Cl]^{2+}$ was found to be broader than the calculated ones, which in combination with the solvent-dependence (cf. Tables 4.11 and 4.12) of these bands suggest a class II picture with comparatively smaller delocalization of the optical electron for these compounds.

(c) Delocalization of the optical electrons:

A close scrutiny of the α^2 values for the three set of complexes (cf. Table 4.13) shows a drastic decrease in the extent of delocalization of the optical electron in going from the pentaammineruthenium (23) dimer to the bis(2,2'-bipyridine)ruthenium (23) dimer. This decreasing trend can be explained by a three-site model involving the interaction of the $d\pi$ orbitals of the metals centers and the LUMO (3π) orbitals of chalcogenocyanates. The LUMO of the bridging species $(E_{3\pi}(SCN) = -4.242$ eV) can mix with the $d\pi$ orbitals of the metal center, with appropriate symmetry. A convenient model given by Ondrechan et al.[102] can be used. Among the split $d\pi$ orbitals of metal centers in an octahedral environment, the combination $d_{xy}(1)-d_{xy}(2)$ and $d_{xz}(1)-d_{xz}(2)$ could interact with the degenerate 3π LUMO orbitals of the NCX ion to yield a pair each of antibonding, non-bonding and bonding orbitals (Figs. 4.21 and 4.22). This interaction would give rise to "localized" metal to ligand charge transfer states, viz., M^+-L^--M (E_1) which can "assist" the delocalization of the optical electron. Similarly participation of the HOMO of the bridging-ligand (if there is any) in the π-bonding scheme

with the metal $d\pi$ orbitals can also be envisaged. This interaction would give rise to "localized" ligand to metal charge transfer states viz., $M-L^{+}-M^{-}$ (E_2) which can "assist" in the delocalization of the optical electron.

Both these interactions, viz., $d\pi(M) \longrightarrow$ LUMO (NCX^{-}) and HOMO $(NCX^{-}) \rightarrow d\pi(M)$, have been recognized by earlier workers.[48,64] The charge distribution within the SCN^{-} ion has been calculated[26] by di Sipio, Wagner and Jones and is given as

```
    S ---- C ---- N          di Sipio
 -0.48   -0.01  -.0.5


    S ---- C ---- N          Wagner
 -0.45   +0.19  -0.71


    S ---- C ---- N          Jones
 -0.54     0    -0.46
```

In all these calculations the charge on sulfur remained almost the same but slightly different polarities for the $C\equiv N$ group were obtained. Further, from an ESCA investigation of a few hexa- and tetra(thiocyanato) complexes of transition metals, it has been observed[27] that donation of electrons from the thiocyanate group results in a considerable reduction of charge on the S atom, which must be due to the interaction of the HOMO of NCS^{-} with the empty $d\pi$ orbitals of the transition metals. The most interesting observation, however, is the pronounced back-donation of electrons from the appropriate transition-metal ions to the

Scheme 2

C-T ion   NCX bridged dimer   Allyl
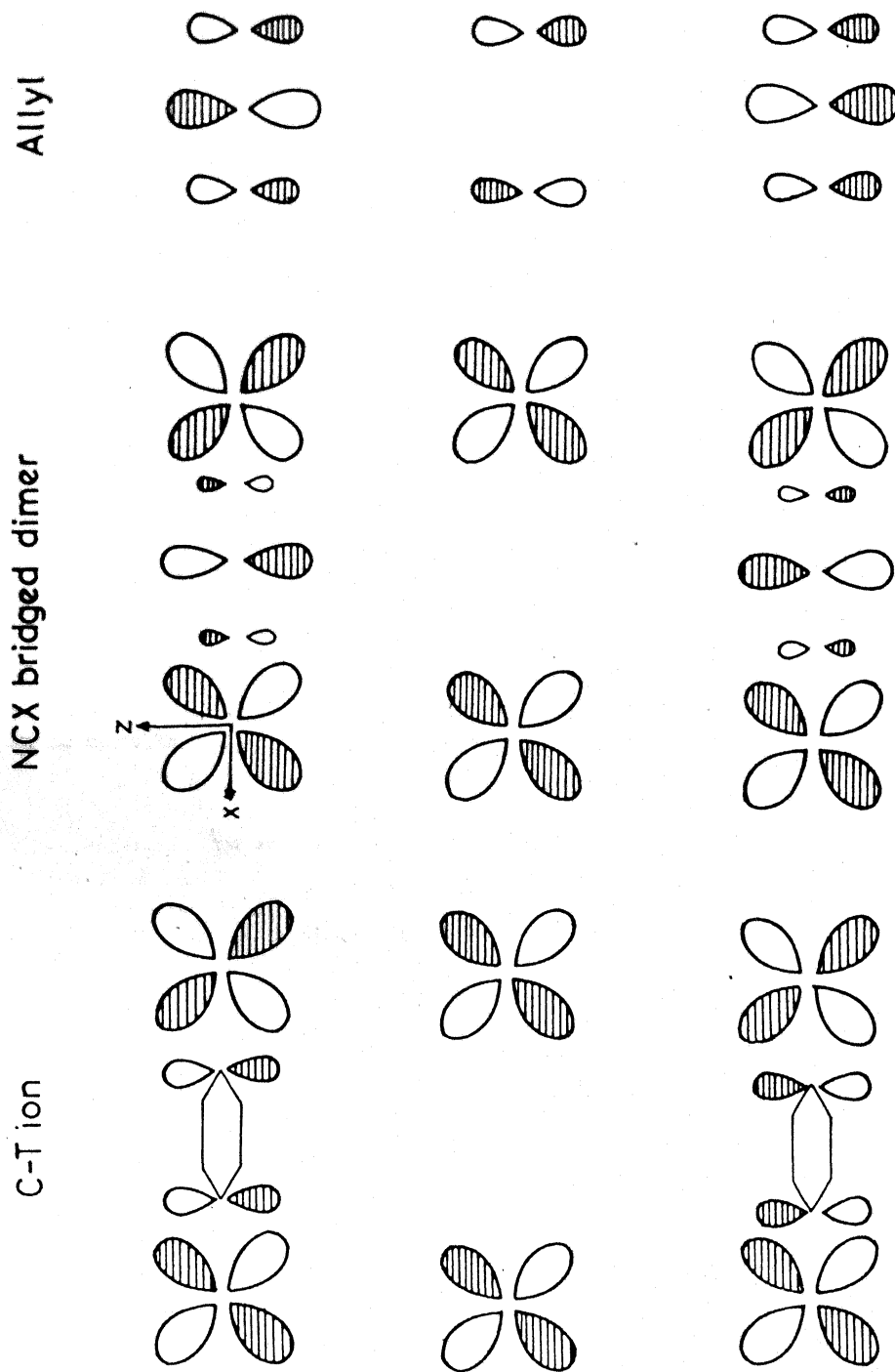
Fig. 4.21 Diagram showing the interaction between 3π LUMO orbitals of NCX^- ion in the xz plane and the filled $d\pi$ orbitals of the metal enters. Similar overlap in the xy plane can be presumed.

FREE ION   CRYSTAL FIELD   DIMER   NCX ION
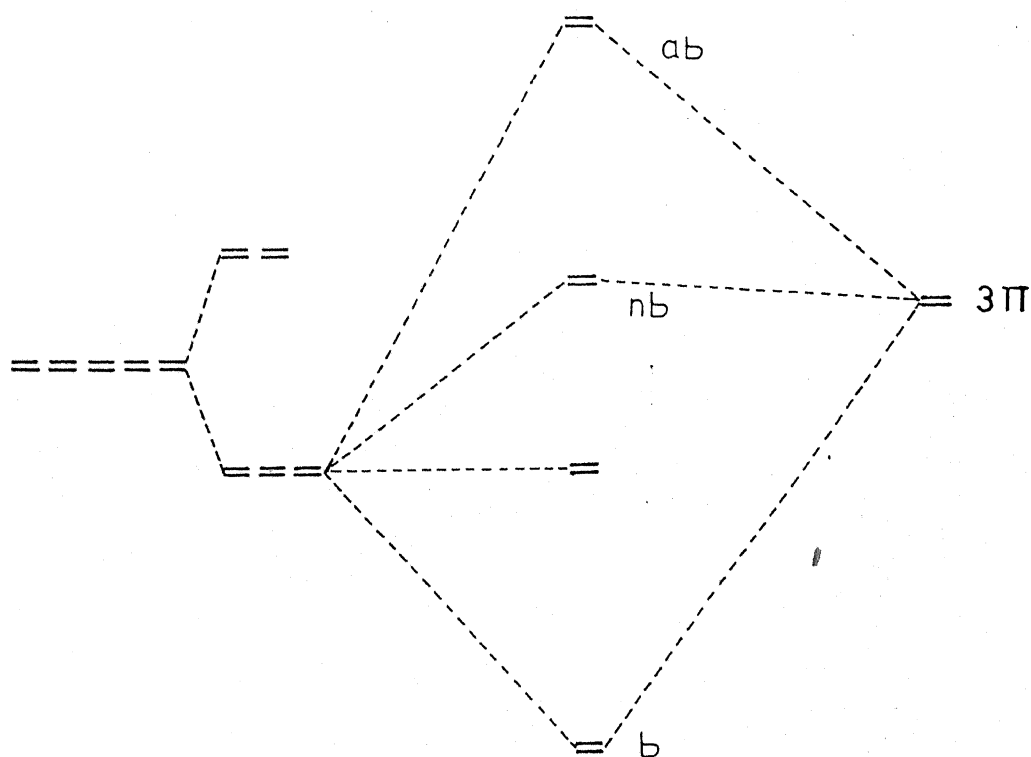
Fig. 4.22 Qualitative MO splitting diagram for the NCX^-
bridged binuclear mixed-valence dimers.

carbon atom of the NCS⁻ ion. This back donation must be the result of the interaction between the filled $d\pi$ orbitals of the transition metal ions and the degenerate LUMO orbitals of NCS⁻ ion resulting in the growth of a considerable amount of negative charge on the carbon atom as is evident from the calculations of charge distributiosn from ESCA measurements.

Further, the "localized" metal to ligand charge transfer state (M^+-L^--M) "assisted" delocalization of the optical electron should decrease in going from a σ-donor nonbridging "spectator" ligand to π-acceptor ones. However, the trend should be reversed if the delocalization of the optical electron is "assisted" by a "localized" ligand to metal charge transfer state ($M-L^+-M^-$).[48] The "localized" MLCT mechanism seems to be operative in the case of pyrazine bridged binuclear ruthenium mixed-valence complex,[48b] while the "localized" LMCT mechanism has been suggested to be operative in the t-butyl malononitrile bridged complexes. Thus, the decrease in the delocalization of the optical electron in going from a σ-donor nonbriding ligand to a π-acceptor nonbridging ligand (cf. Table 4.13) demonstrates conclusively that the mechanism of electron delocalization operative in these set of complexes is the "localized" MLCT. Or atleast it is the effective mechanism. However, in a quantitative calculation, as has been carried out for the C-T ion,[48b] one can take both the excited states, viz., "localized" MLCT and LMCT, into consideration.

Other two factors those have to be considered to explain the delocalization of the optical electron are the energies of the concerned orbitals and the spatial diffusion of the metal $d\pi$ orbitals. There seem to be more of energy matching of the LUMO of NCX^- ions with the ruthenium 4d orbitals of $[(NH_3)_5Ru]^{n+}$ unit than that with the iron 3d orbitals of $[(CN)_5Fe]^{n-}$ or the ruthenium 4d orbitals of $[(bpy)_2Ru]^{n+}$ unit. This might also contribute to the lowering of the extent of electron delocalization in the latter set of compounds from the former set. Also the smaller amount of delocalization of the optical electron in the cases of $[(CN)_5FeNCXFe(CN)_5]^{6-}$ compared to that of $[(NH)_5RuNCSRu(NH)_5]^{4+}$ can be attributed to larger mixing of the ruthenium 4d orbitals due to their larger size compared to that of the iron 3d orbitals (Fig. 4.23).

(d) Asymmetry of the Bridging Ligands:

Another interesting observation is that the asymmetry of the chalcogenocyanate bridge is not as manifested as it might look from a purely chemical point of view. The chemical asymmetry around the metal centers of a chalcogenocyanate bridged binuclear complex should increase the barrier (cf. Section 1.5) for the electron transfer and hence the IT band is expected at higher energies compared to the more symmetric species such as C-T ion. But the IT bands in these chalcogenocyanato bridged species are observed at energies which are comparable to those of the analogous symmetric systems. This barrier (ΔE_o) can be qualitatively estimated for the asymmetric

Fe 3d

Ru 4d
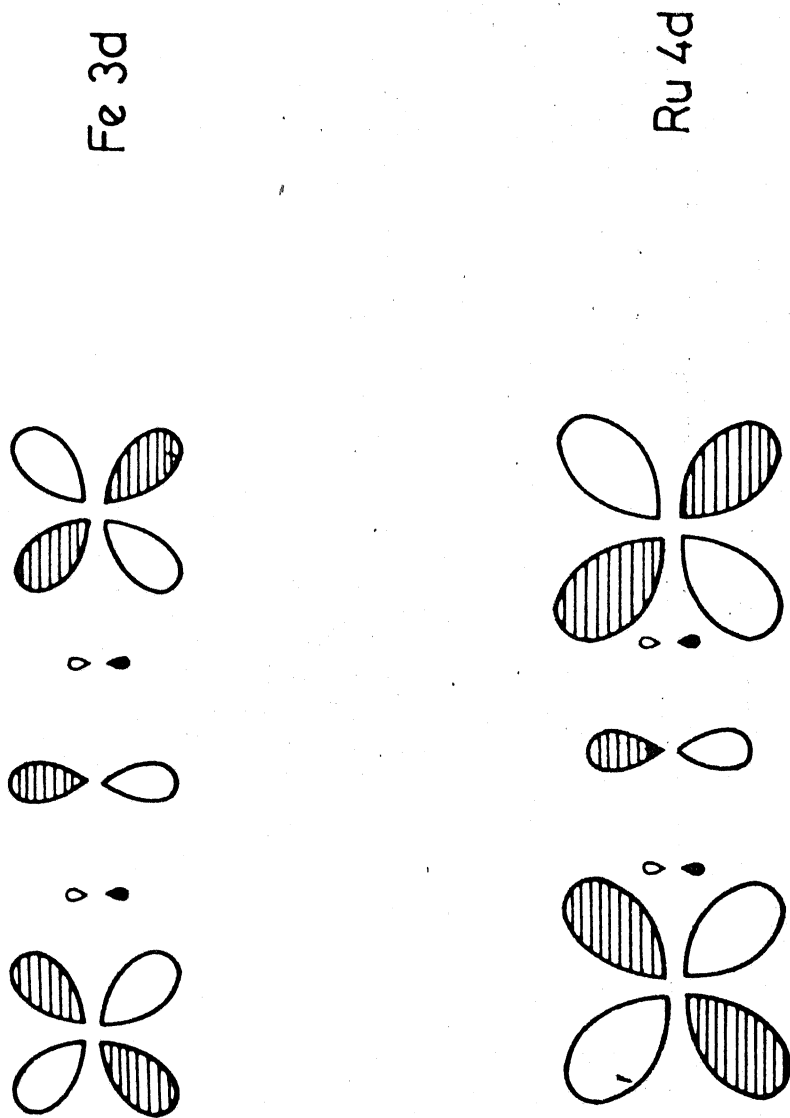
Fig. 4.23 Effect of the orbital size on the $M(d\pi)-L_b$ $(3\pi)-$

$M(d\pi)$ interaction.

systems from the deviation of the IT spectral bandwidth from that of the calculated one from the Hush model. However, the acceptable closeness of the observed and calculated bandwidths of the IT bands is suggestive of the more symmetric nature of the bridge.

This can be explained by the pseudosymmetric nature of the π-overlap (<u>vide</u> <u>infra</u>). The pair of LUMO 3π-acceptor orbitals on the chalcogenocyanate ions (cf. Fig.4.21) are localized mostly (> 92%) on the central carbon atom and the contributions from the end atoms, viz., N and S or Se, are meager. This has been experimentally proved by the ESCA studies (<u>vide</u> <u>infra</u>),[27] where it has been found that the charge on the central carbon atom of the [M-N-C-S] unit decreases drastically. For example,

```
    S ----- C ----- N
  -0.45     +0.19    -0.71
```

```
    S ----- C ----- N ----- Co   in [Co(NCS)_4]^{2-}
  -0.25     -0.02    -0.42    +0.8
```

```
    N ----- C ----- S ----- Pt   in [Pt(SCN)_4]^{2-}
  -0.41     -0.35    +0.02    +0.96
```
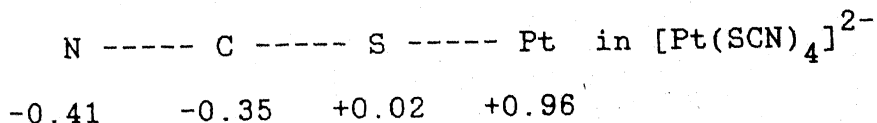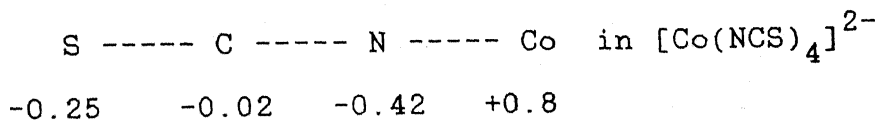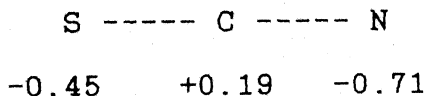
thereby suggesting that the π-backbonding of transition metals with the LUMO of the thiocyanate ion is effectively, the interaction with the carbon atom of the thiocyanate ion. Thus, the π-overlap in the chalcogenocyanate bridged binuclear mixed-valence compounds where the effective electron delocalization mechanism is the "localized" MLCT, could even be thought of as occurring on [M-C-M] unit rather than on [M-NCX-M] unit. The bridge is more a symmetric one rather than asymmetric. However, the applicability of this "pseudo symmetry" in a chemical sense is not clear and does not have any precedence. The small difference in the π-acidities of the N- and S-bonded linkage isomers, noted by earlier workers[24] can be explained using this strategy (vide supra).

(e) π-Bonding Properties: Thiocyanate vis-a-vis Selenocyanate

Another worth mentioning observation is the small difference in the π-acceptor properties between thiocyanate and selenocyanate ions. However, the studies on the bipyridine complexes suggest that the selenocyanate ion has a favorable edge over the thiocyanate ion.

The $d\pi - \pi_1^*$ (bpy) MLCT energies show a linear correlation with the first oxidation potentials of the compounds [(bpy)$_2$Ru(NCX)$_2$], [(bpy)$_2$Ru(NCX)Cl] and the dimeric [Cl(bpy)$_2$RuNCX-Ru(bpy)$_2$Cl]$^+$. However, the slope of the linear plot, $\bar{\nu}_{CT}$ versus $E_{1/2}^{(1)}$ (cf. Fig 4.24) for the selenocyanate compounds is approximately four folds greater than that for the thiocyante complexes. This suggests that the "π-disturbances" in the
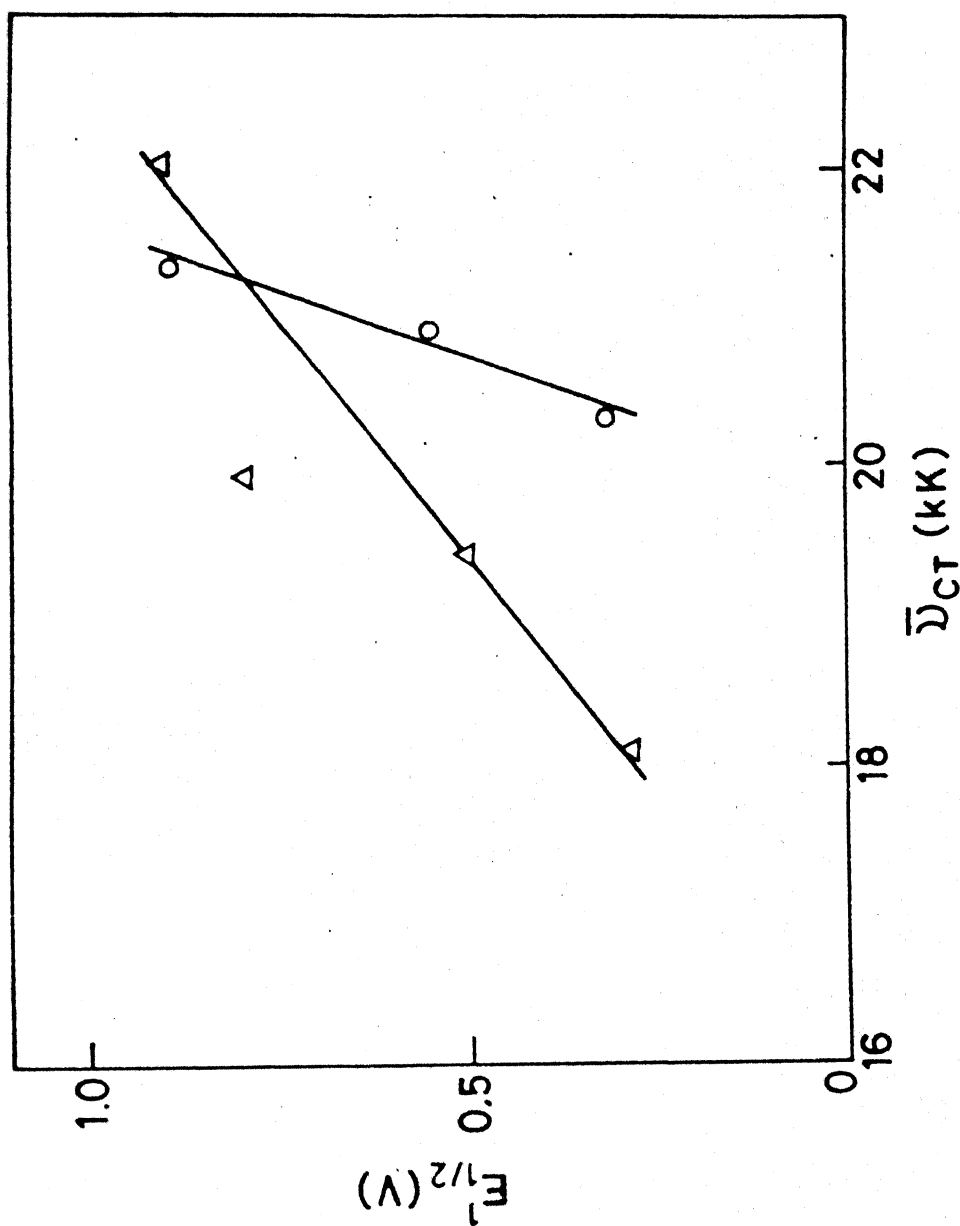
Fig. 4.24 Plot of $\bar{\nu}_{CT}$ vs. $E_{1/2}^{(1)}$ for the thiocyanato and selenocyanatoruthenium-bipyridine compounds.

selenocyanate compounds are greater than that in the thiocyanate compounds. Studies on the linkage isomers (cf. Section III) of the chalcogenocyanate complexes of pentaammineruthenium(III) suggest that the π-back bonding in [M-CNSe] unit is stronger than that in the [M-CNS] unit, i.e., selenocyanate seem to be a better π-acid compared to thiocyanate ion. Thus, given that $SeCN^-$ ion is a better π-acid, it could compete more than thiocyanate ion could do with the 2,2'-bipyridine "spectator ligands" which is a good π-acceptor by itself, for π-back donation from the metal centers. This, in turn, could lead to a slight destabilization of the π-acceptor orbitals of the 2,2'-bipyridine in the case of selenocyanate complexes. Hence, the $d\pi - \pi_1^*$ (bpy) MLCT bands in both $[(bpy)_2Ru(NCSe)_2]$ and $[(bpy)_2RuNCSeCl]$ are observed at slightly higher energies compared to those of the analogous thiocyanate compounds. Further, the reducibility of the metal centers in $[(bpy)_2Ru(NCSe)_2]$ and $[(bpy)_2RuCl_2]$ as seen from their $E_{1/2}$ values, viz., +0.32 and +0.29 V, respectively, is almost similar. In spite of this, the $d\pi - \pi_1^*$ (bpy) MLCT band for $[(bpy)_2Ru(NCSe)_2]$ is observed at considerably higher energy (493 nm) than that for $[(bpy)_2RuCl_2]$ (552 nm). The reason possibly is the stronger π-interaction of the metal centers with selenocyanate ion. The stronger π-interaction destabilizes the π-acceptor orbitals on the 2,2'-bipyridine coligands due to the smaller amount of charge transfer and the $d\pi - \pi_1^*$ (bpy) MLCT is observed at higher energy. The chloro ligands being π-donors, could favorably increase the charge flow to the 2,2'-bipyridine coligands and thus the stabilization of the π-acceptor oribitals

of 2,2'- bipyridine coligands is a cooperative phenomenon of two factors: (i) the larger π-back donation to 2,2'-bipyridine in the absence of any other π-acceptor ligands such as, selenocyanate ions (ii) the π-donation of the chloro ligand to the metal centers, in turn increases the π-back donation to the bipyridine ring.

Other evidences that were observed during the study for the larger π-interaction in case of selenocyanate ions than that in thiocyanate are the following:

(i)   larger values for the comproportionation constants of the selenocyanate (23) dimers compared to that of the thiocyanate analogs (cf. Table 4.20);

(ii) the larger quenching of the luminescence in the selenocyanate compounds (cf. Section 4.5);

(iii) the greater enhancement in intensities of the RR peaks for selenocyanate compounds compared to that of the their thiocyanate analogs (cf. Section 4.6).

However, the greater π-back bonding in [M-NCSe] unit than that in [M-NCS] unit could not be explained satisfactorily on the basis of the energies of the 3π-acceptor orbitals of the chalcogenocyanate ions. The difference in the energies of the 3π-orbitals between cyanate and thiocyanate is very small, i.e., 60 cm^{-1}.[25] A similar trend can be applicable for selenocyanate ion, which essentially means that the energy and symmetry of these

orbitals should give similar π-bonding properties for both thiocyanate and selenocyanate ions.

4.10 Stability of the Binuclear Mixed-Valence Compounds

The stability of the mixed-valence species after allowance for statistical factors (K_c = 4) can be attributed to several factors, the relative contributions of which we are interested in (cf. Section 1.6).

$$\Delta G^{\circ}_{tot} = \Delta G^{\circ}_{del} + \Delta G^{\circ}_{coul} + \Delta G^{\circ}_{struct} + \Delta G^{\circ}_{mag} + \Delta G^{\circ}_{induc}$$

Among these factors, the contribution due to structural variations can be omitted in the case of ruthenium(II,III) and iron(II,III) mixed-valence compounds as the inner-sphere reorganizational effects are meager, when they form robust low-spin octahedral complexes. Similarly, the contribution from the magnetic interaction can also be omitted as the bridging is through a triatomic species.

ΔG°_{del} :   This term has been evaluated in the past by Sutton and Taube[45] for a series of weakly coupled class II mixed-valence compounds:

$$\Delta G^{\circ}_{del} = \frac{H_{AB}^{2}}{E_{op}}$$

However, the calculated values seems to be generally very low (1% of H_{AB}) in almost all the cases. This contribution calculated for the chalcogenocyanate bridged mixed-valence compounds is ~20-25 cal mol^{-1}, which is far less compared to the total

stability of the species (a few kcal mol^{-1}).

ΔG°_{coul}: The contribution due to the purely electrostatic factors has also been evaluated in the past for ruthenium (23) systems bridged by neutral ligands on the basis of the point charge model in a dielectric continum and more recently on the basis of the more sophisticated ellipsoidal model. Qualitatively,[28a] the repulsive forces operative between the positive charges on the metal centers of a dimer can be given as

$$F \propto -\frac{xy}{r^2}$$

where x and y are the magnitudes of charges and r is the distance of separation between charges. For the neutral-ligand-bridged dimeric compounds the repulsive forces operative on (22) + (33) (state A; proportional to $2^2 + 3^2 = 13$) is 1 unit more than those operative on 2(23) (state B; proportional to 2 x 6 = 12) and state B is stabilized over state A due to the smaller repulsive forces even when the electron delocalization is not "turned on". But the situation is completely different for dimers having anionic bridging ligands. Attractive forces are also operative apart from the repulsive forces in these cases. We can consider the dimer M_2L_b:

$$\overset{\displaystyle \longmapsto\!\!\underset{r_1}{-\!-\!-\!-\!-\!-\!-\!-\!-\!-\!-}\!\!\dashv \quad \longmapsto\!\!\underset{r_2}{-\!-\!-\!-\!-\!-\!-\!-\!-\!-\!-}\!\!\dashv}{M_1{}^{x+} \;-\!-\!-\!-\!-\!-\!-\!-\!-\!- \; L_b{}^{-} \;-\!-\!-\!-\!-\!-\!-\!-\!- \; M_2{}^{y+}}$$

$$\longmapsto\!\!\underset{r}{-\!-}\!\!\dashv$$
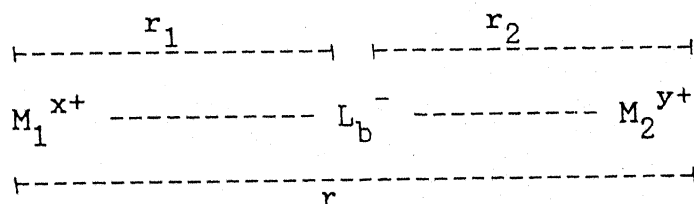
In a qualitative sense the resultant coulombic contribution could be thought of as arising from the attraction between (x+) and (z-) of the M_1-L_b component and (y+) and (z-) of the M_2-L_b component and repulsive forces between the (x+) and (y+) charges and this can be expressed as

$$F_{eff} \propto xy/r^2 - [xz/r_1^2 + yz/r_2^2]$$

(positive sign for repulsive forces as they destabilize the system and a negative sign for attractive forces as they stabilize it are used in a conventional sense.)

State B (proportional to 2) in this case is stabilized over state A (proportional to 0 + 3 = 3) by the additional attractive forces. A value of 100-200 cal mol^{-1} was obtained by Taube, et al., for some of the class II mixed valence compounds[45b] and it is expected that in the chalcogenocyanate bridged complexes this contribution should be more. This again falls short of the few kcal mol^{-1} total stability of these compounds. Thus, it seems the largest contribution to K_c, is from the ΔG^o_{induc}.

ΔG^o_{induc}: The origin of this term is the M(II) back bonding interaction. Its consequences for both (22) and (23) must be taken under consideration. When a (22) species is assembled from bridging ligand and Ru(II) the addition of the second Ru(II) does not produce quite as large a $d\pi$-π^*(L_b) interaction as does the first Ru(II). In contrast when Ru(II) is added to Ru(III)-L_b

there is stabilization because the Ru(II) interaction lowers the $\pi^*(L_b)$ energy. This synergistic inductive effect is general for (23) mixed-valence dimers of all the good -donor metal ions.

Further, it has been pointed out by Taube* that the intrinsic asymmetry of the bridging ligand, viz., NCX^- ions, should increase the separation between the two redox stages further, apart from the contributions of the Franck-Condon barrier. In this case, the enormous increase in K_c values and hence the stability of the mixed-valence species could not be explained in systems that are not comparatively strongly coupled as in our case. This apparent paradox could be solved by study-ing systems with strong coupling between metal centers through intrinsically asymmetric mediators. A probable candidate would be chalcogenocyanato-bridged osmium systems, where more mixing can be expected between the orbitals, favored by appropriate ener-gy and spatial diffusion conditions (cf. Fig. 4.23).

---

* H. Taube, personal correspondence.

SECTION V.   SUMMARY AND FUTURE DIRECTIONS

Thiocyanate ion and chalcogenocyanates (NCO^-, NCS^-, $NCSe^-$ and $NCTe^-$ ions) in general are versatile ambidentate ligands. Their ambidenticity is manifested by a large number of linkage isomers synthesized till date. They have played a crusading role in solving many of the mechanistic problems of inorganic coordination chemistry. Furthermore, these ions exhibit bridging properties resulting in the synthesis of a large number of oligomeric and polymeric chalcogenocyanato bridged metal complexes where they have been recognized to be good mediator for electron transfer. Thiocyanate ion takes part in electron transfer reactions by both inner sphere and outer sphere mechanisms. Following the continued interest on the chemistry of the chalcogenocyanates and their capabilities as bridging ligands in di-, tri- and polynuclear complexes, an effort to quantify the electron mediation properties of the thiocyanate bridge was needed. To accomplish this, the synthesis and a detailed study of the thiocyanato and selenocyanato bridged complexes of the 8th group metals, viz., Fe, Ru and Os were planned.

As a first step, the synthesis and a detailed study of the mononuclear thiocyanato and selenocyanato complexes were

undertaken. The linkage isomers such as, $[(NH_3)_5RuNCS]^{2+}$ and $[(NH_3)_5RuSCN]^{2+}$, $[(NH_3)_5RuNCSe]^{2+}$ and $[(NH_3)_5RuSeCN]^{2+}$, $[(CN)_5FeNCS]^{3-}$, $[Cl(bpy)_2RuNCS]$ and $[Cl(bpy)_2RuSCN]$ and $[Cl(bpy)_2RuNCSe]$ and $[Cl(bpy)_2RuSeCN]$ were identified and characterized using vibrational spectroscopy and other physicochemical methods. These complexes were later reacted with appropriate mononuclear units $([ML_5X]^{n-/n+}$ where X is a labile ligand) to generate the discrete binuclear complexes. Different building blocks such as $[(NH_3)_5Ru]^{n+}$, $[(CN)_5Fe]^{n-}$ and $[(bpy)_2Ru]^{n+}$ were used in the process.

The binuclear complexes were characterized by various physicochemical techniques such as, microanalytical methods, vibrational (IR, Raman and resonance Raman), electronic (absorption and emission), n.m.r. (^1H and ^{13}C) and Mossbauer spectroscopy and electrochemical methods (cyclic voltammetry). All the thiocyanato- and selenocyanato bridged binuclear mixed valence compounds exhibited fairly intense intervalence transfer (IT) bands (Eqn. 1):

$$[L_5M(II)-L_b-M(III)L_5] \xrightarrow[IT]{h\nu_{IT}} [L_5M(III)-L_b-M(II)L_5]^{n+*} \quad ..(1)$$

in the near infrared region of their electronic spectra. This in combination with the conceptual model proposed by Hush was used in evaluating the electron mediation properties of the bridge.

A few of the several important results those emerged from this study are:

(i) In the case of $[(NH_3)_5MCNX]^{2+}$, where M = Ru and Os and X = S and Se and the coligands are mainly σ-donors the X-bonded (S or Se) isomers are favored over the N-bonded isomers. If the coligands are substituted by π-acceptors, as in the cases of $[(CN)_5FeCNX]^{3-}$ and $[Cl(bpy)_2RuCNX]$, the N-bonded isomer is favored over the X-(S or Se) bonded isomers. These results are in concordance with earlier studies.

(ii) In binuclear complexes, the interaction between the metal centers via the chalcogenocyanate bridge is suggested to occur through a π-overlap, viz., $d\pi(M)-3\pi*(NCX^-)-d\pi(M)$.

(iii) The electron mediation properties of the chalcogenocyanate bridges in the mixed-valence compounds, as obtained from the delocalization factor, α^2, are interesting. For example,

Complex	α^2 (X = S)	α^2 (X = Se)
$[(NH_3)_5RuNCSRu(NH_3)_5]^{4+}$	Delocalized	–
$[(CN)_5FeNCXFe(CN)_5]^{6-}$	5.3×10^{-3}	5.0×10^{-3}
$[Cl(bpy)_2RuNCXRu(bpy)_2Cl]^{2+}$	1.9×10^{-3}	1.9×10^{-3}

The inference is that the change in the "spectator ligands" (from σ-donor to π-acceptor) affects the delocalization of the optical electron as one would expect. A further point is that the interaction between the metal centers could be "tuned" as to our requirements by deliberately changing the nature of the coligands. This will have large impact on biological electron transfer processes, where the driving force (a function of redox asymmetry) plays an important role.

(iv) The asymmetry of the chalcogenocyanate bridge is not as manifested as it might look from a purely chemical point of view. The reason for this could be the pseudosymmetric π-overlap (vide infra). The pair of LUMO π*-acceptor orbitals on the chalcogenocyanate ions (3π -orbitals) are localized mostly (>92%) on the central carbon atom and the contributions from the end atoms, viz., N and S or Se, are meager. Thus, the π-overlap could even be thought of as occurring on [M-C-M] unit rather than [M-NCX-M] unit. The bridge is more a symmetric one rather than asymmetric.

(v) The anionic nature of the bridge, NCX^- (X = S or Se) seems to increase the stability of the mixed-valence species (cf. Table) by a favorably higher contribution from the electrostatic factors to the total free energy change of the comproportionation reaction, ΔG^o_{tot}, $\Delta G^o_{tot} = \Delta G^o_{es} + \Delta G^o_{del} + \Delta G^o_{struct} + \Delta G^o_{mag} + \Delta G^o_{induct}$

(vi) The difference between thiocyanate and selenocyanate ions, as for the π-acceptor properties are concerned is very

small. However, the available evidences suggest that the selenocyanate ion has a favorable edge over the thiocyanate ion.

(vii) The electrochemical studies of the binuclear complexes show that the successive two one-electron redox processes occur within a short range of potential. This may be a desirable property, as, now one could imagine the thiocyanate bridged polymeric coordination compounds to exhibit a multielectron redox process within a short range of potential and this is a primary requirement for any compound to act as an electrocatalyst for multielectron redox processes such as photodissociation of water, etc. As the thiocyanate ion acts as the bridging species in one-, two- and three dimensional networks of coordination complexes, the synthesis of the appropriate polymeric compounds could be planned in future.

Apart from the several obvious extensions of this work such as, chalcogenocyanate-osmium chemistry (which could not be completed) and chalcogenocyanate bridged mixed-metal complexes, there seem to be several things that can be probed in future. For example,

(i)   the implications of the findings reported in this thesis on biological electron transport processes;

(ii)   implications on the chalcogenocyanate bridged polymeric complexes;

(iii)   chemical implications of the pseudosymmetry discussed for the chalcogenocyanate ions;

(iv)   catalytic utility of the 2,2'-bipyridine complexes inmultielectron transfer processes such as, "water-oxidation," "nitrogen-reduction," etc.

Thus, "at this stage, it would be premature to attribute the differences to effects of the kind we are looking for, but it would be equally premature to give up the search" -- Henry Taube.[*]

[*] H. Taube, Ref. 103

References

1. (a) Taube, H. Angew. Chem. Int. Ed. Eng. 1984, 23, 329. (b) Cannon, R.D. "Electron Transfer Reactions;" Butterworths; London, 1980 and references therein.

2. (a) Guarr, T.; McLendon, G. Coord. Chem. Rev. 1985, 68, 1. (b) Gray, H.B. Chem. Soc. Rev. 1986, 15, 17. (c) McLendon, G.; Guarr, T.; McGuire, M.; Simolo, K.; Strauch, S.; Taylor, K. Coord. Chem. Rev. 1985, 64, 113. (d) Isied, S.S. Prog. Inorg. Chem. 1984, 32, 443. (e) "Advances in Inorganic and Bioinorganic Mechanisms, Vol. III"; Sykes, A.G. Ed.; Academic; London, 1984.

3. See for example: (a) "Bioenergetics of Photosynthesis;" Govindjee, E. Ed.; Academic; New York, 1975. (b) "Photosynthesis, Vols. I and II;" Govindjee, E. Ed.; Academic; New York, 1979. (c) Blankenship, R.E. Acc. Chem. Res. 1981, 14, 163.

4. Penfield, K.W.; Miller, J.R.; Paddon-Row, M.N.; Cotsaris, E.; Oliver, A.M.; Hush, N.S. J. Am. Chem. Soc. 1987, 109, 5061 and references therein.

5. Tabushi, I. In "Studies in Organic Chemistry-13: Biomimetic Chemistry;" Yoshida, Z- I.; Ise, N. Eds.; Elsevier; Amsterdam, 1983.

6. Mayer, T.J. In "Inorganic Chemistry Toward 21st Century;" Chisholm, M.H. Ed.; ACS; Washington (D.C.), 1983, p. 157.

7. (a) Ramaraj, R., Kira, A.; Kaneko, M. J. Chem. Soc. Farad. Trans. 1986, 182. (b) Ramaraj, R.; Kira, A.; Kaneko, M. Angew. Chem. Int. Ed. Eng. 1986, 25, 825, 1009. (c) Grätzel, M. In "Energy Resources Through Photochemistry and Catalysis;" Academic; New York, 1983. (d) Grätzel, M. Acc. Chem. Res. 1981, 14, 376. (e) Kalyanasundaram, K. Coord. Chem. Rev. 1982, 46, 159. (f) Gilbert, J.A.; Egglesdon, D.S.; Murphy Jr., W.R.; Geselowitz, D.A.; Gersten, S.W.; Hodgson, D.R.; Meyer, T.J. J. Am. Chem. Soc. 1985, 107, 3855.

8. (a) Ellis, C.D.; Gilbert, J.A.; Murphy Jr.W.R.; Meyer, T.J. J. Am. Chem. Soc. 1983, 105, 4842. (b) Vining, W.J.; Meyer, T.J. Inorg. Chem. 1986, 25, 2023. (c) Doppelt, P.; Meyer, T.J. Inorg. Chem. 1987, 26, 2027.

9. Roecker, L.; Meyer, T.J. J. Am. Chem. Soc. 1986, 108, 4066.

10. Norbury, A.H. Adv. Inorg. Chem. Radiochem. 1975, 17, 231.

11. Jackson, W.G.; Sargeson, A.M. In "Rearrangement in Ground and Excited States;" de Mayo, P., Ed.; Academic: New York, 1980: Vol. 2, pp. 273-378.

12. Huheey, J.E. In "Inorganic Chemistry-Principles of Structure and Reactivity;" 2nd Ed.; Harper International SI Edn.: Cambridge, 1983: pp. 516-521.

13. (a) Jackson, W.G.; Hookey, C.N. Inorg. Chem. 1984, $\underline{23}$, 668. (b) Jackson, W.G.: Jurisson, S.S.; McGregor, B.C. Inorg. Chem. 1985, $\underline{24}$, 1788.

14. (a) Yadav, S.K.S.; Agarwala, U.C. Indian J. Chem. 1982, $\underline{21A}$, 175. (b) Yadav, S.K.S.; Agarwala, U.C. Polyhedron, 1984, $\underline{3}$, 1. (c) Yadav, S.K.S. Ph.D. Thesis, IIT, Kanpur, India, 1982.

15. (a) Poddar, R.K.; Parashad, R.; Agarwala, U.C. J. Inorg. Nucl. Chem. 1980, $\underline{42}$, 837. (b) Parashad, R.; Yadav, S.K.S.; Agarwala, U.C. J. Inorg. Nucl. Chem. 1981, $\underline{43}$, 2359. (c) Parashad, R. Ph.D. Thesis, IIT, Kanpur, India, 1980.

16. Lin, S.W.; Scheiner, A.F. Inorg. Chim. Acta 1971, $\underline{5}$, 290.

17. Gutterman, D.F.; Gray, H.B. Inorg. Chem. 1972, $\underline{11}$, 1727.

18. Wajda, S.; Rachlewicz, K. Inorg. Chim. Acta 1978, $\underline{31}$, 35.

19. Haim, A. Prog. Inorg. Chem. 1983, $\underline{30}$, 273.

20. (a) Espenson, J.H.; Birk, J.P. J. Am. Chem. Soc. 1965, $\underline{87}$, 3280. (b) Birk, J.P.; Espenson, J.H. J. Am. Chem. Soc. 1968, $\underline{90}$, 1153.

21. For example see ref. 14c and 15c.

22. Che, C.M.; Jamal, M.; Poon, C.K.; Chung, W.C. Inorg. Chem. 1985, $\underline{24}$, 2868.

23. (a) Von Kameke, A.; Tom, G.M.; Taube, H. Inorg. Chem. 1978, $\underline{17}$, 1790. (b) Bauman, J.A.; Wilson, S.T.; Salmon, D.J.; Hood, P.L.; Meyer, T.J. J. Am. Chem. Soc. 1979, $\underline{101}$, 2916. (c) Bignozzi, C.A.; Roffia, S.; Scandola, F. J. Am. Chem. Soc. 1985, $\underline{107}$, 1644.

24. Lim, H.S.; Barclay, D.I.; Anson, F.C. Inorg. Chem. 1972, $\underline{11}$, 1460.

25. Rabalais, J.W.; McDonald, J.M.; Sherr, V.; McGlynn, S.P.M. Chem. Rev. 1971, $\underline{71}$, 73.

26. diSipio, L.; Oleari, L.; de Michelis, G. Coord. Chem. Rev. 1966, $\underline{1}$, 7.

27. Folkensson, B.; Larsson, R .J. Electron. Spectrosc. Relat. Phenom. 1982, 26, 157.

28. (a) Richardson, D.E.; Taube, H. Coord. Chem. Rev. 1984, 60, 107 and references therein. (b) Stein, C.A.; Taube, H. J. Am. Chem. Soc. 1981, 103, 693. (c) Stein, C.A.; Lewis, N.A.; Seitz, G. J. Am. Chem. Soc. 1982, 104, 2596.

29. Hush, N.S. Coord. Chem. Rev. 1985, 64, 135.

30. (a) Marcus, R.A. J. Chem. Phys. 1956, 24, 966. (b) Marcus, R.A. Discuss. Faraday Soc. 1960, 29, 21. (c) Marcus, R.A. Ann. Rev. Phys. Chem. 1964, 28, 962. (d) Marcus, R.A. J. Chem. Phys. 1965, 43, 679.

31. (a) Hush, N.S. J. Chem. Phys. 1958, 28, 962. (b) Hush, N.S. Trans. Faraday Soc. 1961, 57, 557.

32. (a) Laidler, K.J. Can. J. Chem. 1959, 37, 138. (b) Sacher, E.; Laidler, K.J. Trans. Faraday Soc. 1963, 59, 396.

33. (a) Dogonadze, R.R.; Kuznetsov, A.M.; Zakaraya, M.G.; Ulstrup, J. In "Tunneling in Biological Systems;" Chance, B.; DeVautt, D.; Fraueufelder, H.; Marcus, R.A.; Schrieffer, J.R.; Sutin, N. Eds.; Academic: New York, 1979. (b) Hopfield, J.J. Proc. Natl. Acad. Sci. U.S.A. 1974, 71, 3640. (c) Bukhs, E.; Bixon, M.; Jortner, J. Chem. Phys. 1981, 55, 41. (d) Sarai, S. Biochim. Biophys. Acta 1980, 589, 71.

34. (a) Thanabal, V.; Krishnan, V. J. Am. Chem. Soc. 1982, 104, 3644. (b) Bhaskar Maiya, G. Ph.D. Thesis, I.I.Sc. Bangalore, India, 1985 and references therein. (c) Bolton, J.R. In ref. 6. (d) Seta, P.; Bienvenue, E.; Moore, A.L.; Mathis, P.; Bensasson, R.V.; Liddel, P.A.; Pessiki, P.J.; Joy, A.; Moore, T.A.; Gust, D. Nature, 1985, 316, 653. (e) Wasielewski, M.R.; Liddel, P.A.; Barret, D.; Moore, T.A.; Gust, D. Nature, 1986, 322, 570.

35. Sykes, A.G. In ref. 6.

36. (a) Isied, S.S.; Vassilian, A.; Magnuson, R.H.; Schwarz, S. J. Am. Chem. Soc. 1985, 107, 7432. (b) Isied, S.S.; Vassilian, A. J. Am. Chem. Soc. 1984, 106, 1732.

37. Creutz, C. Prog. Inorg. Chem. 1983, 30, 1 and references therein.

38. Day, P. In "Mixed-Valence Compounds;" Brown, D.B.; Ed.; D. Reidel: Boston, 1980. p 1.

39. Robin, M.B.; Day. P. Adv. Inorg. Chem. Radiochem. 1967, 10, 247.

40. (a) Hush, N.S. Prog. Inorg. Chem. 1967, 8, 391, (b) Hush, N.S.; Allen, G.C. Prog. Inorg. Chem. 1967, 8, 357. (c) Hush, N.S.; Electrochim. Acta, 1968, 13, 1005. (d) ref. 63.

41. Creutz, C.; Taube, H. J. Am. Chem. Soc. 1969, 91, 3988; 1973, 95, 1086.

42. Sullivan, B.P.; Curtis, J.C.; Kober, E.M.; Meyer, T.J. Nouv. J. Chim. 1980, 4, 643.

43. (a) Piepho, S.B.; Krausz, E.R.; Schatz, P.N. J. Am. Chem. Soc. 1978, 100, 2006. (b) Schatz, P.N. In ref. 38. (c) Wong, K.Y.; Schatz, P.N. Prog. Inorg. Chem. 1981, 28, 369.

44. Buhks, E. Ph.D.Thesis, Tel Aviv University, 1980.

45. (a) Sutton, J.E.; Sutton, P.M.; Taube, H. Inorg. Chem. 1979, 18, 1017. (b) Richardson, D.E.; Taube, H. Inorg. Chem. 1981, 20, 1278.

46. (a) Mandal, S.K.; Adhikary, B.; Nag, K. J. Chem. Soc. Dalton Trans. 1986, 1175. (b) Gagne, R.R.; Spiro, C.L.; Smith, T.J.; Hamann, C.A.; Thies, W.R.; Schiemke, A.K. J. Am. Chem. Soc. 1981, 103, 4073. (c) Sutton, J.E.; Taube, H. Inorg. Chem. 1981, 20, 3125. (d) Pherlps, J.; Bard, A.J. J. Electrochim. Acta 1976, 68, 313.

47. See Ludi, A. In ref. 38.

48. (a) Mayoh, B.; Day, P. Inorg. Chem. 1974, 13, 2273. (b) Richardson, D.E.; Taube, H. J. Am. Chem. Soc. 1983, 105, 40.

49. (a) Ondrechen, M.J.; Ko, J.; Root, L.J.; J. Phys. Chem. 1984, 88, 5919. (b) Ko, J.; Ondrechen, M.J. Chem. Phys. Lett. 1984, 112, 507.

50. (a) Glauser, R.; Hauser, U.; Herren, F.; Ludi, A.; Roder, P.; Schmidt, E.; Siegnhaler, H.; Wenk, F. J. Am. Chem. Soc. 1973, 95, 8457. (b) Ludi, A. Chimia, 1972, 26, 647. (c) Hennig, H.; Rehorek, A.; Rehorek, D.; Thomas, Ph. Inorg. Chim. Acta, 1984, 86, 41. (d) Hennig, H.; Rehorek, D.; Archer, R.D. Coord. Chem. Rev. 1985, 61, 1.

51. (a) Brant, P.; Stephenson, T.A.; Inorg. Chem. 1987, 26, 22. (b) Dubicki, L.; Krausz, E.R. Inorg. Chem. 1985, 24, 4461.

52. (a) Taube, H. Ann. N.Y. Acad. Sci. 1978, 313, 481. (b) Magnuson, R.H.; Taube, H. J. Am. Chem. Soc. 1972, 94, 7213.

53. Tom, G.; Taube, H. J. Am. Chem. Soc. 1975, 97, 5310.

54. (a) Weaver, T.R.; Meyer, T.J.; Adeyemi, S.A.; Brown, G.M.; Eckberg, R.P.; Hatfield, W.E.; Johnson, E.C.; Muray, R.W.;

Untereker, D. J. Am. Chem. Soc. 1975, 97, 3039. (b) Bauman, J.A.; Meyer, T.J. Inorg. Chem. 1980, 19, 345.

55. Strekas, T.C.; Spiro, T.G. Inorg. Chem., 1976, 15, 974.

56. Creutz, C.; Good, M.L.; Chandra, S. Inorg. Nucl. Chem. Lett. 1973, 9, 171.

57. Citrin, P. J. Am. Chem. Soc. 1973, 95, 6472.

58. Beattie, J.K.; Hush, N.S.; Taylor, R.P. Inorg. Chem. 1976, 15, 992.

59. Elias, J.; Drago, R.S. Inorg. Chem. 1972, 11, 415.

60. Bunker, B.C.; Drago, R.S.; Hendrickson, D.N.; Richman, R.M.; Kessel, S.L. J. Am. Chem. Soc. 1978, 100, 3805.

61. Beattie, J.K.; Hush, N.S.; Taylor, P.R.; Raston, C.L.; White, A.H. J. Chem. Soc. Dalton Trans. 1977, 1121.

62. Stebler, A.; Ammeter, J.H.; Furholz, U.; Ludi, A. Inorg. Chem. 1984, 23, 2764.

63. Hush, N.S. Chem. Phys. 1975, 10, 361.

64. (a) Mayoh, B.; Day, P. J. Am. Chem. Soc. 1972, 94, 2885. (b) ref. 48(a).

65. Koppel, I.A.; Palm, V.A. In "Advances in Linear Free Energy Relationship;" Chapman, N.B.; Shorter, N.J., Eds. Plenum: London, 1972: pp 254-258.

66. Allen, A.D.; Bottomley, F.; Remsolu, V.P.; Senoff, C.V., J. Am. Chem. Soc. 1967, 89, 5595.

67. Bruauer, G. "Handbook of Preparative Inorganic Chemistry;" 2nd Ed.; Academic: New York, 1965, p 1511.

68. Jwo, J.J.; Haim, A. J. Am. Chem. Soc. 1976, 98, 1172.

69. Michiels, L.P.; Kolks, G.; Nesbitt, E.R.; Dimauro, P.T., Krichner, R.M.; Waszczak, J.V. Inorg. Chim. Acta, 1985, 100, 211.

70. Herington, E.F.; Kynaston, W. J. Chem. Soc. 1955, 3555.

71. Goodwin, J.B.; Meyer, T.J. Inorg. Chem. 1971, 10, 471.

72. (a) Bryant, G.M.; Fergusson, J.E.; Powell, H.K. J. Aust. J. Chem. 1971, 24, 257. (b) Bryant, G.M.; Fergusson, J.E. Aust. J. Chem. 1971, 24, 275. (c) Johnson, E.C.; Callahan, R.W.;

Eckberg,R .P.; Hatfield,W.E.; Meyer,T.J. Inorg.Chem. 1979,18,618.

73. Vogel, A. I. "Practical Organic Chemistry;"Longmans. Green and Co.; London,1951.

74. Wharton, D. C.; McCarty, R. E. "Experiments and Methods in Biochemistry;" Macmillan: New York, 1972, p 105.

75. Khan, M. I. Ph.D. Thesis, IIT, Kanpur, India, 1984.

76. (a) Vogel, A. I. "A Textbook of Quantitative Inorganic Analysis,"2nd edn.: Longmans Green Co.: London, 1951, p 441. (b) Williams, J. W. "Handbook of Anion Determination;" Butterworths; London, 1979.

77. Lamba, O. P.; Bist, H. D.: Jain, Y.·S. Can. J. Chem. 1983, 61. 608.

78. Dollish, F. R.; Fateley, W. G.; Bentley, F.F. "Characteristic Raman Frequencies of Organic Compounds; "John Wiley: New York, 1974.

79. Swaminathan, M.; Dogra, S.K. Indian J. Chem. 1983,22A. 853.

80. Sengupta, S.K.; Johri, U.C.; Singru, R.M.; Kunzru, D.; Srivastava, R.D. J.Catal. (in press).

81. Miller , F.J.; Meyer, T.J. J. Am. Chem. Soc. 1971, 93. 1294.

82. (a) Chang, J.P.; Fung, E.Y.; Curtis, J.C.Inorg. Chem. 1986, 25. 4233.
(b) Ennix, K. S.; Mcmahon. P. T.; Rosa, R. D. L.; Curtis, J. C. Inorg. Chem. 1987, 26 2660.

83. Offenhartz, P. O D'. "Atomic and Molecular Orbital Theory;" McGraw Hill; New York, 1970.

84. Lever, A. B. P. "Inorganic Electronic Spectroscopy;" 2nd ed.: Elsevier: New York, 1984; p 453.

85. Taube, H. Pure Appl. Chem. 1979,51,901.

86. See ref 41.

87. Callahan, R. W.; Keene, F.R.; Meyer, T.J.; Salmon,D.J. J. Am. Chem. Soc. 1977,99,1064.

88. Nakamoto, K. "Infrared and Raman Spectroscopy"

89. (a) Yeh, A.; Haim, A.: Tanner, M.: Ludi, A. Inorg.

Chim. Acta 1979,33, 51; (b) Yeh, A.; Haim, A. J Am. Chem. Soc. 1985,107,369.

90. Dows, D. A.; Wilmarth, W. K.; Haim, A. J. Inorg. Nucl. Chem. 1961,21,23

91. Treitel, I. M.; Flood,M. T.; Marsh, R. E.; Gray, H. B. J. Am. Chem. Soc. 1969,91, 6512.

92. Felix, F.; Ludi,A. Inorg. Chem. 1978,17, 1782.

93. (a) Fucks, Y.; Lofters, S.;Dieter, T.; Shi, W. ;Morgan R.; Strekas,T .C.; Gafney, H. D.;Baker,A. D. J. Am. Chem.Soc. 1987, 109, 2691.(b) Braunstein,C.H.;Baker, A.D.;Strekas, T. C.; Gafney, H. D. Inorg. Chem. 1984, 23,857.(c) Haga,M. A. Inorg. Chim. Acta 1980,45, L183.

94. Basu ,A.; Gafney, H. D.; Strekas, T.C. Inorg. Chem. 1982,21, 1085

95. (a) Rillema, D. P.; Mack, K. B. Inorg. Chem. 1982,21, 3849.(b) Rillema, D. P.; Callahan, R.W.; Mack, K. B.Inorg. chem. 1982,21, 2589. (c) Dallinger, R. F.; Woodruff, W.H. J. Am. Chem. Soc. 1979,101,4391.(d) Bradley, P. G.; Kress, N.; Hoornberger, B. A.; Dallinger,R. F.; Woodruff, W. H. J Am. Chem .Soc. 1981,103, 7441.(e) Basu, A.;Gafney, H. D.; Strekas, T. C. Inorg. chem. 1982, 21, 2231.

96. Smothers, W.K.; Wrighton, M. S. J Am. Chem. Soc. 1983,105, 1067.

97. (a) Work by D. N. Hendrickson on the biferrocenium salts should be mentioned in this regard. (b) Ito, A.; Suenaga, M.; Ono, K. J. Chem. Phys. 1968,48, 3597.(c) van Steenwijk, F. J.; Roder, P. Helv. Phys. Acta 1979,52, 18.

98. Mathur, H. B. In" Spectroscopy in Inorganic Chemistry,vol,I.;" Rao, C. N. R.; Ferraro, J. R.; Eds.; Academic: New York, 1970,p 347.

99. Callahan, R.W.; Meyer, T. J. Chem. Phys. Lett. 1976,39, 82.

100. (a) Nicholson, R. S.; Shain, I. Anal. Chem. 1964,36, 406. (b) Bard, A. J.; Faulkner, L. R."Electrochemical Methods- Fundamentals and Application;" John Wiley: New York, 1980.

101. (a) Manoli, J. M.; Potvin, C.; Secheresse, F.; Marzak, S. J Chem. Soc. Chem Commun. 1986, 1557. (b)

Taniguchi, M.; Sugita, Y.; Ouchi. A. Bull. Chem. Soc. Jpn. 1987, 60, 1321. (c) Nakao, Y.: Nakmura, H.; Mori, W.; Sakurai, T.; Suzuki, S.; Nakahara, A. Bull. Chem. Soc. Jpn. 1986. 59, 2755.

102.   Ondrechen, M. J.; Ratner, M. A.; Ellis, D. E. J. Am. Chem. Soc. 1981, 103, 1656.

103.   Taube, H. In " Complex Ions in Solution;" Plenum; New York, 1970.